

In Vivo and in Vitro Studies on the Localisation and Kinetics of Porphyrin Related Drugs for Photodetection and Photodynamic Therapy

In vivo en in vitro studies naar de lokalisatie en kinetiek van
porfyrine-achtige stoffen voor fotodetectie en fotodynamische therapie

PROEFSCHRIFT

ter verkrijging van de graad van doctor aan de
Erasmus Universiteit Rotterdam
op gezag van de Rector Magnificus
Prof.dr.ir. J.H. van Bommel
en volgens besluit van het College voor Promoties.

De openbare verdediging zal plaatsvinden op
donderdag 13 november 2003 om 13.30 uur

door

Johanna Theodora Hendrica Maria van den Akker

geboren te Helmond

Promotiecommissie

Promotoren	Prof.dr. P.C. Levendag Prof.dr. S.B. Brown
Overige leden	Prof.dr. R. Kanaar Prof.dr. H.A.M. Neumann Prof.dr. P. de Witte
Copromotor	Dr.ir. H.J.C.M. Sterenborg

The studies presented in this thesis were performed at

the Department of Radiation Oncology, Daniel den Hoed Cancer Centre, Erasmus Medical Centre, Rotterdam, The Netherlands; the Department of Biophysics, Institute for Cancer Research, Norwegian Radium Hospital, Oslo, Norway; the School of Biochemistry and Molecular Biology, University of Leeds, Leeds, United Kingdom.

The studies described in this thesis were supported by

grant BMH4-CT97-2260 from the European Community; the Norwegian Radium Hospital Research Foundation; Yorkshire Cancer Research; the Willem H. Kroger Foundation.

This thesis was made possible thanks to financial contributions of

biolitec pharma ltd.; Galderma Nederland; Harlan Nederland; Hope Farms; NDDO Oncology; Novartis Ophthalmics the Netherlands.

Table of Contents

CHAPTER 1	Introduction and outline	11
CHAPTER 2	Photodynamic therapy based on 5-aminolevulinic acid: Applications in dermatology	19
CHAPTER 3	Localisation and accumulation of a new carotenoporphyrin in two primary tumour models.	37
CHAPTER 4	Protoporphyrin IX fluorescence kinetics and localization after topical application of ALA pentyl ester and ALA on hairless mouse skin with UVB-induced early skin cancer.	53
CHAPTER 5	Topical application of 5-aminolevulinic acid hexyl ester and 5-aminolevulinic acid to normal nude mouse skin: Differences in protoporphyrin IX fluorescence kinetics and the role of the stratum corneum.	69
CHAPTER 6	Systemic component to protoporphyrin IX production in the nude mouse skin upon topical application of aminolevulinic acid depends on the application conditions.	87
CHAPTER 7	Comparative in vitro percutaneous penetration of 5-aminolevulinic acid and two of its esters through excised hairless mouse skin.	99
CHAPTER 8	Chronic UVB exposure enhances in vitro percutaneous penetration of 5-aminolevulinic acid in hairless mouse skin.	113
CHAPTER 9	Effect of elevating the skin temperature during topical ALA application on in vitro ALA penetration through mouse skin and in vivo PpIX production in human skin.	123
CHAPTER 10	General discussion and summary	135
	Samenvatting en conclusies	147
	Curriculum Vitae	156
	List of publications	157
	Tenslotte...	158

Abbreviations

AK	Actinic keratosis
ALA	5-Aminolevulinic acid
ALAHE	5-Aminolevulinic acid hexyl ester
ALAME	5-Aminolevulinic acid methyl ester
ALAPE	5-Aminolevulinic acid pentyl ester
ANOVA	Analysis of variance
BCC	Basal cell carcinoma
BD	Bowen's disease
CC	Pearson product-moment correlation coefficient
CCD	Charge-coupled device
CP	Carotenoporphyrin
CP3	Trimethoxylated carotenoporphyrin
CP6	Hexamethoxylated carotenoporphyrin
DMSO	Dimethylsulphoxide
EAI	Epithelial atypia index
HE	Haematoxylin and eosin
HPE-101	1-[2-(Decylthio)ethyl]azacyclopentan-2-one
K-W	Kruskal-Wallis statistic
M-W	Mann-Whitney rank-sum test
4-NQO	4-Nitroquinoline-1-oxide
PDT	Photodynamic therapy
PpIX	Protoporphyrin IX
SCC	Squamous cell carcinoma
SNK	Student-Newman-Keuls
<i>t</i> -test	Unpaired Student <i>t</i> -test

Voor ons pap en ons mam

CHAPTER 1

Introduction and outline

Background

The techniques of photodetection and photodynamic therapy (PDT) of malignant and premalignant lesions are based on the activation of a photosensitive drug (photosensitiser) with (laser) light (1,2). The photosensitiser can be administered exogenously, which is the case for porphyrin derivatives. Alternatively, the photosensitiser can be produced endogenously upon administering a suitable precursor: aminolevulinic acid (ALA) induces the production of protoporphyrin IX (PpIX) which is an intermediate in the haem biosynthetic pathway with and has excellent photodynamic properties (3-6). The apparent accumulation of PpIX in (pre)cancerous tissue and lesions has been observed in several studies (2,7-14).

The ideal photosensitiser accumulates selectively in the (pre)malignant tissue. Upon illumination with light of an appropriate wavelength, the photosensitiser fluoresces and reacts with cellular substances and/or produces singlet oxygen. The reaction with cellular substances and the highly reactive singlet oxygen are responsible for the photodynamic action, which is causing cell death and thus destruction of the (pre)-malignant tissue (1). The fluorescent properties can be used for diagnosis of (pre)malignant tissue, which is not visible for the eye (2).

The photodynamic properties of porphyrin derivatives and PpIX can induce undesired side effects like prolonged skin photosensitivity and erythema. These side effects can be too severe to allow the use of these agents for purely diagnostic purposes. An alternative to the use of porphyrin derivatives may be photosensitive drugs which are chemically modified in such a way that these agents have lost their ability to induce photodynamic effects, but have preserved their fluorescent properties and their ability to localise in (pre)malignant tissue. Another solution to this problem may be the use of chemically altered ALA, for example esterified ALA which is more lipophilic than ALA itself. The higher lipophilicity of the ALA esters is expected to increase the penetration depth, improve the distribution and enhance the cellular uptake. The administration of ALA esters could then result in higher PpIX levels, a more uniform and deeper PpIX distribution, or a greater difference in PpIX levels (and thus fluorescence) between normal and (pre)malignant tissue as compared to ALA. The improved ratio of PpIX in (pre)malignant tissue versus normal tissue allows the use of lower PpIX concentrations, therewith reducing the chance that undesirable photodynamic effects occur.

Motivation

The starting point of this thesis was to evaluate the use of other agents than porphyrin derivatives or protoporphyrin IX (PpIX) for photodetection purposes in order to avoid undesired side effects which are related to the use of photodynamically active drugs. This was done in the PDT laboratory in the Daniel den Hoed Cancer Center in Rotterdam

as a participant of an EC project in which several different photodetection techniques for diagnosis of gynaecological cancer were developed and evaluated in laboratory and clinical settings (Fluorescence imaging in Gynaecology, BMH4 CT97-2260).

In the first study within this EC project (1997), a chemically modified porphyrin (hexamethoxylated carotenoporphyrin) was tested *in vivo* in two animal models with primary tumours. From this study it appeared that the use of this carotenoporphyrin was not a successful approach for the photodetection of (pre)malignant lesions with a fluorescent porphyrin that lacks the photodynamic effects.

The next step then was to investigate if esterification of aminolevulinic acid (ALA) could be a successful approach for photodetection with minimal photodynamic effects. The *in vivo* PpIX fluorescence kinetics and distribution in mice with primary skin lesions was determined upon topical application of ALA pentyl ester. The results showed that the *in vivo* ratio in PpIX fluorescence between (pre)malignant lesions and normal tissue was slightly higher for ALA pentyl ester than for ALA. These results were quite in contrast to our expectations, which were based on the *in vitro* and *in vivo* studies in which ALA esters, and ALA hexyl ester in particular, proved to be successful in improving PpIX production in cells and in skin and PpIX production and distribution in bladder mucosa (15-24).

The results from the study with ALA pentyl ester application to mouse skin lead to the decision to further investigate the use of ALA esters for PpIX photodetection as well as PDT in skin. This decision was partly influenced by the fact that the EC project had finished and that I had moved to the PDT laboratory in the Norwegian Radium Hospital in Oslo (1999). The design of the next study was therefore based on the questions whether ALA hexyl ester and ALA have different properties regarding penetration and PpIX production in normal nude mouse skin after topical application and if possible differences between ALA and ALA hexyl ester regarding the *in vivo* PpIX fluorescence kinetics are dependent on application time and applied concentration.

In the same animals in which the *in vivo* PpIX fluorescence kinetics were measured in the application area of ALA and ALA hexyl ester to answer the above mentioned questions, the *in vivo* PpIX fluorescence kinetics were also determined in the skin contralateral to the ALA and ALA hexyl ester application area. These latter measurements were performed to further investigate the phenomenon that in case of ALA application to nude mouse skin, PpIX is not only produced within the application area but also in skin distant from the application area (22,25-28). This PpIX production outside the ALA application area is induced by ALA that has penetrated through the skin into the circulation.

From the results from the ALA pentyl ester study and the ALA hexyl ester study, which showed that esterified ALA does not induce substantial improvement of PpIX production in mouse skin, the next question arose: Is it possible that the increased lipophilicity of

ALA esters not only induces an increased cellular uptake but also a decreased penetration into the skin? A difference between ALA esters and ALA regarding the skin penetration properties might be (co-)responsible for the finding that ALA esters do not perform as well in the skin as they do in cells and the bladder mucosa. To find an answer for this question, an *in vitro* percutaneous penetration model for measuring the penetration of ALA and ALA esters across freshly excised skin was needed. Such a model was in development in the PDT laboratory of Prof. Brown in Leeds. In the final 11 months of my research I stayed in his lab (2000 and 2001) to further develop this *in vitro* percutaneous penetration model and to perform skin penetration experiments with ALA and ALA esters in this model.

The same *in vitro* percutaneous penetration model was used to investigate if the preferential accumulation of PpIX in (pre)cancerous lesions is (partly) the result of a higher penetration rate of ALA into these lesions as compared to normal skin, due to differences in permeation properties of the stratum corneum.

The above-described studies with the ALA esters demonstrated that the use of ALA esters on skin is not a suitable approach in order to increase the PpIX production in skin as compared to ALA. The next step was therefore to further investigate in healthy human skin the effect of skin temperature (during ALA application) on the PpIX production in human skin (in the PDT laboratory in Rotterdam). Furthermore it was investigated if increased ALA penetration into the skin at higher skin temperature is a contributing factor in increasing the PpIX production in the skin (in the PDT laboratory in Leeds).

Outline of the thesis

Chapter 2 reviews the application of photodynamic therapy (PDT) based on aminolevulinic acid (ALA)-induced protoporphyrin IX (PpIX) in dermatological conditions. Firstly, the principles and mechanism of ALA-based PDT in general and the general approach to PDT in skin are outlined. Then, this chapter presents an overview of the results of published patient studies and case reports on ALA-based PDT treatment of Bowen's disease, basal cell carcinoma, actinic keratosis, psoriasis, acne, T-cell lymphoma and erythroplasia of Queyrat. Furthermore, this chapter describes the limitations of the ALA-based PDT in skin and different methods that are under investigation or have been applied successfully to overcome these limitations.

In **chapter 3**, the *in vivo* fluorescence kinetics and tumour localising properties of a hexamethoxylated carotenoporphyrin were investigated in two primary tumour models: UVB-induced early skin cancer in mice and chemically induced mucosal dysplasia in the rat palate. The *in vivo* fluorescence kinetics were determined at different time points after the carotenoporphyrin administration by measuring *in vivo* fluorescence spectra and images. The tumour localising properties were studied by means of fluorescence

microscopy of tissue samples taken at different time point after administration of the carotenoporphyrin.

Chapter 4 describes an investigation on the *in vivo* fluorescence kinetics (with *in vivo* fluorescence spectroscopy and imaging) and tumour localising properties (with fluorescence microscopy) of PpIX induced by either ALA or ALA pentyl ester. The study was performed in hairless mice with and without UVB-induced early skin cancer.

In **chapter 5**, ALA hexyl ester was compared with ALA with regard to the *in vivo* PpIX fluorescence kinetics in nude mouse skin. Application times and concentrations of ALA hexyl ester and ALA were varied. Furthermore, the effect of a penetration enhancer and the effect of tape stripping were investigated.

Chapter 6 presents results what the effect is of the ALA concentration in the cream, the application time, the presence of a penetration enhancer, the presence of the stratum corneum, or esterification of ALA, on the PpIX production in nude mouse skin outside the area where ALA is applied.

In **chapter 7**, the penetration of ALA and its methyl and hexyl ester across freshly excised hairless mouse skin was investigated in an *in vitro* percutaneous penetration model. The influence of different application concentrations and the effect of the stratum corneum barrier function on the percutaneous penetration of ALA, ALA methyl ester and ALA hexyl ester were investigated.

Chapter 8 describes the results from another *in vitro* experiment with the percutaneous penetration model. In this chapter it was investigated if the preferential accumulation of PpIX in (pre)cancerous lesions is the result of a higher percutaneous penetration rate of ALA into the lesions. The penetration of ALA across diseased hairless mouse skin with dysplastic and thickened epidermis was compared to normal healthy hairless mouse skin and to normal hairless mouse skin with reduced stratum corneum.

Chapter 9 describes what the effect is of higher skin temperature during ALA application to skin on the penetration of ALA through the skin and the production of PpIX production in the skin. The *in vitro* penetration of ALA through hairless mouse skin was determined in the percutaneous penetration model. The PpIX production was measured with *in vivo* fluorescence spectroscopy measurements in temperature controlled areas on healthy human skin.

The results presented in this thesis are reviewed in **chapter 10**.

References

1. Henderson BW, Dougherty TJ. How does photodynamic therapy work? *Photochem Photobiol* 1992; 55(1):145-157.
2. Wagnières GA, Star WM, Wilson BC. *In vivo* fluorescence spectroscopy and imaging for oncological applications. *Photochem Photobiol* 1998; 68(5):603-632.
3. Kennedy JC, Pottier RH, Pross DC. Photodynamic therapy with endogenous protoporphyrin IX: basic principles and present clinical experience. *J Photochem Photobiol B* 1990; 6:143-148.

4. Kennedy JC, Pottier RH. Endogenous protoporphyrin IX, a clinically useful photosensitizer for photodynamic therapy. *J Photochem Photobiol B* 1992; 14:275-292.
5. Kennedy JC, Marcus SL, Pottier RH. Photodynamic therapy and photodiagnosis using endogenous photosensitization induced by 5-aminolevulinic acid: mechanisms and clinical results. *J Clin Laser Med Surg* 1996; 14(5):289-304.
6. Peng Q, Berg K, Moan J, Kongshaug M, Nesland JM. 5-Aminolevulinic acid-based photodynamic therapy: principles and experimental research. *Photochem Photobiol* 1997; 65(2):235-251.
7. Szeimies R-M, Sassy T, Landthaler M. Penetration potency of topical applied d-aminolevulinic acid for photodynamic therapy of basal cell carcinoma. *Photochem Photobiol* 1994; 59(1):73-76.
8. Roberts DJH, Stables GI, Ash DV, Brown SB. Distribution of protoporphyrin IX in Bowen's disease and basal cell carcinomas treated with topical 5-aminolaevulinic acid. *Proc SPIE* 1995; 2371:490-494.
9. Peng Q, Warloe T, Moan J, Heyerdahl H, Steen HB, Nesland JM, Giercksky K-E. Distribution of 5-aminolevulinic acid-induced porphyrins in nodulo-ulcerative basal cell carcinoma. *Photochem Photobiol* 1995; 62:906-913.
10. van der Veen N, de Bruijn HS, Berg RJW, Star WM. Kinetics and localisation of PpIX fluorescence after topical and systemic ALA application, observed in skin and skin tumours of UVB-treated mice. *Br J Cancer* 1996; 73:925-930.
11. van der Veen N, de Bruijn HS, Star WM. Photobleaching during and re-appearance after photodynamic therapy of topical ALA-induced fluorescence in UVB-treated mouse skin. *Int J Cancer* 1997; 72:110-118.
12. Orenstein A, Kostenich G, Malik Z. The kinetics of protoporphyrin fluorescence during ALA-PDT in human malignant skin tumors. *Cancer Letters* 1997; 120:229-234.
13. Fritsch C, Lehmann P, Schulte KW, Blohm E, Lang K, Sies H, Ruzicka T. Optimum porphyrin accumulation in epithelial skin tumours and psoriatic lesions after topical application of δ -aminolaevulinic acid. *Br J Cancer* 1999; 79(9/10):1603-1608.
14. af Klinteberg C, Enejeder AMK, Wang I, Andersson-Engels S, Svanberg S, Svanberg K. Kinetic fluorescence studies of 5-aminolaevulinic acid-induced protoporphyrin IX accumulation in basal cell carcinomas. *J Photochem Photobiol B* 1999; 49:120-128.
15. Kloek J, Beijersbergen van Henegouwen GMJ. Prodrugs of 5-aminolevulinic acid for photodynamic therapy. *Photochem Photobiol* 1996; 64(6):994-1000.
16. Gaullier J-M, Berg K, Peng Q, Anholt H, Selbo PK, Ma L-W, Moan J. Use of 5-aminolevulinic acid esters to improve photodynamic therapy on cells in culture. *Cancer Res* 1997; 57:1481-1486.
17. Kloek J, Akkermans W, Beijersbergen van Henegouwen GMJ. Derivatives of 5-aminolevulinic acid for photodynamic therapy: enzymatic conversion into protoporphyrin. *Photochem Photobiol* 1998; 67(1):150-154.
18. Marti A, Lange N, van den Bergh H, Sedmera D, Jichlinski P, Kucera P. Optimisation of the formation and distribution of protoporphyrin IX in the urothelium: an *in vitro* approach. *J Urol* 1999; 162:546-552.
19. Casas A, del C. Battle AM, Butler AR, Robertson D, Brown EH, MacRobert A, Riley PA. Comparative effect of ALA derivatives on protoporphyrin IX production in human and rat skin organ cultures. *Br J Cancer* 1999; 80(10):1525-1532.
20. Uhlinger P, Zellweger M, Wagnières GA, Juillerat-Jeanneret L, van den Bergh H, Lange N. 5-Aminolevulinic acid and its derivatives: physical chemical properties and protoporphyrin IX formation in cultured cells. *J Photochem Photobiol B* 2000; 54:72-80.
21. Eléout S, Rousset N, Carre J, Bourre L, Vonarx V, Lajat Y, Beijersbergen van Henegouwen GMJ, Patrice T. *In vitro* fluorescence, toxicity and phototoxicity induced by δ -aminolevulinic acid (ALA) or ALA esters. *Photochem Photobiol* 2000; 71(4):447-454.
22. Peng Q, Moan J, Warloe T, Iani V, Steen HB, Bjorseth A, Nesland JM. Build-up of esterified aminolevulinic-acid-derivative-induced porphyrin fluorescence in normal mouse skin. *J Photochem Photobiol B* 1996; 34:95-96.
23. Peng Q, Warloe T, Moan J, Heyerdahl H, Steen HB, Giercksky K-E, Nesland JM. ALA derivative-induced protoporphyrin IX build-up and distribution in human nodular basal cell carcinoma. *Photochem Photobiol* 1995; 61:Abstract 82S
24. Peng Q, Moan J, Iani V, Steen HB, Nesland JM. Studies on ALA derivative-induced proto-

porphyrin IX build-up in normal mouse skin. *Photochem Photobiol* 1995; 61:Abstract 82S

25. Sørensen R, Juzenas P, Iani V, Moan J. Formation of protoporphyrin IX in mouse skin after topical application of 5-aminolevulinic acid and its methyl ester. *Proc SPIE* 1999; 3563:77-81.

26. Casas A, Fukuda H, del C. Battle AM. Tissue distribution and kinetics of endogenous porphyrins synthesized after topical application of ALA in different vehicles. *Br J Cancer* 1999;

81(1):13-18.

27. Casas A, Fukuda H, di Venosa G, del C. Battle AM. The influence of the vehicle on the synthesis of porphyrins after topical application of 5-aminolaevulinic acid. Implications in cutaneous photodynamic sensitization. *Br J Dermatol* 2000; 143:564-572.

28. Moan J, Ma L-W, Iani V. On the pharmacokinetics of topically applied 5-aminolevulinic acid and two of its esters. *Int J Cancer* 2001; 92:139-143.

CHAPTER 2

Photodynamic therapy based on 5-aminolevulinic acid: Applications in dermatology

This chapter has been adapted from JTHM van den Akker and SB Brown. In *Photobiology for the 21st Century* (Edited by TP Coohill and DP Valenzano) 2001, Valdenmar Publishing Company, Kansas, USA: pp 165-181.

Introduction and context

Photodynamic therapy (PDT) requires three components for success, a photosensitiser, light and molecular oxygen. All three components are necessary if the PDT effect is to occur and the aim of successful PDT is to ensure adequate amounts of each in the target tissue. Most of the development work, both experimentally and clinically, has been aimed at ensuring that there is sufficient photosensitiser and light in the target tissue at the time of treatment. It is much more difficult to control the levels of molecular oxygen but, again, successful PDT is absolutely dependent on having sufficient oxygen present.

Most drugs for PDT have been developed as photosensitisers which are given systemically. However, a quite different approach has been developed over the past ten years in order to produce an adequate quantity of photosensitiser in the target tissue. This involves the administration of 5-aminolevulinic acid (ALA), which is a very simple 5 carbon compound, the structure of which is shown in figure 1. ALA was first used by Kennedy and Pottier (1) to treat various dermatological conditions using a topical preparation of the drug. Since that first demonstration that ALA-PDT was feasible, the approach has been extended a great deal both within dermatology and to other applications in gynaecology, in bladder, in the gastrointestinal tract and in the brain. The drug has been used both topically, in a variety of formulations and systemically through oral administration. This brief review is intended to give an indication of the scope and potential of PDT using ALA and its derivatives, particularly in dermatology, since this was the area which was focused on in the recent Photobiology Congress on which this book is based. It is not intended to be a comprehensive review, even in the dermatology field and references are given to more detailed reviews and papers both in the dermatology area and elsewhere.

Principles of ALA-based PDT

Haem is a vital component of a large number of enzymes and proteins throughout nature. In mammals, it is most abundant as the active centre of haemoglobin but is also a component of myoglobin, cytochromes of the respiratory chain, the cytochrome P450 family of proteins which are essential in oxidative metabolism and many other enzymes. Virtually all mammalian cells have the capacity to synthesize haem, a major exception being the mature red blood cell which has already lost its haem synthesizing capacity during development following synthesis of its complement of haemoglobin. It is this

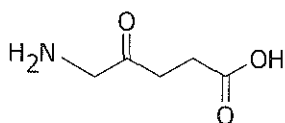


Figure 1 Molecular structure of 5-aminolevulinic acid.

ubiquitous pathway of haem biosynthesis which is utilized in ALA-PDT.

An outline of this pathway is shown in figure 2. Haem is a tetrapyrrolic derivative and the first committed step in the pathway is the condensation of two molecules of ALA to form the first pyrrolic derivative known as porphobilinogen (PBG). Four molecules of porphobilinogen then assemble together to make a linear tetrapyrrolic derivative known as a hydroxymethylbilane which then ring closes to form a porphyrinogen. When this process occurs without enzymatic control, the porphyrinogen formed is a symmetrical derivative known as a Type 1 isomer. However, in the normal biological situation, an enzyme called uroporphyrinogen cosynthetase ensures that there is a rearrangement during the cyclisation to give the Type 3 isomer. Porphyrinogens may be considered as pyrrole rings joined by four CH_2 bridges. They are colourless and not photoactive, because the conjugation does not extend around the macrocyclic ring. Further modification of the side chains is then carried out to convert uroporphyrinogen to coproporphyrinogen and then to protoporphyrinogen. At this point, the side chains are those which are seen in the final product haem. However, the oxidation state of the molecule is still at the level of the porphyrinogen and the molecule is colourless and not photoactive. At this point, under the action of the enzyme protoporphyrinogen oxidase,

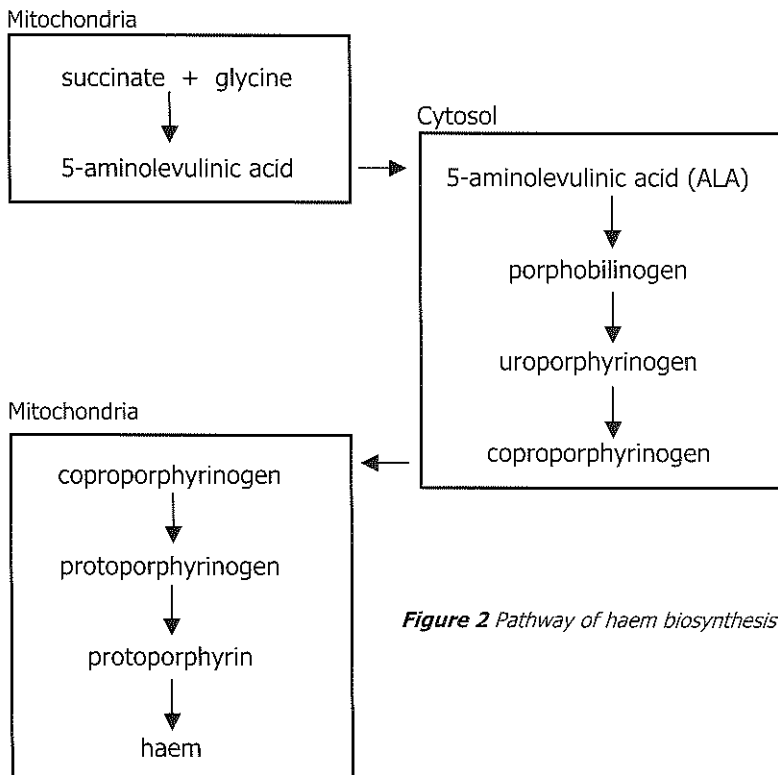


Figure 2 Pathway of haem biosynthesis.

four oxidation steps occur which result in the formation of protoporphyrin IX (PpIX, the IX refers to the particular isomer which is formed based on the order of the side chains, figure 3). Because there is now complete delocalisation of electrons around the macrocyclic ring, protoporphyrin is highly coloured and is a highly photoactive molecule. Indeed, it is a very efficient photosensitiser. The final step in the synthesis involves the insertion of an iron atom into the protoporphyrin ring to make haem. Although haem remains highly coloured because of the delocalisation, it is not a photosensitiser itself because of the presence of the iron atom. Thus the biosynthesis of haem involves the transient formation of a very powerful photosensitiser, PpIX.

This whole process is normally under very tight enzymatic control and there is a strong feed-back control mechanism of haem on ALA synthetase. There exists a group of diseases known as the porphyrias in which one of the enzymes of the pathway is genetically deficient and this can lead to a range of clinical problems. In one particular porphyria, known as erythropoietic protoporphyria, there is a defect in ferrochelatase, the enzyme responsible for inserting iron into PpIX. This leads to a build-up of PpIX in red cells and in other tissues and this can lead to photosensitivity in sufferers.

In ALA photodynamic therapy, an excess exogenous dose of ALA is given to a patient. This dose of ALA temporarily overloads the porphyrin pathway and creates a build-up of PpIX. If this build-up occurs in the target tissue and light is applied at the appropriate time, then a very powerful PDT effect can occur. This is the principle of photodynamic therapy using ALA.

Mechanism of ALA-based PDT

Several factors are involved in the achievement of selectivity of therapy by PDT. Since it is a local technique, clearly a major factor is the ability to direct light precisely to the lesion which is being treated. For the skin, this is usually a relatively easy process but even for internal treatments using ALA (for example in the bladder or in the uterus) this is now a relatively routine procedure because of major advances in lasers and fibre optic

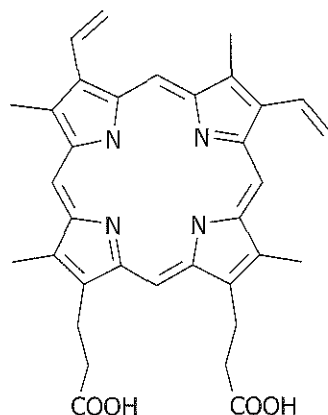


Figure 3 Molecular structure of protoporphyrin IX.

delivery systems in recent years. Detailed consideration of light delivery during PDT is outside the scope of this review.

Selectivity is also determined by preferential accumulation of photosensitiser in the target lesion and, in many cases, ALA is able to induce such localization of the PpIX produced. It should be noted that, whilst increased levels of PpIX in target tissue over surrounding normal tissue is highly desirable for ALA therapy, it is absolutely essential for ALA-based photodiagnosis, which depends upon the observation of increased fluorescence in the lesion compared with the surrounding normal tissue.

The reasons why tumours such as basal cell carcinoma (BCC) in the skin and carcinoma *in situ* in the bladder produce more PpIX than the surrounding normal tissue are not fully understood, though the phenomenon is now extremely well documented both in terms of fluorescence imaging (2-8), fluorescence spectroscopy (2,5,8-11), fluorescence microscopy (4,8,12) and in terms of biochemical analysis (13,14). The localization extends to pre-cancerous dysplastic tissues such as cervical intraepithelial neoplasia (CIN) and Barrett's oesophagus as well as to benign proliferative tissue such as the endometrium. Many theories have been advanced to account for this selectivity including the following: i) tumours may contain a lower level of ferrochelatase (the enzyme responsible for inserting iron into PpIX) than surrounding normal tissue, resulting in a greater build-up of the enzyme's substrate, protoporphyrin; ii) tumours may have less readily accessible iron which is also required for the conversion of PpIX into haem; iii) the lower pH of tumours may result in more PpIX formation; iv) the permeability properties of the skin or epithelium overlying the tumour or lesion are different from the permeability properties of normal skin or epithelium.

Clearly, the reason why tumours and other lesions produce more PpIX must be linked with the reason for which PpIX itself accumulates, rather than other intermediates in the pathway. Whilst it is tempting to use the simple argument that PpIX accumulates because the next enzyme in the pathway, ferrochelatase, is limiting, it is now clear that this represents an oversimplification of the true picture. First, it is possible that other intermediates in the pathway before protoporphyrin do indeed accumulate but that they may be readily removed and only PpIX remains. Alternatively, the immediate precursor of PpIX, protoporphyrinogen IX, may accumulate and may be non-enzymatically oxidized to PpIX. Here, intracellular compartmentation is important, because protoporphyrinogen IX may be released into the cytoplasm. It may be oxidized there to PpIX non-enzymatically, or it may be released into the extracellular compartments and oxidized there to PpIX. In the former case, PpIX may accumulate in subcellular compartments outside of the mitochondria which is its normal organelle of synthesis. A fluorescence microscopy study upon co-incubating cells with ALA and rhodamine 123 (a fluorescent mitochondrial probe), indicated that PpIX is located in the mitochondria (15). Whilst some of these considerations may not be directly relevant to therapy or to

photodetection, they do illustrate the complexity of this apparently simple system and warn against oversimplification.

ALA-based PDT in the skin

Introduction to skin and skin lesions

Healthy human skin consists of a stratified, cellular epidermis and an underlying dermis of connective tissue. The dermis, situated between the epidermis and the subcutaneous fat layer, is a supporting matrix that consists of linked polysaccharides and proteins (mainly collagen and elastin). It supplies nutrition to the epidermis and the cutaneous appendages and is a protective layer for the body against mechanical injury. The epidermis is largely composed of keratinocytes, which are formed by dividing cells in the basal layer of the epidermis, adjacent to the dermo-epidermal junction. The keratinocytes move outwards while differentiating progressively to give several distinguishable layers. They eventually form the stratum corneum, a layer of cells without nucleus and other organelles. These so-called corneocytes, mainly contain keratin and are embedded in a lipid matrix. The rate of keratinocyte production and differentiation (epidermopoiesis) is regulated by a balance between stimulatory and inhibitory signals. Among the stimulating factors are interleukines and other cytokines, and growth factors, such as the epidermal growth factor, transforming growth factor α and fibroblast growth factors. Transforming growth factor β , peptides called chalone, interferons and tumour necrosis factor have a negative feedback on the epidermal growth. One can understand that any disruption in the complex balances or cascades can result in diseases of the skin. We will focus on skin diseases which are currently treated (in clinical trials) with ALA-PDT.

General approach to PDT in the skin

In terms of numbers of lesions treated, there has been more PDT application to the skin than to any other organ. In part this is due to the accessibility of the skin and the fact that cheap, non-laser light sources appear to be as effective as lasers. However, it is also due to the good results obtained, especially the excellent cosmesis as will be seen below. The great majority of skin lesions treated by PDT are non-life threatening – as yet there has been little attempt to treat malignant melanoma. For this reason, there has been a reluctance to use systemic photo-sensitisers, especially if they cause prolonged photosensitivity. This has led to a preference for topical agents, but it has proved extremely difficult to develop topical preparations of most of the photosensitisers which are in use systemically. It is in this arena that ALA makes its major contribution to dermatology, because topical preparations of ALA have been highly successful in inducing photosensitization of target lesions. This was first demonstrated by the pioneering work of Kennedy and Pottier (1) who used typically 20% ALA in an oil-in-water emulsion. Clinical PDT with topical ALA has now become extremely simple

and cheap. First, ALA contained in a cream or other vehicle is spread across the lesion and over a margin of healthy tissue. In some protocols, the skin may be tape stripped or otherwise disrupted to aid penetration. The ALA is left in place for a period of 3 to 4 hours depending upon the particular protocol. During this time, the patient feels no discomfort and the ALA penetrates into the lesion and is metabolised into PpIX. At this time, light is applied in a pre-determined dose, typically for a period of between 10 and 20 minutes. During this phase, the patient may feel effects ranging from discomfort to acute pain and analgesia may be necessary. The treatment is then complete. For some indications (e.g. for Bowen's disease) one treatment is usually sufficient but in other cases (such as in some protocols for BCC) a repeat treatment may be necessary.

The precise mechanism causing the pain during ALA-PDT is not been fully understood. The generally accepted theory is that ALA is taken up in nerve endings and converted to PpIX, which leads to pain when light is applied. Certainly the evidence is that the pain is closely synchronized with the light i.e. the pain begins when the light is switched on and quickly disappears when the light is removed and begins again when the light is reapplied.

ALA-PDT for Bowen's disease

Bowen's disease, actinic keratosis and BCC belong to the group of epidermal non-melanoma (pre)malignancies. Bowen's disease (squamous carcinoma *in situ*) is a premalignant condition located in the epidermis and is characterized as an erythematous, non-elevated scaly or crusted plaque. Atypical squamous cells and individually keratinising cells are present throughout the epidermis, which shows hyperkeratosis, parakeratosis and acanthosis. The atypia and proliferation is limited to the epidermis because of the intact dermo-epidermal junction. The disease can develop into squamous cell carcinoma by invasion into the dermis. Conventional treatments are surgical excision, cryotherapy, laser ablation or topical 5-fluorouracil.

There are now many studies which show that ALA-based PDT can be extremely effective in the treatment of Bowen's disease. The approach is particularly well suited to treatment of the large lesions which sometimes occur in this condition because of the excellent healing which is achieved. Achievement of more than 90% complete response, without recurrence, is now relatively routine for PDT of this condition. Early work carried out by Kennedy (1) and subsequently in Leeds (16,17), Lund (18) and elsewhere (19-22) clearly showed the efficacy of the approach. The treatment is very simple and may be carried out in an outpatient clinic or even in a general practitioner's surgery. Although the formulations in different studies have varied, a 20% preparation of ALA has been typically used. A single treatment is sufficient to cure the Bowen's disease in more than 90% of cases. The only side effect is local pain as described above.

One of the best studies of Bowen's disease has been a clinical trial randomising lesions

to treatment either with cryotherapy or with PDT (19). Cryotherapy produced clearance in 10 of 20 lesions with one treatment, the remaining lesions requiring one or more additional treatments. PDT resulted in the clearance of 15 of 20 lesions with one treatment and all the remaining 5 lesions after a second treatment. The probability that a lesion would be cleared with one treatment was significantly greater with PDT than with cryotherapy. The study also showed that PDT was better for treatment of larger lesions. Finally, the study demonstrated that after 12 months, visible scarring was absent for the PDT-treated lesions, but present in some of the cryotherapy-treated lesions. This excellent healing has come to be accepted as a characteristic benefit of ALA-PDT.

ALA-PDT for basal cell carcinoma

Basal cell carcinoma is a tumour and the lesions are characterized as small, waxy, (semi)translucent raised areas around a central depression which may be ulcerated, crusted and bleeding. Often, the nodules are covered by a thin epidermis through which superficial blood vessels are visible. BCC is generally considered to arise from immature pluripotent cells of the epidermis. Different types of BCC occur with different clinical course and histopathological appearances. Commonly used treatments are surgical and nonsurgical, including Moh's microsurgery, cryosurgery, electrosurgery, curettage, radiotherapy and topical 5-fluorouracil.

ALA-PDT has been applied to the treatment of BCCs in a similar fashion as for Bowen's disease. However, whilst Bowen's is always relatively superficial, BCCs may be nodular or invasive. Not surprisingly therefore, the results achieved with ALA-PDT have depended very much upon the nature of the lesion being treated. For the superficial BCCs, initial data suggested a complete response rate similar to that of Bowen's disease (18,23-27). However, some studies with long follow-up showed a significant recurrence rate, typically up to 50% following a single treatment (17,21,25). Further studies in our laboratory suggested that the failure rate was not due to poor light penetration and was likely caused by poor penetration of the ALA into the deeper parts of the lesion. However, more recent studies have demonstrated that much better results with BCCs may be obtained with repeat treatments (new drug and light) at intervals varying from two days to one week (20-22). Responses of nodular BCCs to ALA-PDT have been much less (18,20,21), probably due to the poor penetration of ALA into the deeper layers of the nodular BCCs (13,28,29). Whether ALA-PDT can compete with alternative therapies if it requires repetition for complete response is an important question. Clearly, there would be major advantages if the technique could be improved with only a single treatment, to give results comparable with alternative therapies.

ALA-PDT for actinic keratosis

Actinic or solar keratosis is found in chronically sun-exposed skin areas. The lesions are small, usually multiple and manifest as rough, scaly, erythematous patches. The

epidermal changes are hyperkeratosis, parakeratosis, dyskeratosis, acanthosis and keratinocyte atypia. Dermatology handbooks describe actinic keratosis as a premalignant condition that can progress into an invasive squamous cell carcinoma. However, other authors state that actinic keratosis is in fact non-invasive squamous cell carcinoma, which has a chance to become invasive (30,31). Approximately 1% of the lesions convert to squamous cell carcinoma. Established treatments are cryotherapy, topical 5-fluorouracil and dermabrasion.

Treatment of actinic keratoses with ALA-PDT has been successful in a number of studies (20,21,23,32). Indeed, this is the lead indication for DUSA Pharmaceuticals with their proprietary product Levulan® (ALA) which has recently been approved by the FDA. So far, this is the only approved use of ALA. In 1997, DUSA completed two Phase III studies using Levulan®-PDT for actinic keratoses at a total of 16 centres across the USA with over 1500 lesions treated in 243 patients. Treatment was either with a 20% Levulan® topical solution or a placebo vehicle, using blue light, which penetrates less than red light. Patients whose lesions did not clear completely were retreated after 8 weeks. In one of the studies (117 patients) after a single treatment with Levulan®-PDT, 86% of the actinic keratoses responded completely, with 94% clearing after two treatments. In contrast, after two treatments, only 32% of lesions cleared when treated with placebo and light. In the other study (126 patients), after a single treatment 81% of the lesions gave a complete response with 90% clearing after two treatments, whereas after two treatments with placebo, only 20% cleared. All of these results were highly significant statistically. As expected, a well-tolerated burning or stinging discomfort was experienced during light exposure, but there were no other treatment-related side effects and no systemic photosensitivity. Cosmetic responses were rated by both patients and doctors as good to excellent. 85% of patients said that they would prefer Levulan® PDT if they had to be treated again in the future.

ALA-PDT for psoriasis

Psoriasis is a chronic, recurrent, inflammatory and proliferative disease of the skin and it is characterized by round erythematous, red, dry, scaly plaques. The cause is still unknown, but heredity is of significance in some cases. The psoriatic lesions are the result of increased keratin production by the keratinocytes caused by abnormal differentiation and hyperproliferation of the keratinocytes as a response to inflammation. It is not clear whether the increased rate of epidermopoiesis or the increased amount of keratinocytes in the epidermopoiesis process is the basic fault in psoriasis. Established treatment methods are either topical treatment with corticosteroids, tars, dihydroxy-anthralin, tazarotene, vitamin D analogues, salicylic acid, or phototherapy with UV-B irradiation or PUVA (psoralen + UV-A irradiation), or systemic treatment with corticosteroids, methotrexate, cyclosporine, retinoids or hydroxyurea, or surgery, or laser clearance of the dermis. Sometimes a combination of above treatments is employed.

ALA-PDT is potentially a good option for psoriasis, because it can treat large areas, the healing is excellent and there are no long-term effects as is the case with PUVA therapy. A number of groups, including our own, have attempted to exploit this potential (33-38). Overall, the results have been disappointing so far. The responses have been variable and the reasons for this are not understood. Certainly adequate levels of PpIX are achieved in at least some of the plaque, but this may not be uniform throughout the lesion. In an attempt to improve response, multiple treatments, up to three times per week, were performed in one study (36). Although clinical efficacy did improve with multiple treatments, unpredictable response and patient discomfort during treatment led to the conclusion that ALA-PDT did not offer advantages over other therapies.

Other photosensitisers may be more suited to treatment of psoriasis. For example, in one study both ALA and methylene blue used topically, gave responses comparable with treatment by dithranol, but methylene blue did not induce the patient discomfort seen with ALA (33). Also, it may be that derivatives of ALA, such as the esters (see below) may be more effective. Finally, it is possible that treatment of psoriasis using a systemic sensitiser may be more successful. A photosensitiser which does not cause skin photosensitivity would be essential and there is evidence that PDT using verteporfin (benzoporphyrin derivative) has potential in this regard (39).

ALA-PDT for acne

Acne vulgaris is a chronic inflammatory disease of the sebaceous glands, resulting in comedos (blackheads), papules, pustules, cysts, nodules and often scars. It is a follicular disease and the comedo formation is caused by keratinous plugs (tightly packed horny cells) in the hair follicles, which fail to be properly discharged from the follicular opening. The formation of inflammatory papules, pustules, cysts and nodules is caused by follicular contents that are discharged into the dermis, permitted by a disrupted follicular epithelium. Another important factor in the formation of papules and pustules is the production of free fatty acids, which induce inflammation, by *Propionibacterium acnes*. Common treatments are either systemic with antibacterials, hormones, spironolactone, dexamethasone, prednisone or isotretinoin, or topical with benzoyl peroxide, retinoids or antibacterials, or use of an abrasive cleanser, or surgery.

The use of ALA-PDT for treatment of acne has been discussed for a number of years, but there are relatively few studies (40,41). There are, however, sound reasons for believing that ALA-PDT will be helpful in this condition. A very recent study by Anderson and co-workers (40) concluded that potentially, ALA plus red light might be useful for some patients with acne. This was based on a study of 22 subjects, each of which was treated in four sites on the back with ALA plus red light, ALA alone, light alone and untreated control. Sebum excretion was eliminated for several weeks and decreased for 20 weeks following PDT with clinical and statistical clearance of inflammatory acne. DUSA Pharmaceuticals are currently beginning a trial to test a non-laser, blue light

source in the treatment of acne.

Other dermatological conditions

A number of other conditions have been treated with ALA-PDT. These include T-cell lymphoma in which a partial response was observed (18) and erythroplasia of Queyrat. However the number of cases is very small and it is not possible at present to make any judgment on the effectiveness of ALA-PDT in these indications.

Improving ALA-based PDT of skin lesions

Problems with topical ALA application

Like other small molecules, ALA can penetrate through skin (42) and into superficial skin tumours and other skin diseases upon topical application. However, high doses of ALA (20% w/w is a standard concentration for a topical formulation) have to be applied in order to achieve sufficiently high PpIX levels in superficial BCC (13,17,29). Fluorescence microscopy studies have shown that there is no or little (inhomogeneous) PpIX fluorescence in the deeper layers of nodular BCC after topical application (3-4 hours) of ALA (13,28,29). Thus, the bioavailability of PpIX is low in deeper layers of the skin (lesions), largely due to poor penetration of ALA into the skin. One reason for the poor penetration of ALA into the skin (and cells) is the fact that ALA is a hydrophilic molecule and at physiological pH a zwitter ion. Hydrophilic and charged compounds poorly penetrate lipophilic barriers, such as cellular membranes and the stratum corneum. In addition, the penetration of compounds is limited by the structure of the skin itself. The stratum corneum, the outermost layer of the epidermis, is the main barrier against the external environment (43-45). This barrier function is attributed to the structure of the stratum corneum, which is often described as a "brick and mortar" structure (43-46). The stratum corneum consists of several layers of dead cells (corneocytes, mainly containing keratin) that are embedded in a lipid matrix. The diffusion of drugs into and through the epidermis is believed to be passive (43,44), mainly across the epidermis and little via the skin appendages (hair follicles and sweat glands). The rate determining step in the epidermal route is the diffusion across the stratum corneum. The diffusion pathway through the stratum corneum can be transcellular (across the corneocytes and the intercellular lipids) or intercellular (via the lipid matrix between the corneocytes). The latter route is believed to be the principal route and thus the major barrier for drug permeation (43,44). Results from animal studies indicate that diffusion of ALA across the stratum corneum is an important limiting factor for ALA penetration into normal skin (47,48).

Penetration enhancement

PDT effects in normal skin of hairless guinea pigs were increased when the thickness of

the stratum corneum was reduced by tape stripping before ALA application (47) and more PpIX was produced in normal nude mouse skin when the stratum corneum was removed by tape stripping the skin prior to ALA application (48).

Besides tape stripping, several other methods to increase ALA penetration into skin and skin lesions have been applied successfully or are presently under investigation. Iontophoretic ALA delivery to normal human skin resulted in increased PpIX fluorescence and PDT effects (49). ALA delivery across the stratum corneum is fast and the amount of ALA in the skin can be increased with increasing charge. Furthermore, the use of ultrasound during ALA application enhances PpIX production in the skin (50). The use of penetration enhancers prior to or during ALA application increases the ALA penetration into the skin. Penetration enhancers are chemicals that improve the permeation properties of the stratum corneum, either by creating disorder in the alkyl chains of the lipids or by altering the solubility characteristics of the lipids. Dimethylsulphoxide (DMSO) has proven to increase PpIX fluorescence in deeper layers of nodular BCC (29) and has been used as a penetration enhancer in several clinical studies with ALA-PDT of BCC (22,24,51). However, one should keep in mind that DMSO is also a potentiator of haem biosynthesis (52-55). ALA- and ALA hexyl ester-induced PpIX production in nude mouse skin was increased by another penetration enhancer, an azacycloalkane derivative (48). Reducing the tumour volume of BCC by curettage of the lesions prior to ALA application has also been used in some clinical studies on ALA-PDT of BCC (51,56,57). The effect of temperature on ALA penetration and PpIX production in cells and skin has also been investigated (11,58,59). *In vitro* ALA uptake into cells is increased when ALA incubation takes place at higher temperatures (59). Higher PpIX fluorescence levels were measured in nude mouse skin (11) and the skin of three healthy volunteers (58) when the skin temperature was increased after, but not during a short-term (10 or 15 minutes) topical ALA application. In the skin of the healthy volunteers, PpIX production could also be increased when the skin was kept at a higher temperature during a 5 to 6 hours topical application of ALA (58). The authors from these two studies therefore concluded that mainly the PpIX production, and not the ALA penetration into the skin, is temperature dependent. However, this is contradictory with the *in vitro* results (59), and therefore more research into this is needed.

ALA esters and other derivatives

ALA prodrugs have been synthesized in order to overcome the limited penetration of ALA into the skin, which is (partly) caused by the hydrophilic and zwitter ionic characteristics of ALA. A prodrug is a chemically inactive derivative of the biologically

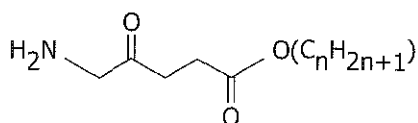


Figure 4 Molecular structure of 5-aminolevulinic acid alkyl esters.

active compound, but is, after administration, converted to the active compound. The most common prodrug linkage is a covalent ester bond (figure 4) which is enzymatically cleaved by intracellular esterases (60). The lipophilicity of ALA can be increased by esterifying the carboxyl group and this higher lipophilicity might then increase the penetration depth, distribution and uptake. Several ALA derivatives, i.e. esters and amide derivatives have been synthesized and tested *in vitro* (61-66), *ex vivo* (67,68), *in vivo* (8,48,63,69,70) and in patients (71).

Several (but not all) ALA esters increased the PpIX production in different cell lines (61-64,66), with the long-chained esters being more efficient than the shorter ones (61,64,66). Some short-chained ALA esters did not increase the PpIX production in cells, dependent on the cell line used in the different studies. ALA methyl ester induced lower PpIX production in all cell lines used (61,63-66), whereas the ethyl ester (64,66) and the propyl ester (66) induced lower PpIX production in some of the cell lines. The differences between ALA and the ALA esters might be explained by the fact that ALA, but not ALA esters, is transported by β -amino acid and γ -aminobutyric acid carriers (59). In a study where *ex vivo* human and rat skin explant cultures were incubated with ALA or ALA esters in the medium, ALA hexyl ester was the only one that increased PpIX production (68). However, in this set-up, ALA and its derivatives are absorbed from the medium through the dermis to reach the epidermis, thus resembling rather systemic than topical administration of the compounds to the skin. After topical application of ALA or esters to *ex vivo* pig skin, there was no difference between ALA and the esters with regard to the amount of PpIX produced in the epidermis. However, in accordance with the previous *in vitro* studies (61-64,66), incubation of freshly isolated pig skin keratinocytes (from the epidermis) with ALA or esters showed that these keratinocytes produce more PpIX when incubated with ALA esters, compared to ALA (personal communication G.M.J. Beijersbergen van Henegouwen).

In vivo PpIX levels in the epidermis and hair follicles of normal nude mouse skin were higher after long-term application (14 hours) of ALA methyl, ethyl or propyl ester than after 14 hours ALA application (69). After 1 or 3.5 hours application, the PpIX levels were similar for ALA and these three short-chained esters.

ALA hexyl ester-induced PpIX fluorescence levels are only slightly higher (compared to ALA) in the normal nude mouse skin during long-term (24 hours) application (48). However, ALA-induced PpIX fluorescence was higher than ALA hexyl ester-induced PpIX fluorescence after short application times (1 to 60 minutes) with a 20% cream and after a 10 minutes application with creams containing 0.5 to 40% ALA (hexyl ester). Removing the stratum corneum by tape stripping the skin prior to application or the use of a penetration enhancer increased the ALA hexyl ester-induced PpIX production more than the ALA-induced PpIX production. Therefore, the results from this study indicate that the stratum corneum is an important barrier for the penetration of both ALA and

ALA hexyl ester into the skin, but to a higher extent for ALA hexyl ester.

In an *in vivo* PpIX fluorescence kinetics study after 30 minutes topical application of ALA and ALA pentyl ester to the back skin of hairless mice with and without UV-B induced (pre)cancerous lesions, it was shown that ALA pentyl ester induced slightly more *in vivo* PpIX fluorescence in the (pre)cancerous lesions, but not in the skin without (pre)cancerous lesions (8). However, microscopic fluorescence images showed these higher ALA pentyl ester-induced PpIX fluorescence levels were in the stratum corneum, but not in the dysplastic layer of the epidermis in which the ALA and ALA pentyl ester-induced PpIX fluorescence levels were the same. This, together with the fact that the PpIX fluorescence levels were also the same in the deeper layers, indicates that ALA pentyl ester does not penetrate deeper into skin than ALA.

In a study with healthy volunteers, ALA and the butyl and hexyl ester were delivered into the skin iontophoretically (70). Slightly higher PpIX levels were reached earlier with ALA hexyl ester, compared to ALA and ALA butyl ester. Furthermore, they observed a higher phototoxicity with ALA hexyl ester. There was no difference in microscopic PpIX levels and depth between the three compounds, but the ALA hexyl ester- and ALA butyl ester-induced microscopic PpIX fluorescence appeared to be distributed more homogeneously than the ALA-induced PpIX fluorescence.

Therapy using ALA esters

So far, ALA methyl ester is the only ALA ester tested in a clinical study for application to skin disease (71). ALA and ALA methyl ester were applied to patients with actinic keratosis and the PpIX levels in the lesions and surrounding normal skin was measured. The PpIX levels for both compounds were higher in the lesions than the surrounding normal skin, with the maximum PpIX levels in the lesions higher after ALA application than after ALA methyl ester. However, the ratio between PpIX in the lesions and PpIX in the surrounding normal skin was higher with ALA methyl ester. ALA methyl ester is being developed as a proprietary product, Metvix, by PhotoCure, a company based in Oslo. PhotoCure ASA are carrying out several pivotal clinical trials to assess the efficacy of Metvix PDT with red light in comparison to placebo and other treatment modalities in AK and BCC. In a phase II trial in primary BCC (nodular and superficial) Metvix PDT with 3 hours application time in one or two treatment sessions gave an overall complete lesion response rate of 95%. In addition, the same Metvix PDT regimen gave an overall cure rate of 90% of AK lesions in a phase II trial. Moreover, in a phase III study in 202 patients with 699 AK lesions, a single PDT session with Metvix showed similar efficacy, better cosmetic outcome, and high patient preference compared to cryotherapy. Based on these finalized phase II and III studies in AK, PhotoCure ASA have prepared and submitted an application for regulatory approval in Europe, with Sweden as reference country.

Other approaches

Several other approaches to the enhancement of ALA-PDT have been looked at. These include the use of agents to influence the PpIX production or breakdown. Iron chelators, like ethylenediaminetetraacetic acid, hydroxypyridones and desferrioxamine, reduce the intracellular conversion of PpIX into haem. This results in greater and longer accumulation of PpIX in cells (*in vitro*) and *ex vivo* skin explants (68,72-74). Iron chelators have been used in the ALA-PDT treatment of skin lesions in patients with Bowen's disease, actinic keratosis and BCCs (21,22,24). Interrupting the illumination for a long period of time (up to several hours) has also shown to be successful in improving the ALA-PDT in hairless mice with or without precancerous lesions (75). After the first light treatment, new PpIX is formed (5,75) which is then used for the second illumination. New formation of PpIX after ALA-PDT was also found to occur in human superficial (3,9) and nodular (3) BCC. Increased ALA-PDT effect in hairless mouse skin with precancerous lesions could also be achieved by decreasing the irradiance or fluence rate (75-77).

Acknowledgements

We thank Yorkshire Cancer Research for financial support.

References

- Kennedy JC, Pottier RH, Pross DC. Photodynamic therapy with endogenous protoporphyrin IX: basic principles and present clinical experience. *J Photochem Photobiol B* 1990; 6:143-148.
- Wagnières GA, Star WM, Wilson BC. *In vivo* fluorescence spectroscopy and imaging for oncological applications. *Photochem Photobiol* 1998; 68(5):603-632.
- Orenstein A, Kostenich G, Malik Z. The kinetics of protoporphyrin fluorescence during ALA-PDT in human malignant skin tumors. *Cancer Letters* 1997; 120:229-234.
- van der Veen N, de Bruijn HS, Berg RJW, Star WM. Kinetics and localisation of PpIX fluorescence after topical and systemic ALA application, observed in skin and skin tumours of UVB-treated mice. *Br J Cancer* 1996; 73:925-930.
- van der Veen N, de Bruijn HS, Star WM. Photobleaching during and re-appearance after photodynamic therapy of topical ALA-induced fluorescence in UVB-treated mouse skin. *Int J Cancer* 1997; 72:110-118.
- D'Hallewin M-A, Vanherzeele H, Baert L. Fluorescence detection of flat transitional cell carcinoma after intravesical instillation of aminolevulinic acid. *Am J Clin Oncol* 1998; 21(3):223-225.
- Jichlinski P, Forrer M, Mizeret J, Gianzmann T, Braichotte D, Wagnières GA, Zimmer G, Guillou L, Schmidlin F, Graber P, van den Bergh H, Leisinger H-J. Clinical evaluation of a method for detecting superficial transitional cell carcinoma of the bladder by light-induced fluorescence of protoporphyrin IX following topical application of 5-aminolevulinic acid: preliminary results. *Lasers Surg Med* 1997; 20:402-408.
- van den Akker JTHM, de Bruijn HS, Beijersbergen van Henegouwen GMJ, Star WM, Sterenborg HJCM. Protoporphyrin IX fluorescence kinetics and localization after topical application of ALA pentyl ester and ALA on hairless mouse skin with UVB-induced early skin cancer. *Photochem Photobiol* 2000; 72(3):399-406.
- af Klinteberg C, Enejeder AMK, Wang I, Andersson-Engels S, Svanberg S, Svanberg K. Kinetic fluorescence studies of 5-aminolaevulinic acid-induced protoporphyrin IX accumulation in basal cell carcinomas. *J Photochem Photobiol B* 1999; 49:120-128.
- Heil P, Stocker S, Sroka R, Baumgartner R. *In vivo* fluorescence kinetics of porphyrins follo-

- wing intravesical instillation of 5-aminolaevulinic acid in normal and tumour-bearing rat bladders. *J Photochem Photobiol B* 1997; 38:158-163.
11. Juzenas P, Sørensen R, Iani V, Moan J. Uptake of topically applied 5-aminolevulinic acid and production of protoporphyrin IX in normal mouse skin: Dependence on skin temperature. *Photochem Photobiol* 1999; 69(4):478-481.
 12. Roberts DJH, Stables GI, Ash DV, Brown SB. Distribution of protoporphyrin IX in Bowen's disease and basal cell carcinomas treated with topical 5-aminolaevulinic acid. *Proc SPIE* 1995; 2371:490-494.
 13. Szeimies R-M, Sassy T, Landthaler M. Penetration potency of topical applied d-aminolevulinic acid for photodynamic therapy of basal cell carcinoma. *Photochem Photobiol* 1994; 59(1):73-76.
 14. Casas A, Fukuda H, del C. Battle AM. Tissue distribution and kinetics of endogenous porphyrins synthesized after topical application of ALA in different vehicles. *Br J Cancer* 1999; 81(1):13-18.
 15. Rossi FM, Campbell DL, Pottier RH, Kennedy JC, Gudgin Dickson EF. *In vitro* studies on the potential use of 5-aminolaevulinic acid-mediated photodynamic therapy for gynaecological tumours. *Br J Cancer* 1996; 74:881-887.
 16. Stables GI, Stringer MR, Robinson DJ, Ash DV. Large patches of Bowen's disease treated by topical aminolaevulinic acid photodynamic therapy. *Br J Dermatol* 1997; 136:957-960.
 17. Cairnduff F, Stringer MR, Hudson EJ, Ash DV, Brown SB. Superficial photodynamic therapy with topical 5-aminolevulinic acid for superficial primary and secondary skin cancer. *Br J Cancer* 1994; 69:605-608.
 18. Svanberg K, Andersson T, Killander D, Wang I, Stenram U, Andersson-Engels S, Berg R, Johansson J, Svanberg S. Photodynamic therapy of non-melanoma malignant tumours of the skin using topical δ -aminolevulinic acid sensitization and laser irradiation. *Br J Dermatol* 1994; 130:743-751.
 19. Morton CA, Whitehurst C, Moseley H, McColl JH, Moore JV, MacKie RM. Comparison of photodynamic therapy with cryotherapy in the treatment of Bowen's disease. *Br J Dermatol* 1996; 135:766-771.
 20. Calzavara-Pinton PG. Repetitive photodynamic therapy with topical δ -aminolevulinic acid as an appropriate approach to the routine treatment of superficial non-melanoma skin tumours. *J Photochem Photobiol B* 1995; 29:53-57.
 21. Fijan S, Honigsmann H, Ortel B. Photodynamic therapy of epithelial skin tumours using delta-aminolaevulinic acid and desferrioxamine. *Br J Dermatol* 1995; 133:282-288.
 22. Harth Y, Hirshowitz B, Kaplan B. Modified topical photodynamic therapy of superficial skin tumors, utilizing aminolevulinic acid, penetration enhancers, red light, and hyperthermia. *Dermatol Surg* 1998; 24(7):723-726.
 23. Wolf P, Rieger E, Kerl H. Topical photodynamic therapy with endogenous porphyrins after application of 5-aminolevulinic acid. *J Am Acad Dermatol* 1993; 28:17-21.
 24. Soler AM, Angell-Petersen E, Warloe T, Tausjø J, Steen HB, Moan J, Giercksky K-E. Photodynamic therapy of superficial basal cell carcinoma with 5-aminolevulinic acid with dimethylsulfoxide and ethylenediaminetetraacetic acid: A comparison of two light sources. *Photochem Photobiol* 2000; 71(6):724-729.
 25. Fink-Puches R, Soyer HP, Hofer A, Kerl H, Wolf P. Long-term follow-up and histological changes of superficial nonmelanoma skin cancers treated with topical δ -aminolevulinic acid photodynamic therapy. *Arch Dermatol* 1998; 134:821-826.
 26. Fink-Puches R, Wolf P, Kerl H. Photodynamic therapy of superficial basal cell carcinoma by instillation of aminolevulinic acid and irradiation with visible light. *Arch Dermatol* 1997; 133:1494-1495.
 27. Hürlimann AF, Hänggi G, Panizzon RG. Photodynamic therapy of superficial basal cell carcinomas using topical 5-aminolevulinic acid in a nanocolloid lotion. *Dermatology* 1998; 197:248-254.
 28. Martin A, Tope WD, Grevelink JM, Starr JC, Fewkes JL, Flotte TJ, Deutsch TF, Anderson RR. Lack of selectivity of protoporphyrin IX fluorescence for basal cell carcinoma after topical application of 5-aminolevulinic acid: implications for photodynamic treatment. *Arch Dermatol Res* 1995; 287:665-674.
 29. Peng Q, Warloe T, Moan J, Heyerdahl H, Steen HB, Nesland JM, Giercksky K-E. Distribution of 5-aminolevulinic acid-induced porphyrins in nodulo-ulcerative basal cell carcinoma. *Photochem Photobiol* 1995; 62:906-913.
 30. Lober BA, Lober CW. Actinic keratosis is squamous cell carcinoma. *South Med J* 2000; 93(7):650-655.
 31. Cockerell CJ. Histopathology on incipient intraepidermal squamous cell carcinoma ("actinic keratosis"). *J Am Acad Dermatol* 2000; 42(1):s11-s17.
 32. Jeffes EW, McCullough JL, Weinstein GD,

- Fergin PE, Nelson JS, Shull TF, Simpson KR, Bukaty LM, Hoffman WL, Fong NL. Photodynamic therapy of actinic keratosis with topical 5-aminolevulinic acid. *Arch Dermatol* 1997; 133:727-732.
33. Schick E, Rück A, Boehncke W-H, Kaufmann R. Topical photodynamic therapy using methylene blue and 5-aminolevulinic acid in psoriasis. *J Dermatol Treatment* 1997; 8:17-19.
34. Stringer MR, Collins P, Robinson DJ, Stables GI, Sheehan-Dare RA. The accumulation of protoporphyrin IX in plaque psoriasis after topical application of 5-aminolevulinic acid indicates a potential for superficial photodynamic therapy. *J Invest Dermatol* 1996; 107:76-81.
35. Boehncke W-H, Sterry W, Kaufmann R. Treatment of psoriasis by topical photodynamic therapy with polychromatic light. *Lancet* 1994; 343:801.
36. Robinson DJ, Collins P, Stringer MR, Vernon DI, Stables GI, Brown SB, Sheehan-Dare RA. Improved response of plaque psoriasis after multiple treatments with topical 5-aminolevulinic acid photodynamic therapy. *Acta Derm Venereol* 1999; 79:451-455.
37. Collins P, Robinson DJ, Stringer MR, Stables GI, Sheehan-Dare RA. The variable response of plaque psoriasis after a single treatment with topical 5-aminolevulinic acid and photodynamic therapy. *Br J Dermatol* 1997; 137:743-749.
38. Stringer MR, Robinson DJ, Collins P. The establishment of treatment parameters for ALA-PDT of plaque psoriasis. *Proc SPIE* 1996; 2924:314-318.
39. Boehncke W-H, Elshorst-Schmidt T, Kaufmann R. Systemic photodynamic therapy is a safe and effective treatment for psoriasis. *Arch Dermatol* 2000; 136:271-272.
40. Hongcharu W, Taylor CR, Chang Y, Aghassi D, Suthamjarai K, Anderson RR. Topical ALA-photodynamic therapy for the treatment of acne vulgaris. *J Invest Dermatol* 2000; 115:183-192.
41. Itoh Y, Ninomiya Y, Tajima S, Ishibashi A. Photodynamic therapy for acne vulgaris with topical 5-aminolevulinic acid. *Arch Dermatol* 2000; 136:1093-1095.
42. De Rosa FS, Marchetti JM, Thomazini JA, Tedesco AC, Bentley MVLB. A vehicle for photodynamic therapy of skin cancer: influence of dimethylsulphoxide on 5-aminolevulinic acid *in vitro* cutaneous permeation and *in vivo* protoporphyrin IX accumulation determined by confocal microscopy. *J Control Rel* 2000; 65:359-366.
43. Williams AC, Barry BW. Skin absorption enhancers. *Crit Rev Ther Drug Carrier Syst* 1992; 9(3,4):305-353.
44. Suhonen TM, Bouwstra JA, Urtti A. Chemical enhancement of percutaneous absorption in relation to stratum corneum structural alterations. *J Controlled Release* 1999; 59:149-161.
45. Landmann L. The epidermal permeability barrier. *Anat Embryol* 1988; 178:1-13.
46. Menton DN, Eisen AZ. Structure and organisation of mammalian stratum corneum. *J Ultrastruct Res* 1971; 35:247-264.
47. Goff BA, Bachor R, Kollias N, Hasan T. Effects of photodynamic therapy with topical application of 5-aminolevulinic acid on normal skin of hairless guinea pigs. *J Photochem Photobiol B* 1992; 15:239-251.
48. van den Akker JTHM, Iani V, Star WM, Sterenberg HJCM, Moan J. Topical application of 5-aminolevulinic acid hexyl ester and 5-aminolevulinic acid to normal nude mouse skin: Differences in protoporphyrin IX fluorescence kinetics and the role of the stratum corneum. *Photochem Photobiol* 2000; 72(5):681-689.
49. Rhodes LE, Tsoukas MM, Anderson RR, Kollias N. Iontophoretic delivery of ALA provides a quantitative model for ALA pharmacokinetics and PpIX phototoxicity in human skin. *J Invest Dermatol* 1997; 108(1):87-91.
50. Ma L-W, Moan J, Peng Q, Iani V. Production of protoporphyrin IX induced by 5-aminolevulinic acid in transplanted human colon adenocarcinoma of nude mice can be increased by ultrasound. *Int J Cancer* 1998; 78:464-469.
51. Soler AM, Warloe T, Tausjø J, Berner A. Photodynamic therapy by topical aminolevulinic acid, dimethylsulphoxide and curettage in nodular basal cell carcinoma: A one-year follow-up study. *Acta Derm Venereol* 1999; 79:204-206.
52. Malik Z, Kostenich G, Roitman L, Ehrenberg B, Orenstein A. Topical application of 5-aminolevulinic acid, DMSO and EDTA: protoporphyrin IX accumulation in skin and tumours of mice. *Photochem Photobiol* 1995; 28:213-218.
53. Malik Z, Djaldetti M. 5-Aminolevulinic acid stimulation of porphyrin and hemoglobin synthesis by uninduced Friend erythroleukemic cells. *Cell Differentiation* 1979; 8:223-233.
54. Conder L, Woodard SI, Dailey HA. Multiple mechanisms for the regulation of haem synthesis during erythroid cell differentiation. Possible role for coproporphyrinogen oxidase. *Biochem J* 1991; 275:321-326.
55. Marks PA, Rifkind RA. Erythroleukemic differentiation. *Ann Rev Biochem* 1978; 47:419-448.

56. Itoh Y, Henta T, Ninomiya Y, Tajima S, Ishibashi A. Repeated 5-aminolevulinic acid-based photodynamic therapy following electro-curettage for pigmented basal cell carcinoma. *J Dermatol* 2000; 27:10-15.
57. Thissen MRTM, Schroeter CA, Neumann HAM. Photodynamic therapy with delta-aminolaevulinic acid for nodular basal cell carcinoma using a prior debulking technique. *Br J Dermatol* 2000; 142:338-339.
58. Moan J, Berg K, Gadmar ØB, Iani V, Ma L-W, Juzenas P. The temperature dependence of protoporphyrin IX production in cells and tissues. *Photochem Photobiol* 1999; 70(4):669-673.
59. Rud E, Gederaas O, Hogset A, Berg K. 5-Aminolevulinic acid, but not 5-aminolevulinic acid esters, is transported into adenocarcinoma cells by system BETA transporters. *Photochem Photobiol* 2000; 71(5):640-647.
60. Waller DG, George CF. Prodrugs. *Br J Clin Pharmacol* 1989; 28:497-507.
61. Kloek J, Akkermans W, Beijersbergen van Henegouwen GMJ. Derivatives of 5-aminolevulinic acid for photodynamic therapy: enzymatic conversion into protoporphyrin. *Photochem Photobiol* 1998; 67(1):150-154.
62. Eléout S, Rousset N, Carre J, Bourre L, Vonarx V, Lajat Y, Beijersbergen van Henegouwen GMJ, Patrice T. *In vitro* fluorescence, toxicity and phototoxicity induced by δ-aminolevulinic acid (ALA) or ALA esters. *Photochem Photobiol* 2000; 71(4):447-454.
63. Kloek J, Beijersbergen van Henegouwen GMJ. Prodrugs of 5-aminolevulinic acid for photodynamic therapy. *Photochem Photobiol* 1996; 64(6):994-1000.
64. Ühlinger P, Zellweger M, Wagnières GA, Juillerat-Jeanneret L, van den Bergh H, Lange N. 5-Aminolevulinic acid and its derivatives: physical chemical properties and protoporphyrin IX formation in cultured cells. *J Photochem Photobiol B* 2000; 54:72-80.
65. Washbrook R, Riley PA. Comparison of δ-aminolaevulinic acid and its methyl ester as an inducer of porphyrin synthesis in cultured cells. *Br J Cancer* 1997; 75(10):1417-1420.
66. Gaullier J-M, Berg K, Peng Q, Anholt H, Selbo PK, Ma L-W, Moan J. Use of 5-aminolevulinic acid esters to improve photodynamic therapy on cells in culture. *Cancer Res* 1997; 57:1481-1486.
67. Marti A, Lange N, van den Bergh H, Sedmera D, Jichlinski P, Kucera P. Optimisation of the formation and distribution of protoporphyrin IX in the urothelium: an *in vitro* approach. *J Urol* 1999; 162:546-552.
68. Casas A, del C.Battle AM, Butler AR, Robertson D, Brown EH, MacRobert A, Riley PA. Comparative effect of ALA derivatives on protoporphyrin IX production in human and rat skin organ cultures. *Br J Cancer* 1999; 80(10):1525-1532.
69. Peng Q, Moan J, Warloe T, Iani V, Steen HB, Bjorseth A, Nesland JM. Build-up of esterified aminolevulinic-acid-derivative-induced porphyrin fluorescence in normal mouse skin. *J Photochem Photobiol B* 1996; 34:95-96.
70. Gerscher S, Connelly JP, Griffiths J, Brown SB, MacRobert AJ, Wong G, Rhodes LE. Comparison of the pharmacokinetics and phototoxicity of protoporphyrin IX metabolized from 5-aminolevulinic acid and two derivatives in human skin *in vivo*. *Photochem Photobiol* 2000; 72(4):569-574.
71. Fritsch C, Homey B, Stahl W, Lehmann P, Ruzicka T, Sies H. Preferential relative porphyrin enrichment in solar keratoses upon topical application of δ-aminolevulinic acid methylester. *Photochem Photobiol* 1998; 68(2):218-221.
72. Bech Ø, Phillips D, Moan J, MacRobert AJ. A hydroxypyridinone (CP94) enhances protoporphyrin IX formation in 5-aminolaevulinic acid treated cells. *J Photochem Photobiol B* 1997; 41:136-144.
73. Tan WC, Krasner N, O'Toole P, Lombard M. Enhancement of photodynamic therapy in gastric cancer cells by removal of iron. *Gut* 1997; 41(1):14-18.
74. Berg K, Anholt H, Bech Ø, Moan J. The influence of iron chelators on the accumulation of protoporphyrin IX in 5-aminolevulinic acid-treated cells. *Br J Cancer* 1996; 74(5):688-697.
75. van der Veen N, Hebeda KM, de Bruijn HS, Star WM. Photodynamic effectiveness and vasoconstriction in hairless mouse skin after topical 5-aminolevulinic acid and single- or two-fold illumination. *Photochem Photobiol* 1999; 70(6):921-929.
76. Robinson DJ, de Bruijn HS, van der Veen N, Stringer MR, Brown SB, Star WM. Fluorescence photobleaching of ALA-induced protoporphyrin IX during photodynamic therapy of normal hairless mouse skin: the effect of light dose and irradiance and the resulting biological effects. *Photochem Photobiol* 1998; 67(1):140-149.
77. Robinson DJ, de Bruijn HS, van der Veen N, Stringer MR, Brown SB, Star WM. Protoporphyrin IX fluorescence photobleaching during ALA-mediated photodynamic therapy of UVB-induced tumors in hairless mouse skin. *Photochem Photobiol* 1999; 69(1):61-71.

CHAPTER 3

Localisation and accumulation of a new carotenoporphyrin in two primary tumour models

This chapter has been adapted from JTHM van den Akker, OC Speelman, HJ van Staveren, AL Moore, TA Moore, D Gust, WM Star and HJCM Sterenborg.
J Photochem Photobiol B 2000; 54:108-115.

Summary

We investigated the tumour localising properties and *in vivo* fluorescence kinetics of a hexamethoxylated carotenoporphyrin (CP6) in two primary tumour models: UVB-induced early skin cancer in hairless mice and chemically induced mucosal dysplasia in the rat palate. CP6 fluorescence kinetics were investigated by measuring *in vivo* fluorescence spectra and images of the mouse skin and the rat palate at different time points after injection. For the tumour localising properties, microscopic phase contrast and fluorescence images were recorded. The *in vivo* fluorescence kinetics in the mouse skin showed localisation of CP6 in the tumours. However, fluorescence microscopy images showed that CP6 localises in the dermis and structures that are not related to the malignant transformation of the mouse skin. The fluorescence kinetics in the rat palate showed a significant correlation between the degree of malignancy and the CP6 fluorescence build-up time in the palate. The microscopic images showed that CP6 fluorescence localises in the connective tissue and not in the dysplastic epithelium. In conclusion, CP6 does not localise preferentially in (pre-)cancerous tissue in the two primary tumour models studied here, in contrast to reports about localisation of carotenoporphyrins in transplanted tumours. However, the CP6 build-up time in rat palates correlates with the degree of malignancy and might therefore be a promising parameter in tumour detection.

Introduction

Early detection of malignant and premalignant lesions is an important factor in successful treatment of cancer. One approach for *in vivo* discrimination between normal tissue and malignancies or premalignancies is to make use of auto-fluorescence, the fluorescence of endogenous chromophores in the tissue. Another approach is to make use of exogenous fluorescent agents that localise in pre-cancerous or cancerous tissues (1). Porphyrin derivatives are a class of agents that are used as photosensitisers for the treatment of malignancies by photodynamic therapy. The porphyrins localise to some extent in cancerous tissues and, when illuminated with light of an appropriate wavelength, they are fluorescent but also produce singlet oxygen, which is highly reactive and responsible for the photodynamic action (2). These photosensitising properties may also result in undesired effects such as prolonged skin photosensitivity, which make these agents less suitable for photodiagnostic purposes.

Carotenoporphyrins are substances that have similar fluorescent properties as the porphyrins, but they are not phototoxic. A carotenoid polyene is attached covalently to the porphyrin ring through a linker that enables direct triplet-triplet energy transfer between the porphyrin and the carotenoid polyene. Hence, the excited porphyrin triplet state is quenched rapidly and efficiently by the carotenoid polyene. Thus, the short-lived

porphyrin triplet state does not result in the formation of $^1\text{O}_2$ (3,4). The compound, however, is still fluorescent. These photophysical and spectroscopic properties make carotenoporphyrins suitable candidates for the use as photodiagnostic agents.

Other investigators have shown that trimethoxylated carotenoporphyrins have promising tumour localising properties *in vivo* in animals with transplanted tumours (5-8). The purpose of the present study is to perform a detailed investigation on the localising properties of a hexamethoxylated carotenoporphyrin in two primary tumour models: chemically induced oral mucosal dysplasia in rats and UVB-induced early skin cancer in hairless mice.

Materials and methods

Chemicals

The carotenoporphyrin with six methoxy groups (figure 1) was synthesised at Arizona

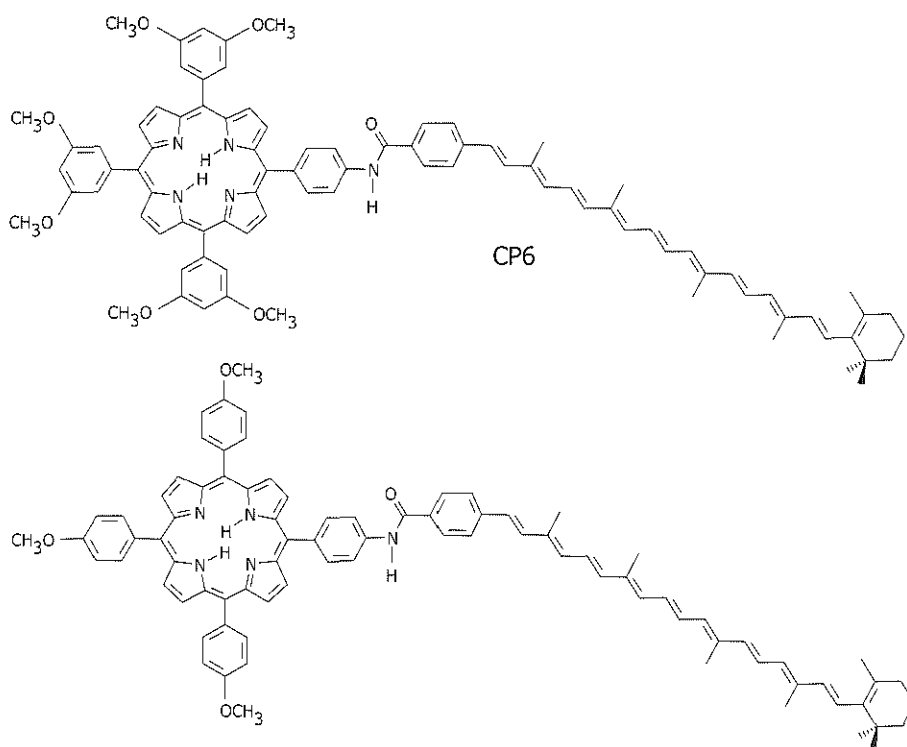


Figure 1 Chemical structure of the hexamethoxylated carotenoporphyrin (CP6) and, for comparison, the trimethoxylated carotenoporphyrin (CP3) that was studied earlier (5,6,7,8).

State University, according to a method described previously by Gust et al (9). Sigma Chemical Co. (St. Louis, USA) supplied Cremophor EL, other chemicals and solvents were of analytical grade.

Animal models and tumour induction

For the hairless mouse model, inbred female albino hairless mice (SKH HR1, Dept. of Dermatology, Academic Hospital Utrecht, The Netherlands) were used. The dorsal skin was irradiated daily with UVB light for 90 days according to a method described by De Gruijl et al (10), causing small primary lesions of actinic and seborrhoeic keratosis and squamous cell carcinoma (10,11). Non-irradiated animals of the same age were used for investigation of normal skin.

For the rat palate model, male Wistar rats (Harlan, Zeist, The Netherlands) were used. Different stages in premalignant dysplasia in the palate were induced by application of 4-nitroquinoline-1-oxide (4-NQO) three times a week for 6, 12 or 18 weeks (12-14). Control animals without dysplasia were also studied.

Preparation and administration of drug solution

After adding 5.3 mg of CP6 in 50 μ l dimethyl sulfoxide to 0.5 ml of Cremophor-EL, the mixture was sonicated until the carotenoporphyrin was completely dispersed. The solubilise was added to 0.15 ml of ethanol and sonicated again. The final volume was made up to 5 ml by dropwise adding phosphate buffered saline, pH 7.3. Before injection, the solution was filtered through a 0.2 μ m filter.

Hairless mice and Wistar rats were anaesthetised with a mixture of ethrane, oxygen and N₂O before drug injection. A dose of 5.4 μ mol.kg⁻¹ CP6 was injected i.v. in rats and i.p. in mice.

Instrumentation: in vivo fluorescence measurements

The excitation source was a 150 W Xenon lamp with monochromator (Photomax 60100, monochromator 77250, Oriel Instruments Corporation, Stratford, CT, USA). Tissues were illuminated with 425 nm light, bandwidth 15 nm (FWHM), for CP6 excitation. Reflection measurements, as reference to compensate for variations in measurement geometry (distance) and lamp output, were performed with 610 nm light, bandwidth 15 nm (FWHM). Spectra were recorded with a cooled CCD-camera (TEA/CCD512-TXB/1, Princeton Instruments inc., Trenton, NJ, USA) with spectrometer (Spectrapro-150, Acton Research Corporation, Acton, MA, USA) with additional 570 nm long wavelength pass filter (Schott OG570). Images were recorded with an intensified CCD-camera (ADIMEC, Eindhoven, The Netherlands) with additional 590 nm long wavelength pass filter (Schott OG590). An optical building block with filters, dichroic mirrors and lenses as described previously (15) was used for illumination of a 10 mm circular area as well as to record tissue fluorescence from that illuminated area.

Instrumentation: fluorescence microscopy

A cooled CCD-camera (TEA/CCD512-TXB/1, Princeton Instruments inc., Trenton, NJ, USA) with spectrometer (Spectrapro-150, Acton Research Corporation, Acton, MA, USA) were coupled to a fluorescence microscope (Leitz DMRB, Leica Mikroskopie und Systemen GmbH, Wetzlar, Germany). Within this set-up, phase contrast, fluorescence images and fluorescence spectra were recorded. Excitation was performed with a halogen lamp and two bandpass filters (370-430 nm and 420-520 nm) resulting in 420-430 nm excitation light. Emission light was transmitted through a bandpass filter (630-670 nm).

Experimental procedures: in vivo fluorescence kinetics

Before each measurement, the animals were anaesthetised with a mixture of ethrane, oxygen and N₂O.

Hairless mouse model: A lesion or a group of lesions on the back was selected to be followed in time. In three untreated and 13 chronically UVB-irradiated hairless mice, fluorescence measurements were made before CP6 injection and at various time points up to 600 h post injection.

Rat palate model: Fluorescence measurements were performed before CP6 injection and at various time points up to 200 h post injection, on untreated rat palates (n=5) and on rat palates that were treated with 4-NQO for 6 weeks (n=6), 12 weeks (n=6) and 18 weeks (n=6).

For measurements on the rat palate, a palatoscope, which is a conical tube with an additional mirror, was fixed to the set-up (12). Before each measurement, the animals were placed in a stereotactic frame to make the palate accessible for measurements with the palatoscope. The mucosa of the hard palate between the molars was placed in the centre of the beam. The fluorescence images included the mucosa and the molars. After the last measurement, the rats were sacrificed and the degree of dysplasia was graded histologically by the epithelial atypia index (EAI) as described by Nauta et al (16). Squamous cell carcinoma can not be graded by the EAI and is therefore separately noted.

Experimental procedures: fluorescence microscopy

At different time points after drug injection (see below), the animals were sacrificed and samples were collected. The samples were kept at -80°C and from these samples, frozen 20 µm and 5 µm sections were made and kept at -20°C. The 20 µm sections were used for the recording of phase contrast and fluorescence emission images. The 5 µm sections were stained with haematoxylin and eosin (HE) for histological examination.

The microscopic fluorescence images were superimposed on their accompanying phase contrast image. The localisation of CP6 fluorescence in cell types and tissues was determined from these images with help of adjacent HE stained sections.

Hairless mouse model: The different samples are defined as follows. Normal skin is skin of untreated mice, altered skin is apparently normal skin of chronically UVB-exposed mice and lesions are the visible lesions on the back of chronically UVB-exposed mice. From the untreated hairless mice, a single sample of the dorsal skin was collected. From the UVB-exposed hairless mice, a single sample of altered skin and up to three macroscopically visible lesions were collected from the dorsal skin. CP6 fluorescence was examined before injection and at 5.5, 18, 100 and 300 hours post injection. At each time interval, four untreated and four UVB-exposed mice were sacrificed.

Rat palate model: Frozen sections were made of untreated palates and palates that were treated with 4-NQO for 18 weeks. CP6 fluorescence was examined before injection and at 3, 20 and 90 hours post injection. At each time interval, three untreated and three treated rats were sacrificed.

Data analysis: fluorescence kinetics

Hairless mouse model: The fluorescence kinetics and localisation of CP6 in the hairless mouse skin were determined from the fluorescence images, because the skin lesions as well as the adjacent altered skin could be recognised easily in the images. Normal skin can be studied only in non UVB-exposed mice. The mean grey scale value was determined of each area and was corrected for lamp output and variations in geometry using the reflection measurements. Then, the mean grey scale values were corrected for autofluorescence and plotted versus time post injection.

Rat palate model: The fluorescence kinetics in the rat palate were determined from the fluorescence spectra rather than from the images, because an additional fluorescence

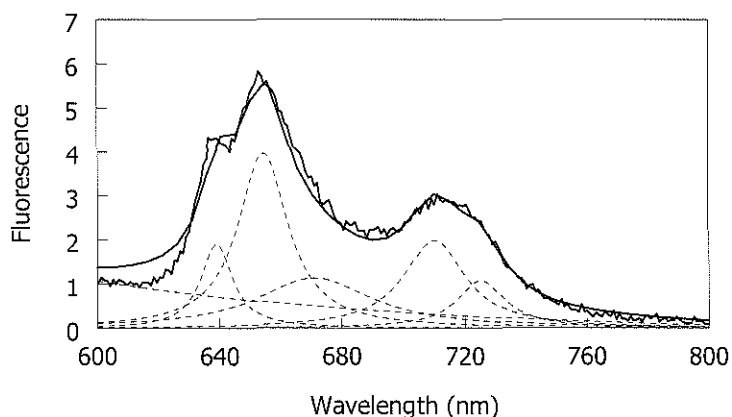


Figure 2 Determination of the peak heights in rat palate fluorescence spectra after CP6 injection. Dotted lines represent the exponential and multiple Lorentzian fitting functions and solid lines represent the measured and fitted spectrum.

peak at 635 nm (figure 2), close to the main CP6 peak at 655 nm, was found to contribute to the mean grey scale value of the images. The heights of the different peaks were determined using an exponential and a multiple Lorentzian fitting function, as follows (figure 2). First, an exponential fitting function was subtracted from the measured spectrum for autofluorescence baseline correction. The multiple Lorentzian fitting procedure was then performed on this corrected spectrum. The height of the 655 nm CP6 peak (from the Lorentzian fitting function) was plotted versus time post injection.

Data analysis: fluorescence kinetics curve fitting

The mouse skin fluorescence showed two maxima as a function of time post injection. To these measurements we fitted the curve mathematically described by:

$$F(t) = A(1 - e^{-t/\tau_1})e^{-t/\tau_2} + B(1 - e^{-t/\tau_3})e^{-t/\tau_4} \quad \text{equation (1)}$$

This is the sum of two standard pharmacokinetics curves, where $F(t)$ represents the measured fluorescence, A and B represent the amplitudes (not the peak heights) of the first and second maximum respectively. The parameters τ_1 and τ_2 , and τ_3 and τ_4 represent the accumulation and removal times of the first and second maximum, respectively. The curves were obtained from the data using a χ^2 -fit. Fits were considered statistically acceptable at (double sided) $P < 0.05$.

On the rat palate only one maximum was observed. Initially, we fitted a curve represented by the first term of equation (1), but this did not yield an acceptable fit. Especially at later time in the curve, the differences between measurements and fit were increasing. Apparently, a second wave occurs here too. However, we did not have enough data at later time points to allow a fit of the complete model. The fit to the following function yielded the best results:

$$F(t) = A(1 - Be^{-t/\tau_1})e^{-t/\tau_2} \quad \text{equation (2)}$$

Statistics

The curve fitting parameters from equation (1) were tested with two-sample z-test to see whether they are different for the different skin types. (The proper procedure would be to calculate the correlation between the curve fitting parameters and skin type, using the Spearman rank correlation test. However, with only 3 groups the best possible p value is 0.333.)

For the rat palates, we tested whether the 635 nm peak heights were different for different 4-NQO treatment periods, using analysis of variance and Student-Newman-Keuls test. By the same procedure we also tested whether the EAI's of the rat palates were different for different 4-NQO treatment periods. Furthermore, the Spearman rank correlation coefficient was calculated to test for a trend in EAI with increasing 4-NQO

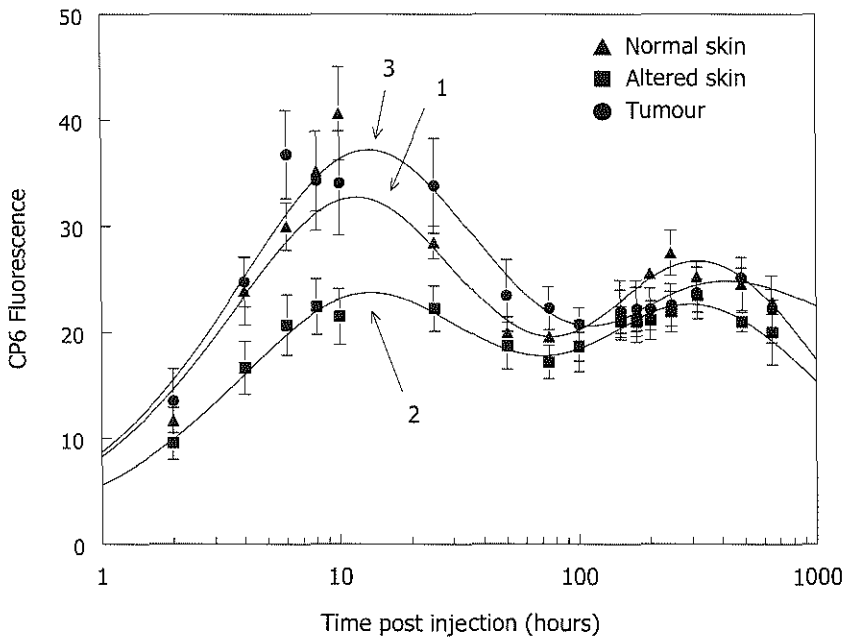


Figure 3 Fluorescence kinetics of CP6 in hairless mouse normal skin (\blacktriangle , curve 1), altered skin (\blacksquare , curve 2) and visible lesion (\bullet , curve 3). Per time point 6 animals and error bars represent standard error of the mean. Lines represent curve fits, described by equation (1).

treatment period. The Pearson product-moment correlation coefficient was calculated to test for correlation between the EAI and the curve fitting parameters from equation (2).

Results

Hairless mouse model

In each fluorescence spectrum of the mouse skin, there is a small autofluorescence peak present at 670 nm. After injection of CP6, two peaks appear, corresponding with the *in vitro* emission peaks of CP6. Images of UVB-treated hairless mouse skin before and after injection of CP6 show that fluorescence increases more in the visible lesions than in the altered skin. Fluorescence increases homogeneously in untreated skin.

Fluorescence kinetics show two waves in both untreated skin and in UVB-irradiated skin (figure 3). CP6 fluorescence is still detectable in all three skin types after 27 days. The curve fitting parameters are given in table 1. No curve fitting parameter has significantly different values for the different skin types.

Typical CP6 microscopic fluorescence localisation in UVB-irradiated mouse back skin and lesions is shown in figure 4. In all sections, no CP6 fluorescence is observed in the

Table 1 Parameters of the fitting function equation (1) for the fluorescence kinetics in hairless mice. Statistics are described in the results section.

Parameter	Value \pm stdev		
	Normal skin	Altered skin	Lesions
A	49 \pm 8	33 \pm 9	51 \pm 12
τ_1	5.4 \pm 1.3	5.5 \pm 2.4	5.3 \pm 1.9
τ_2	32 \pm 7	35 \pm 16	43 \pm 15
B	38 \pm 13	29 \pm 11	29 \pm 16
τ_3	137 \pm 74	108 \pm 77	125 \pm 123
τ_4	1300 \pm 800	1550 \pm 1730	3300 \pm 10000
χ^2	24.0	2.67	6.35
v	9	9	9

Table 2 CP6 fluorescence distribution in hairless mouse skin at different time points after injection (p.i.).

Time p.i. (h)	Epidermis	Dermis	Keratin containing structures
0	No	No	No
5.5	No	No or little	Yes
18	No	Little	Yes
100	No	Yes	Yes
300	No	Yes	Yes

epidermis. CP6 fluorescence is distributed inhomogeneously in cells within the dermis and in keratin containing structures like crusts on the lesions, remnants of hair follicles and keratin cysts. The distribution of CP6 fluorescence at the different time points is given in table 2.

Rat palate model

In all spectra of the rat palates, there is a small autofluorescence peak present at 670 nm. Also a high peak at 635 nm is present in all these spectra. The 635 nm peak heights are plotted versus 4-NQO application period in figure 5.

The 635 nm peak height from the group that was treated with 4-NQO for 18 weeks was significantly different from that of the groups that were treated for 0, 6 and 12 weeks ($P < 0.01$). The 635 nm peak heights from the 0, 6 and 12 weeks treated groups were not significantly different from each other. After injection of CP6, two additional fluorescence peaks appear, corresponding with the *in vitro* emission peaks of CP6. The fluorescence in the images increases homogeneously within the whole area between the molars after injection of CP6.

The epithelial atypia indices (EAI) of the rat palates are plotted versus 4-NQO treatment

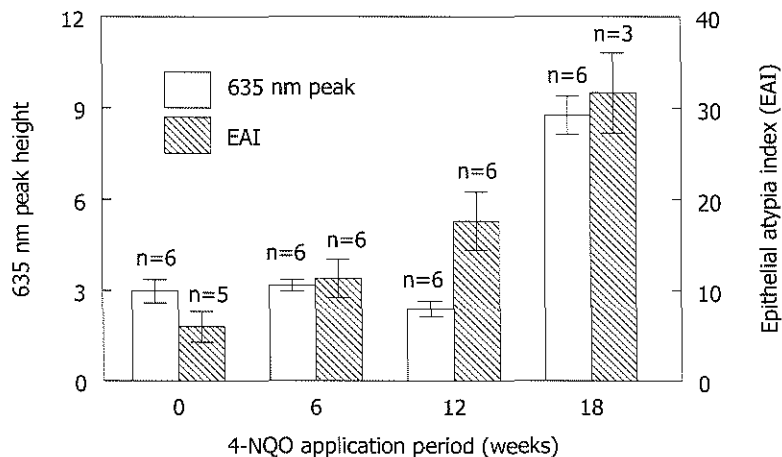


Figure 5 Fluorescence intensities of the 635 nm peak in spectra of rat palates (white bars, left axis) and epithelial atypia index (shaded bars, right axis) versus 4-NQO application period. Error bars represent standard error of the mean.

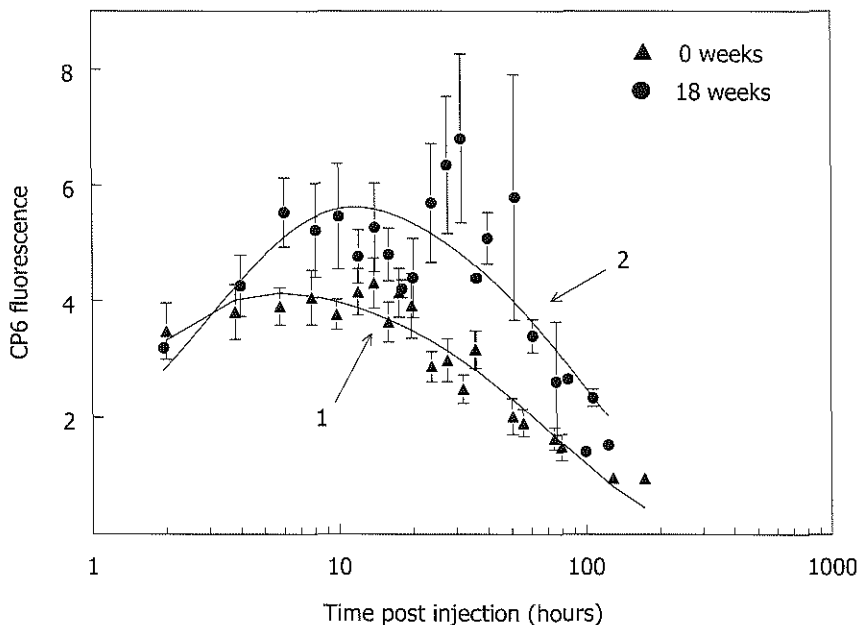


Figure 6 Fluorescence kinetics of CP6 in rat palates that were treated with 4-NQO for 0 weeks (\blacktriangle , curve 1) and 18 weeks (\bullet , curve 2). The curves of the rat palates that were treated for 6 and 12 weeks are not shown in this figure because they are very similar to the curve of the 0 weeks treated palates. Per time point 6 animals and error bars represent standard error of the mean. Lines represent curve fits, described by equation (2).

Table 3 Parameters of the fitting function equation (2) for the fluorescence kinetics in rat palate and the Pearson product-moment correlation coefficient (CC; *, not significant; **, $P < 0.05$) between the parameters and epithelial atypia index (EAI).

Parameter	Value \pm stdev				CC
	Normal	6 weeks	12 weeks	18 weeks	
EAI	6 ± 4	11 ± 5	18 ± 8	32 ± 8	
A	4.1 ± 0.1	4.28 ± 0.08	3.48 ± 0.08	6.40 ± 0.08	0.78*
B	1.00 ± 0.02	1.00 ± 0.04	0.874 ± 0.02	0.980 ± 0.02	-0.72*
τ_1	0.094 ± 0.02	0.12 ± 0.01	1.1 ± 0.2	2.9 ± 0.2	0.98**
τ_2	95 ± 5	72 ± 5	133 ± 6	93 ± 5	0.16*
χ^2	1.85	3.58	5.76	7.72	
ν	15	9	14	17	

Table 4 CP6 fluorescence distribution in rat palate at different time points after injection (p.i.).

Time p.i. (h)	Horny layer	Epithelium	Connective tissue
0	No	No	No
3	Little	No	Yes
20	Little	No	Yes
90	Little	No	Yes

period in figure 5. Three rats from the 18 weeks group did not receive an EAI because they had developed squamous cell carcinoma. The following groups are different from each other with $P < 0.01$: 0 and 18 weeks, 0 and 12 weeks, 6 and 18 weeks, 12 and 18 weeks. The 6 and 12 weeks group are different from each other with $P < 0.05$. The 0 and 6 weeks group are not significantly different from each other. The Spearman rank correlation coefficient between EAI and 4-NQO treatment period is 0.83. This is a significant association between 4-NQO treatment period and EAI ($P < 0.001$).

The fluorescence kinetics of CP6 in the rat palates treated with 4-NQO for 0 and 18 weeks are plotted in figure 6. The curves of the rat palates that were treated for 6 and 12 weeks are very similar to the curve of the palates that were treated for 0 weeks. After 8 days, CP6 fluorescence is still detectable in the palates. The curve fitting parameters are given in table 3. For these parameters, the Pearson product-moment correlation coefficient with the EAI is also given in table 3. Only the CP6 build-up time (τ_1) shows a significant Pearson correlation of 0.98 with the EAI ($P < 0.05$).

Typical microscopic fluorescence localisation in the rat palate is shown in figure 7. Before CP6 injection, autofluorescence (670 nm) is observed in the surface of the horny layer. This autofluorescence is measured in normal as well as 4-NQO treated palate. After injection, CP6 fluorescence is in the connective tissue where it is distributed

inhomogeneously. Because of the autofluorescence in the horny layer before injection, fluorescence spectra of the horny layer were recorded to see if there is CP6 fluorescence in the horny layer after CP6 injection. In these fluorescence spectra, a shoulder appears at 655 nm on the flank of the 670 nm autofluorescence peak after injection of CP6. This shoulder at 655 nm corresponds with CP6 emission. No CP6 fluorescence was observed at any time in the epithelium except in the horny layer. The distribution of CP6 fluorescence at the different time points is given in table 4.

Discussion

Other investigators previously reported on *in vivo* fluorescence kinetics of trimethylated and trimethoxylated carotenoporphyrins (CP3) (5-8). The carotenoporphyrin investigated in our study (CP6) is different from trimethoxylated carotenoporphyrin in having three extra methoxy groups (figure 1). Pharmacokinetics studies by Reddi et al. (5) showed that in mice, an i.v. dose of $4.2 \mu\text{mol.kg}^{-1}$ CP3 is cleared from the blood in 4 days. Maximum accumulation in transplanted tumours occurs at 24-48 hours post injection and accumulation in skin and muscle was very low ($< 2 \mu\text{g.g}^{-1}$) throughout the measurement time span of 168 hours. Furthermore, Reddi's investigation showed that CP3 accumulates in the liver, in which the concentration had not decreased after 8 weeks. Nilsson et al. (6,7) reported on laser-induced CP3 fluorescence measurements in mice with transplanted tumours. They measured an increased fluorescence ratio between surgically exposed tumours and peritumoural muscle. Saarnak et al. (8) performed CP3 fluorescence measurements on rat and mouse skin, exposed tumour and tumour covered with overlying skin. The measured fluorescence from the covered tumour was smaller than that of the exposed tumour. These results led to the conclusion that the depth of the tumour is important, even with a highly tumour-selective agent. These reports by Reddi et al. (5), Nilsson et al. (6,7) and Saarnak et al. (8) show that carotenoporphyrins have promising localising properties in transplanted tumours. In our study we investigated the localising properties of a new carotenoporphyrin in primary tumour models.

In the hairless mouse model, the CP6 fluorescence kinetics showed two waves in both untreated skin and in UVB-irradiated skin (figure 3). At 5.5 and 18 hours after injection, we observed little or no CP6 fluorescence in the dermis compared to the later time points (table 2). Reddi et al. (5) reported that carotenoporphyrins are cleared from the blood within 4 days. They also reported that, due to their high lipophilicity, the delivery of carotenoporphyrins from Cremophor micelles is a slow process. Thus the two waves in the kinetics curve may reflect the sum of the relatively fast plasma kinetics as reported by Reddi et al. (5) plus a much slower tissue kinetics curve.

The difference in peak fluorescence intensities between normal and altered skin may be due to differences in epidermal thickness. In the HE stained sections we observed that



Figure 4 Combined microscopic phase contrast and fluorescence image of the back skin of a UVB-treated mouse, showing the distribution of CP6 fluorescence (red). CP6 fluorescence is inhomogeneously distributed in the dermis (lower part of the image). Very little CP6 fluorescence is present in the epidermal dysplastic tissue (dark gray) and much CP6 fluorescence is present in the horny crust on top of the dysplastic tissue. The white bar represents 500 μm .

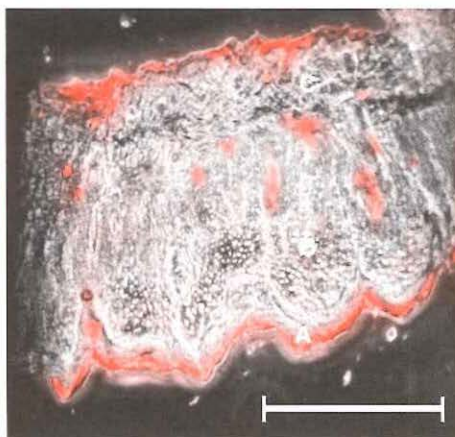


Figure 7 Combined microscopic phase contrast and fluorescence images of a rat palate treated with 4-NQO for 18 weeks, showing the distribution of CP6 fluorescence (red). The fluorescence in the horny layer (A) is the sum of 670 nm autofluorescence and little CP6 fluorescence. These components could be distinguished in the fluorescence spectrum, but not separated from each other in the fluorescence image. No CP6 fluorescence is present in the dysplastic epithelium (B) and the CP6 fluorescence in the connective tissue (C) is distributed inhomogeneously. The white bar represents 500 μm .

the epidermis of altered skin is thickened compared to normal skin. This is a well-known feature of this model (10,17,18). When the epidermis is thickened, less excitation light will reach the dermally located CP6 and less of the fluorescence signal can reach the surface, leading to a decrease in the measured fluorescence signal.

In the microscopic fluorescence images, no CP6 fluorescence was observed in the epidermal cells throughout the duration of the experiment. The CP6 fluorescence in the lesions is located in keratin containing structures like crusts on the lesions, remnants of hair follicles and keratin cysts. These structures, and thus the high CP6 fluorescence intensities in the skin lesions measured *in vivo*, are not directly related to the dysplastic or malignant stage of the epidermal lesions.

A small autofluorescence peak at 670 nm occurs in the spectra that were measured in both mice and rats. This 670 nm autofluorescence is related to the degradation products

of chlorophyll a, namely pheophytin a and pheophorbide a (19,20). Chlorophyll a and its degradation products are present in the food pellets. This 670 nm autofluorescence does not influence the CP6 fluorescence results, because this autofluorescence peak has been excluded from the CP6 fluorescence values in the data analysis.

In the rat fluorescence spectra, a peak is also present around 635 nm. This may be due to porphyrins produced by Harderian glands (21-23). The fluorescence intensity of this peak is significantly higher in rat palates that were treated with 4-NQO for 18 weeks compared to the 0, 6 and 12 weeks treated rat palates. Porphyrin production by the Harderian glands increases with increasing age of the rat (21) or when the rat is stressed (24). Nauta et al (25) reported small but distinctive PDT damage in normal rat palate after PDT with light alone. They explain this damage by the presence of endogenous porphyrins, produced by the Harderian gland. Van der Breggen et al. (26) reported a significant increase in porphyrin fluorescence in the hamster cheek pouch model during the DMBA induced transformation from normal to premalignant to malignant lesions. In hamster buccal mucosa that was treated with DMBA for 16 weeks, this peak fluorescence increased significantly compared to buccal mucosa that was treated with DMBA for 2, 9 and 14 weeks. They refer to this peak as autofluorescence, as no exogenous fluorescent dye was administered. However, from the perspective of the mucosa, the porphyrins from the Harderian glands are exogenously administered.

The EAI and thus the stage of dysplasia showed a strong Spearman rank correlation of 0.83 with the 4-NQO application period ($P < 0.001$). Nauta et al. (27) reported also a strong correlation between the EAI of rat palates and 4-NQO application period. The build-up time (τ_1) from the *in vivo* fluorescence kinetics is the only curve fitting parameter that showed a strong and significant Pearson correlation of 0.98 with the EAI ($P < 0.05$). These results suggest that the fluorescence kinetics of CP6 in the rat palate change with increasing degree of dysplasia. However, we did not observe differences in CP6 fluorescence intensity and localisation that correlated with dysplastic changes in the palate in the microscopic fluorescence images of untreated and 18 weeks treated palates. In both the untreated and treated group, the CP6 fluorescence was observed in the horny layer and connective tissue, but not in the (dysplastic) epithelium.

Conclusions

In our two primary tumour models, CP6 does not localise preferentially in pre-cancerous or cancerous tissues. However, the fluorescence kinetics in the rat palate showed that CP6 fluorescence build-up time in the rat palate increases with increasing degree of malignancy and might therefore be a promising parameter for tumour detection. Furthermore, in our opinion, fluorescence microscopy is vitally important for the understanding of *in vivo* fluorescence measurements for diagnostic purposes.

Acknowledgements

This work was supported by the European Community, contract number BMH4-CT97-2260 (JTHMvdA) and the Dutch Cancer Society, project number DDHK-95-1062 (OCS and HJvS). The authors wish to thank Konnie Hebeda for her assistance in analysing the haematoxylin/eosin stained sections, Max Witjes for performing the EAI grading and Hans Vuijk for his assistance in preparing the photographs.

References

1. Wagnières GA, Star WM, Wilson BC. *In vivo* fluorescence spectroscopy and imaging for oncological applications. *Photochem Photobiol* 1998; 68(5):603-632.
2. Henderson BW, Dougherty TJ. How does photodynamic therapy work? *Photochem Photobiol* 1992; 55(1):145-157.
3. Gust D, Moore TA, Moore AL, Jori G, Reddi E. The photochemistry of carotenoids. Some photosynthetic and photomedical aspects. *Ann NY Acad* 1993; 691:32-47.
4. Gust D, Moore TA, Moore AL, Devadoss C, Lidell PA, Hermant R, Nieman RA, Demanche LJ, DeGraziano JM, Gouni I. Triplet and singlet energy transfer in carotene-porphyrin dyads: role of linkage bonds. *J Am Chem Soc* 1992; 114:3590-3603.
5. Reddi E, Segalla A, Jori G, Kerrigan PK, Lidell PA, Moore AL, Moore TA, Gust D. Carotenoporphyrins as selective photodiagnostic agents for tumours. *Br J Cancer* 1994; 69:40-45.
6. Nilsson H, Johansson J, Svanberg K, Svanberg S, Jori G, Reddi E, Segalla A, Gust D, Moore AL, Moore TA. Laser-induced fluorescence in malignant and normal tissue in mice injected with two different caroteno-porphyrins. *Br J Cancer* 1994; 70:873-879.
7. Nilsson H, Johansson J, Svanberg K, Svanberg S, Jori G, Reddi E, Segalla A, Gust D, Moore AL, Moore TA. Laser-induced fluorescence studies of the biodistribution of carotenoporphyrins in mice. *Br J Cancer* 1997; 76(3):355-364.
8. Saarnak AE, Rodrigues T, Schwartz J, Moore AL, Moore TA, Gust D, van Gemert MJC, Sterenberg HJCM, Thomsen SL. Influence of tumour depth, blood absorption and autofluorescence on measurements of exogenous fluorophores in tissue. *Lasers Med Sci* 1998; 13:22-31.
9. Gust D, Moore TA, Moore AL, Lidell PA. Synthesis of carotenoporphyrin models for photosynthetic energy and electron transfer. In *Methods of enzymology; volume 213* (Edited by L Packer) 1992, Academic Press, San Diego.
10. de Gruijl FR, van der Meer JWM, van der Leun JC. Dose-time dependency of tumour formation by chronic UV exposure. *Photochem Photobiol* 1983; 37:53-62.
11. de Gruijl FR, Sterenberg HJCM, Forbes PD, Davies RE, Cole C, Kelfkens G, van Weelden H, Slaper H, van der Leun JC. Wavelength dependence of skin cancer induction by ultraviolet irradiation of albino hairless mice. *Cancer Res* 1993; 53:53-60.
12. Witjes MJH, Speelman OC, Nikkels PGJ, Nooren CAAM, Nauta JM, van der Holt B, van Leengoed HLLM, Roodenburg JLN. *In vivo* fluorescence kinetics and localisation of aluminium phthalocyanine disulphonate in an autologous tumour model. *Br J Cancer* 1996; 73:573-580.
13. Nauta JM, Speelman OC, van Leengoed HLLM, Nikkels PGJ, Roodenburg JLN, Star WM, Witjes MJH, Vermey A. *In vivo* photo-detection of chemically induced premalignant lesions and squamous cell carcinoma of the rat palatal mucosa. *J Photochem Photobiol B* 1997; 39:156-166.
14. Nauta JM, van Leengoed HLLM, Witjes MJH, Nikkels PGJ, Star WM, Vermey A, Roodenburg JLN. Photofrin-mediated photodynamic therapy of chemically-induced premalignant lesions and squamous cell carcinoma of the palatal mucosa in rats. *Int J Oral Maxillofac Surg* 1997; 26:223-231.
15. Robinson DJ, de Bruijn HS, van der Veen N, Stringer MR, Brown SB, Star WM. Fluorescence photobleaching of ALA-induced protoporphyrin IX during photodynamic therapy of normal hairless mouse skin: the effect of light dose and irradiance and the resulting biological effects. *Photochem Photobiol* 1998; 67(1):140-149.
16. Nauta JM, Roodenburg JLN, Nikkels PGJ, Witjes MJH, Vermey A. Comparison of epithelial dysplasia - the 4NQO rat palate model versus

- human oral mucosa. *Int J Oral Maxillofac Surg* 1995; 24:53-58.
17. Sterenborg HJCM, de Gruijl FR, van der Leun JC. UV-induced epidermal hyperplasia in hairless mice. *Photodermatol* 1986; 3:206-214.
18. Sterenborg HJCM, van der Leun JC. Change in epidermal transmission due to UV-induced hyperplasia in hairless mice: a first approximation of the action spectrum. *Photodermatol* 1988; 5:71-82.
19. Weagle GE, Paterson PE, Kennedy JC, Pottier RH. The nature of the chromophore responsible for naturally occurring fluorescence in mouse skin. *J Photochem Photobiol B* 1988; 2:313-320.
20. Gudgin Dickson EF, Holmes H, Jori G, Kennedy JC, Nadeau P, Pottier RH, Rossi F, Russell DA, Weagle GE. On the source of the oscillations observed during *in vivo* zinc phthalocyanine fluorescence pharmacokinetic measurements in mice. *Photochem Photobiol* 1995; 61:506-509.
21. Rodriguez C, Menendez-Pelaez A, Howes KA, Reiter RJ. Age and food restriction alter the porphyrin concentration and mRNA levels for 5-aminolevulinic acid synthase in rat Harderian gland. *Life Sci* 1992; 51:1891-1897.
22. Sakai T. The mammalian Harderian gland: Morphology, biochemistry, function and phylogeny. *Arch Histol Jap* 1981; 44(4):299-333.
23. Eida K, Kikutani M. Harderian gland IV. Porphyrin formation from δ -aminolevulinic acid by the Harderian gland of rats. *Chem Pharm Bull* 1969; 17(5):927-931.
24. Kurisu K, Sawamoto O, Watanabe H, Ito A. Sequential changes in the Harderian gland of rats exposed to high intensity light. *Lab Animal Sci* 1996; 46(1):71-76.
25. Nauta JM, van Leengoed HLLM, Witjes MJH, Roodenburg JLN, Nikkels PGJ, Thomsen SL, Marijnissen JPA, Star WM. Photofrin-mediated photodynamic therapy of rat palatal mucosa: normal tissue effects and light dosimetry. *Lasers Med Sci* 1996; 11:163-174.
26. van der Breggen EWJ, Rem AI, Christian MM, Yang CJ, Calhoun KH, Sterenborg HJCM, Motamedi M. Spectroscopic detection of oral and skin tissue transformation in a model for squamous cell carcinoma: autofluorescence versus systemic aminolevulinic acid-induced fluorescence. *IEEE J Sel Top Quant Electr* 1996; 2(4):997-1006.
27. Nauta JM, Roodenburg JLN, Nikkels PGJ, Witjes MJH, Vermey A. Epithelial dysplasia and squamous cell carcinoma of the Wistar rat palata. 4NQO model. *Head Neck* 1996; 18(5):441-449

CHAPTER 4

Protoporphyrin IX fluorescence kinetics and localization after topical application of ALA pentyl ester and ALA on hairless mouse skin with UVB-induced early skin cancer

This chapter was adapted from JTHM van den Akker, HS de Bruijn, GMJ Beijersbergen van Henegouwen, WM Star and HJCM Sterenborg. *Photochem Photobiol* 2000; 72(3):399-406

Summary

In order to improve the efficacy of 5-aminolevulinic acid-based (ALA) photodynamic therapy (PDT), different ALA derivatives are presently being investigated. ALA esters are more lipophilic and therefore may have better skin penetration properties than ALA, possibly resulting in enhanced protoporphyrin IX (PpIX) production. In previous studies, it was shown that ALA pentyl ester (ALAPE) does considerably enhance the PpIX production in cells *in vitro* compared with ALA. We investigated the *in vivo* PpIX fluorescence kinetics after application of ALA and ALAPE to hairless mice with and without UVB-induced early skin cancer. ALA and ALAPE (20% w/w) were applied topically to the mouse skin and after 30 minutes, the solvent was wiped off and PpIX fluorescence was followed in time with *in vivo* fluorescence spectroscopy and imaging. At 6 and 12 hours after the 30 minutes application, skin samples of visible lesions and adjacent altered skin (UVB-exposed mouse skin) and normal mouse skin were collected for fluorescence microscopy. From each sample, frozen sections were made and phase contrast images and fluorescence images were recorded. The *in vivo* fluorescence kinetics showed that ALAPE induced more PpIX in visible lesions and altered skin of the UVB-exposed mouse skin, but not in the normal mouse skin. In the microscopic fluorescence images, higher ALAPE-induced PpIX levels were measured in the stratum corneum, but not in the dysplastic layer of the epidermis. In deeper layers of the skin, PpIX levels were the same after ALA and ALAPE application. In conclusion, ALAPE does induce higher PpIX fluorescence levels *in vivo* in our early skin cancer model, but these higher PpIX levels are not located in the dysplastic layer of the epidermis.

Introduction

Photodynamic therapy (PDT) of cancer is based on the administration of a photosensitizing compound with tumor-localizing properties, and subsequent irradiation with light of an appropriate wavelength that causes damage to the treated tissue (1). An alternative to administration of a photosensitizing compound is the administration of 5-aminolevulinic acid (ALA) which is the precursor of protoporphyrin IX (PpIX), a clinically useful photosensitizer (2-4).

The clinical use of PDT with ALA-induced PpIX is limited by different factors, like the diffusion of ALA through biological barriers, location of PpIX, available oxygen and rapid photobleaching of PpIX. Different methods for improving ALA-PDT are presently under investigation or have been applied successfully. Rhodes et al. (5) studied iontophoretic ALA delivery to normal human skin and subsequent PpIX fluorescence and phototoxicity. They reported that with iontophoresis, ALA is delivered rapidly across the stratum corneum and the amount of ALA can be increased with increased charge. ALA-PDT combined with iontophoresis has been successfully applied for treatment of carcinoma *in*

situ of the bladder (6). Ma et al. (7) reported that ultrasound enhances transdermal ALA uptake and thus PpIX production. Another method to improve ALA penetration in the skin is utilizing a skin penetration enhancer (8,9). The conversion of PpIX into heme can be reduced by iron chelators, like hydroxypyridinones and desferrioxamine, resulting in greater accumulation of PpIX (10-13). A different approach to improve ALA-PDT is light fractionation. More tissue damage is caused when the illumination is interrupted once for a long period of time (minutes or hours), because after light treatment new PpIX is formed (14-17). In case of short-term light fractionation, the illumination is interrupted once, or several or many short periods of time (seconds) (18,19). The increase in PDT effect may be the result of improved oxygenation, reperfusion of the tissue or relocalization of PpIX. Improved oxygenation, and thus increased PDT effect, may also be achieved by decreasing the irradiance or fluence rate (20,21).

Another approach to improve the bioavailability of PpIX might be the use of esterified ALA instead of ALA as a precursor for PpIX synthesis. ALA in an esterified form is more lipophilic than ALA itself and this lipophilicity may improve the uptake, penetration depth and distribution. Several authors have demonstrated that ALA derivatives can increase PpIX production *in vitro* in different cell lines (22-24). Some ALA derivatives induced higher PpIX levels in the epidermis of *ex vivo* human and rat skin explant cultures floating on medium containing ALA or its derivatives (25). In patients, ALA methyl ester (ALAME) did not improve PpIX production in solar keratoses, but the ratio of PpIX in solar keratoses versus adjacent normal skin was higher (26). ALAHE has proven to be very successful in improving PpIX production and distribution in the bladder mucosa *ex vivo* (27) and in patients (28). *In vivo* PpIX levels in the epidermis of normal nude mouse skin were increased after long-term application of ALAME, ALA ethyl ester or ALA propyl ester (29,30).

Thus, some ALA derivatives have proven to be successful in increasing PpIX production in cells (22-24), in skin culture explants (25), in bladder mucosa (27,28) and in normal nude mouse skin (29,30). In the present study, we investigate whether short-time topical application of ALAPE, which proved to be the best ALA ester in the *in vitro* studies by Kloeck et al. (22,23), is able to improve the *in vivo* PpIX kinetics and PpIX distribution in the hairless mouse skin with and without UVB-induced early skin cancer.

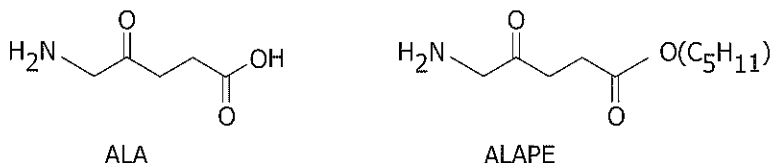


Figure 1 Structure of ALA and ALA pentyl ester (ALAPE). ALAPE was synthesized from ALA and *n*-amyl alcohol and its molecular structure was confirmed by NMR.

Materials and methods

Chemicals

ALA was purchased from FineTech Ltd. (Haifa, Israel) and ALAPE was synthesized as described below. The molecular structures of ALA and ALAPE are shown in figure 1. Reagents and solvents were of analytical grade and were used as purchased.

Synthesis

ALAPE was synthesized from ALA and n-amyl alcohol. The synthesis procedure has been described in detail previously (22). Briefly, 6.0 ml of amyl alcohol was cooled on ice and 1 ml of thionyl chloride was added dropwise. Then, 1 g of ALA was added to the solution and the mixture was kept at 70°C. When ALA had dissolved completely, the reaction was stopped by cooling it to room temperature. The reaction mixture was dissolved in acetone and the excess of alcohol and side products were separated from the reaction product by column chromatography. After recrystallization in diethyl ether, ALAPE was obtained in a yield of 73%. The structure and purity were verified with thin layer chromatography and NMR.

NMR data

The NMR spectra were obtained at 200 MHz on a JEOL FX-200 spectrometer. The NMR characteristics of ALAPE (in ppm relative to tetramethylsilane) were as follows.

8.40 (NH₂, broad, 2H), 4.00 (C[=O]OCH₂, triplet, 2H), 3.94 (H₂NCH₂C[=O], singlet, 2H), 2.81 (C[=O]CH₂CH₂C[=O]O, triplet, 2H), 2.54 (C[=O]CH₂CH₂C[=O]O, triplet, 2H), 1.57 (C[=O]OCH₂CH₂, multiplet, 2H), 1.29 (CH₂CH₂CH₂CH₂, multiplet, 4H), 0.88 (CH₂CH₃, triplet, 3H).

Animal model and tumor induction

Inbred female albino hairless mice (SKH HR1, Dept. of Dermatology, Academic Hospital Utrecht, The Netherlands) were used. The dorsal skin had been irradiated daily with UVB for 90 days according to a method described by de Gruijl et al. (31), causing small primary lesions of actinic and seborrhoeic keratosis and squamous cell carcinoma (31, 32). Non-exposed animals of the same age were used for investigation of normal skin.

Light delivery and in vivo fluorescence measurements

Light from a halogen lamp was passed through a bandpass filter to excite the mouse skin with 500 nm light (bandwidth 40 nm). Low-intensity light (0.1 mW/cm²) was used to avoid photobleaching and photodynamic damage. An optical building block with filters, dichroic mirrors and lenses as described previously (20) was used to illuminate a 10 mm diameter circular area as well as to record tissue fluorescence from that illuminated area. Fluorescence images were acquired with a digital intensified CCD camera (LI-μCAM, Lambert Instruments, Leutingewolde, The Netherlands) with

additional 670 (50 nm bandpass filter (interference filter with very sharp cut-on and cut-off). An optical multi-channel analyzer (InstaSpecTM-IV 77131 CCD camera coupled to a MultiSpecTM 77400 spectrometer, Oriel Instruments, Stratford, USA) with additional 570 nm longpass filter (Schott OG570) was used for spectroscopy. Fluorescence images and spectra were recorded simultaneously. At each time point, fluorescence measurement was also performed on a calibration sample, allowing correction for variations in lamp output.

Fluorescence microscopy

A cooled CCD-camera (TEA/CCD512-TXB/1, Princeton Instruments Inc., Trenton, USA) with spectrometer (Spectrapro-150, Acton Research Corporation, Acton, USA) was coupled to a fluorescence microscope (Leitz DMRB, Leica Mikroskopie und Systemen GmbH, Wetzlar, Germany). Within this set-up, phase contrast and fluorescence images were recorded from 20 μ m sections. Fluorescence was excited with 514 nm light from an argon ion laser. Emission light was transmitted through a 636 ± 5 nm laser line filter (Melles Griot 03FIL050). Before each set of measurements, a microscopic fluorescence image was recorded from a calibration sample for correction of variations in laser output.

ALA and ALAPE administration

ALA and ALAPE (20% w/w) were dissolved in 3% carboxymethylcellulose in water. In case of ALA, NaOH (2M) was added to adjust the solution to pH 5.5 to prevent skin irritation. A thin layer of gauze of 1 cm in diameter was soaked in ALA or ALAPE solution and was applied to the mouse skin and the area was occluded with a polythene dressing (Tegaderm, 3M, The Netherlands). Before the solutions were applied to the skin, the mice received a low dose of Hypnorm[®] (Janssen Pharmaceutica B.V., Tilburg, The Netherlands) and diazepam (Centrafarm, Etten-Leur, The Netherlands) to avoid anxiety caused by the dressing. On each non-UVB-exposed mouse, the solution was applied to one area. In case of UVB-exposed mice, solution was applied to two areas with 1-2 mm diameter tumor(s). After 30 minutes, the solution was wiped off carefully.

Experimental procedures

PpIX fluorescence kinetics measurements were performed on 12 UVB-exposed and 12 non-UVB-exposed mice (table 1). Before each measurement, the animals were anesthetized with a mixture of ethrane, oxygen and N₂O. Prior to application of ALAPE or ALA, an autofluorescence spectrum and image were recorded from each application site. ALAPE and ALA were each applied to 6 UVB-exposed and 6 non-UVB-exposed mice. Fluorescence measurements of the application sites started immediately after the 30 minutes application period and were performed every hour over 14 hours and at 24, 40, 48, 64 and 72 hours post application.

Table 1 Summary of numbers of animals used for the *in vivo* fluorescence kinetics and fluorescence microscopy study.

		UVB-exposed mice			Non-exposed mice			
		Fluorescence kinetics	Fluorescence microscopy 0 h	Fluorescence microscopy 6 h	Fluorescence kinetics	Fluorescence microscopy 0 h	Fluorescence microscopy 6 h	Fluorescence microscopy 12 h
ALAPE	6	2	3	3	6	2	3	3
ALA	6		2	2	6		2	2

Samples for fluorescence microscopy were collected from 12 UVB-exposed and 12 non-UVB-exposed mice. At 6 and 12 hours post application of ALA or ALAPE, mice were sacrificed (for details see table 1) and 2 UVB-exposed and 2 non-exposed mice were sacrificed without receiving ALA or ALAPE. Sites of interest were excised, immediately frozen in liquid nitrogen and kept at -80°C. From each sample, frozen 20 µm and 5 µm sections were obtained. From sets of six 20 µm sections per sample, phase contrast images and fluorescence images were recorded immediately after cutting. The 5 µm sections were stained with hematoxylin and eosin (HE) for histological examination.

Data analysis

The *in vivo* PpIX fluorescence kinetics in the selected areas of normal skin, altered skin and visible lesions were determined from the *in vivo* fluorescence images. Normal skin can only be studied in non-UVB-exposed mice. Visible lesions and adjacent altered skin could easily be recognized in the fluorescence images of UVB-exposed mice (figure 2). The mean gray scale value was determined from each area and was corrected for lamp output using the fluorescence measurements of the calibration sample. After subtraction of the autofluorescence, the corrected mean gray scale values were plotted as a function of time up to 14 hours after the application.

In the phase contrast images, the position and size of the different skin layers were defined with help of the accompanying HE stained sections. The skin layers are: whole epidermis, stratum corneum, epidermis without stratum corneum, dermis, deep dermis, hair follicles and muscle. Only in the epidermis of altered skin and visible lesions, it was

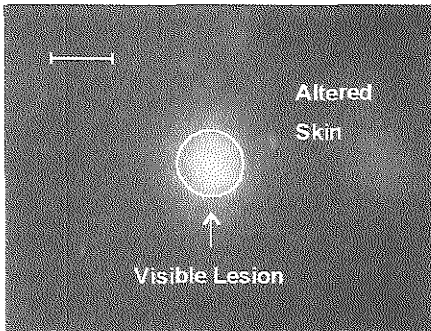


Figure 2 Typical *in vivo* fluorescence image of UVB-exposed mouse skin after application of ALA or ALAPE. Visible lesion and adjacent altered skin are indicated in the image and the white bar represents 1 mm.

possible to define stratum corneum as a separate layer. The mean gray scale values of the PpIX fluorescence were determined in each fluorescence image in the areas of the skin layers that were defined in their accompanying phase contrast image.

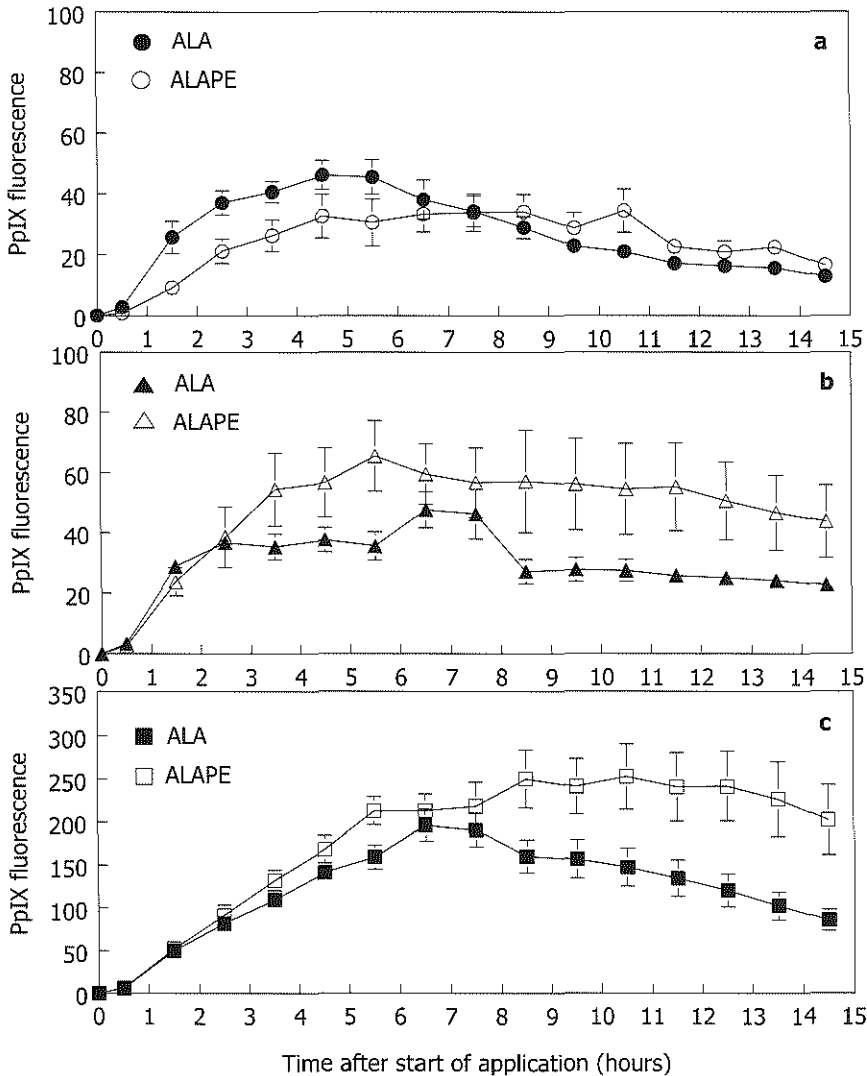


Figure 3 In vivo PpIX fluorescence kinetics in hairless mouse normal skin after ALAPE (open circle) or ALA (solid circle) application (a), hairless mouse UVB-induced altered skin, after ALAPE (open triangle) or ALA (solid triangle) application (b), in hairless mouse UVB-induced visible lesions after ALAPE (open square) or ALA (solid square) application (c). PpIX fluorescence units are arbitrary, but comparable between (a), (b) and (c). Error bars indicate standard error of the mean.

Results

In vivo PpIX fluorescence kinetics

A peak around 635 nm and a smaller peak around 705 nm, corresponding with the emission peaks of PpIX, appear in the fluorescence spectra of the flank after application of ALA and ALAPE. A typical fluorescence image after application to the flank of an UVB-exposed mouse is given in figure 2 and shows that fluorescence increases more in visible lesions than in altered skin. The ALA and ALAPE-induced PpIX fluorescence in normal skin, altered skin and visible lesions is still detectable at 24 hours post application, but returns to autofluorescence levels within 72 hours post application.

Figure 3 shows the ALA and ALAPE-induced PpIX fluorescence kinetics in normal skin, altered skin and visible lesions up to 14 hours post application. Fluorescence measurements beyond 14 hours after start of the application showed many artifacts, probably due to the anesthesia, and are therefore not shown. Compared to ALA, ALAPE does not induce higher PpIX levels in normal skin (figure 3a). In altered skin and visible lesions, ALAPE-induced PpIX levels are higher compared to ALA (figure 3b and c), but these differences are not statistically significant. However, the shapes of these curves do suggest a difference between ALA and ALAPE-induced PpIX fluorescence kinetics. Firstly, the maximum ALA-induced PpIX fluorescence in normal skin, altered skin and visible lesions and the maximum ALAPE-induced PpIX fluorescence in normal skin and altered skin is reached at the same time interval, which is about 4-6 hours post application. The ALAPE-induced PpIX fluorescence maximum in visible lesions is reached at 8 hours post application. Furthermore, ALAPE-induced PpIX fluorescence in all three skin types stays longer at its maximum level compared to ALA-induced PpIX fluorescence.

Microscopic PpIX distribution

Figure 4 shows the ALAPE-induced PpIX fluorescence distribution in normal skin, altered skin and visible lesions (figure 4a-c, respectively) and the ALA-induced PpIX fluorescence in normal skin, altered skin and visible lesions (figure 4d-f, respectively) at 6 hours after the 30 minutes application of ALA or ALAPE. There is no difference between ALA and ALAPE in PpIX fluorescence localization after 30 minutes topical application. Strong PpIX fluorescence in the normal skin, altered skin and visible lesions is mainly restricted to the epidermis, hair follicles and keratin cysts. Weak PpIX fluorescence is visible in the upper dermis, decreasing towards the deeper dermis and muscle layers. Figure 4b-f show that the epidermal PpIX fluorescence in the altered skin and visible lesions is not homogeneous throughout the whole epidermis; PpIX fluorescence is stronger in the stratum corneum than in the rest of the epidermis. This PpIX fluorescence localization is the same in the images recorded from samples taken at 12 hours post application (data not shown). The sequence of the microscopic images in

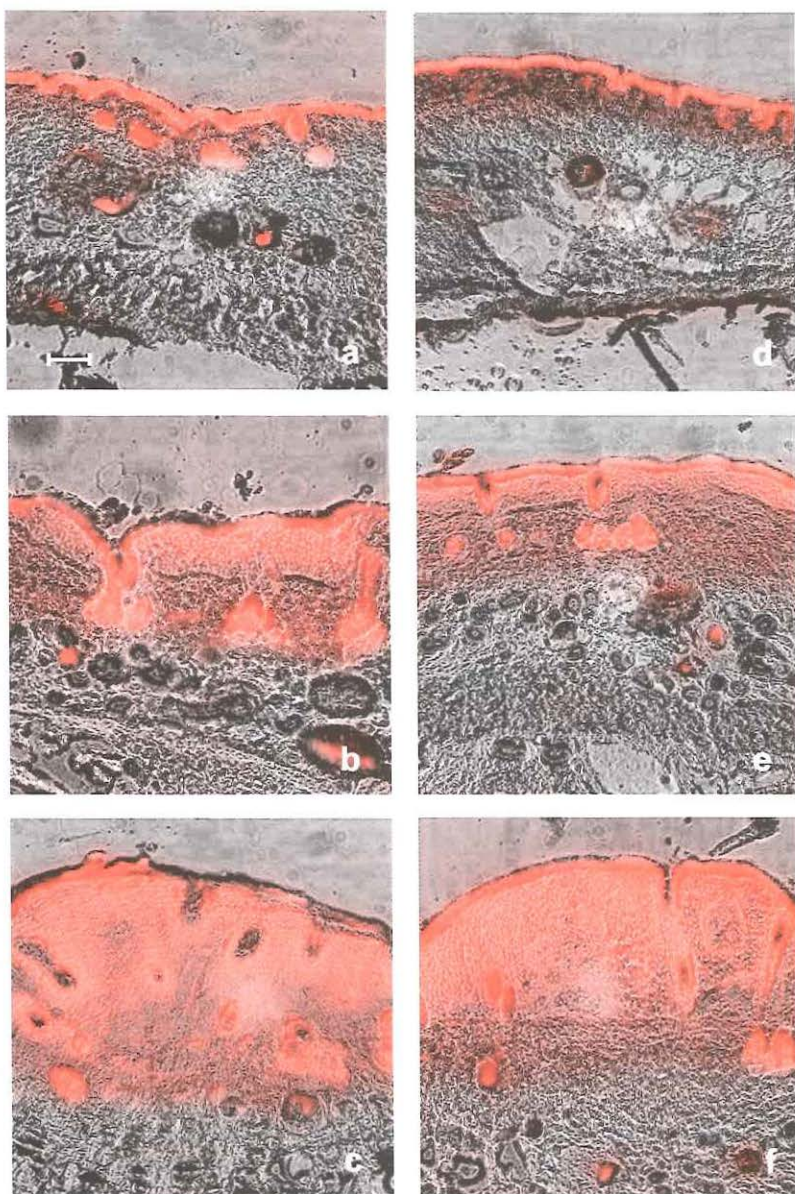


Figure 4 Combined microscopic phase contrast and fluorescence images of mouse normal skin after ALAPE application (a), altered skin after ALAPE application (b), visible lesions after ALAPE application (c), normal skin after ALA application (d), altered skin after ALA application (e), visible lesions after ALA application (f). The images are recorded from skin samples taken at 6 hours after the 30 minutes application of ALA or ALAPE. The PpIX fluorescence distribution is shown in red and the white bar represents 100 μm .

figure 4 clearly illustrates that the increasing *in vivo* fluorescence signals going from normal skin to altered skin and visible lesions reflect an increase in fluorescent epidermal volume rather than an increased fluorophore concentration.

In all skin layers in normal skin, altered skin and visible lesions, the same auto-fluorescence ($t=0$) levels were measured (figure 5 and 6). In dermis, deep dermis and muscle, no or low levels of PpIX fluorescence above autofluorescence were measured after application of ALA or ALAPE (data not shown).

After ALA or ALAPE application, PpIX fluorescence in normal skin, altered skin and visible lesions is mainly located in epidermis and hair follicles (figure 5) and is maximal at 6 hours post application. There is no difference between ALA- and ALAPE-induced PpIX fluorescence in the hair follicles of altered skin and visible lesions. In hair follicles of normal skin, the PpIX fluorescence at 6 and 12 hours application is higher after ALAPE application compared to ALA application. The PpIX fluorescence values in the whole epidermis are similar in normal skin and visible lesions and higher than in altered skin (figure 5b). However, this is different when in altered skin and visible lesions the stratum corneum is being considered as a separate layer from the epidermis, as shown in figure 6. There is no difference between ALA and ALAPE-induced PpIX fluorescence in epidermis without stratum corneum from altered skin and visible lesions (figure 6a). Also

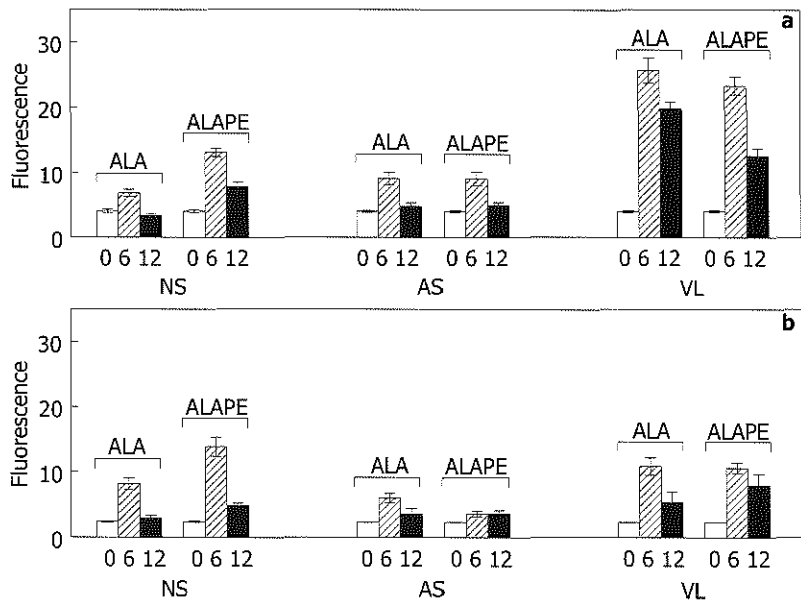


Figure 5 PpIX fluorescence in hair follicles (a) and epidermis (b) from normal skin (NS), altered skin (AS) and visible lesions (VL) after 30 minutes topical application of 20% ALA or 20% ALAPE. Fluorescence before (0) and at 6 hours (6) and 12 hours (12) post application are displayed. PpIX fluorescence units are arbitrary, but comparable between (a), (b) and figure 6. Error bars indicate standard deviation.

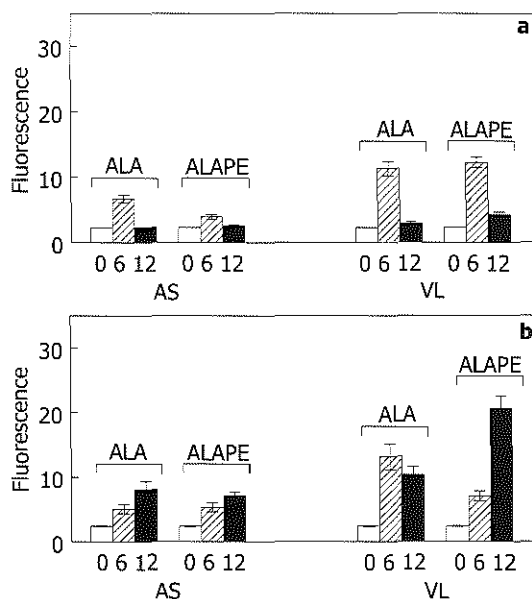


Figure 6 PpIX fluorescence in epidermis without stratum corneum (**a**) and stratum corneum (**b**) from normal skin (NS), altered skin (AS) and visible lesions (VL) after 30 minutes topical application of 20% ALA or 20% ALAPE. Fluorescence before (0) and at 6 hours (6) and 12 hours (12) post application are displayed. PpIX fluorescence units are arbitrary, but comparable between (a), (b) and figure 5. Error bars indicate standard deviation.

in the stratum corneum of altered skin, ALA and ALAPE-induced PpIX fluorescence levels are the same (figure 6b). Figure 6b also shows that ALA-induced PpIX fluorescence in the stratum corneum is maximal at 6 hours post application. In case of ALAPE application, the PpIX fluorescence values are highest at 12 hours post application. This ALAPE-induced PpIX fluorescence in the stratum corneum at 12 hours is higher than the ALA-induced PpIX fluorescence at 12 hours (unpaired Student t-test, $P < 0.01$).

Discussion

We have used PpIX fluorescence as a measure of PpIX content in the tissues both *in vivo* and in fluorescence microscopy. One may wonder whether environmental factors or aggregation could affect the quantum yield and thus invalidate fluorescence for quantification of PpIX content and distribution. Since PpIX is formed in the mitochondria directly from ALA or from ALA after conversion of ALAPE, the PpIX formed in both ways will be in a similar environment, so that fluorescence should be a valid measure in the comparison.

Several ALA derivatives have been investigated for their ability to improve PpIX production, penetration depth and distribution. In *in vitro* studies, several ALA esters increased the PpIX production in different cell lines (22-24), with the long-chained esters being more efficient than the short-chained ones (23,24). Exception is ALAME, which induced lower PpIX production in cells *in vitro* (23,24,33). Also in human solar keratoses and the adjacent normal skin, the ALAME-induced PpIX production was lower when compared with ALA (26). However, the PpIX ratio in the keratoses versus adjacent normal skin was improved with ALAME. Clinical and *in vitro* investigations showed that ALAHE (a long-chained ALA ester) is a much better precursor than ALA for PpIX production in bladder mucosa (27,28). When ALAHE was applied topically to *ex vivo* human or porcine mucosa at much lower concentration than ALA, PpIX synthesis in the urothelium was increased and accelerated (27). Furthermore, the PpIX fluorescence is accumulated and distributed more homogeneously in the urothelium. The clinical study showed that the photodetection of (pre)malignant lesions in the bladder after ALAHE application is better than after ALA application, even at lower concentrations and shorter application times (28). So far, only short-chained ALA esters have been applied topically *in vivo* to nude mouse skin (29,30). ALAME, ALA ethyl ester or ALA propyl ester were applied for 14 hours to normal nude mouse skin. After 3 hours application, the PpIX levels were similar for ALA and these three short-chained esters, but much more PpIX fluorescence was measured in the epidermis and hair follicles after 14 hours application. Thus, so far the long-chained ALAHE seemed to be successful when instilled in the bladder (27,28) and short-chained ALA esters seemed to improve the PpIX production in the nude mouse skin after long application times (29,30).

In our hairless mouse model, ALAPE increased the PpIX production in altered skin and visible lesions of the UVB-irradiated mouse skin, but not in the normal skin of untreated mice (figure 3). However, this slight increase in altered skin and visible lesions is much less compared to what was found in the *in vitro* study with ALAPE in cells (23). Also in the *in vivo* study, short-chained esters increased the PpIX production much more in the nude mouse skin after long-term application than ALAPE in the hairless model (29,30). These differences might be explained as follows. The diffusion of drugs into the skin is believed to be passive and to be limited by the barrier function of the stratum corneum, which is the outermost layer of the skin (34,35). The stratum corneum probably also has a strong barrier effect on the diffusion of ALA and its derivatives. The passive diffusion of ALA esters across or into the stratum corneum might be enhanced compared to ALA because of the higher lipophilicity of these esters. The diffusion of ALAPE through the stratum corneum may be less increased compared to the short-chained esters, because ALAPE may be too lipophilic and therefore not diffuse through but into the lipophilic stratum corneum. Another explanation for the difference between our ALAPE observations and the short-chained ester data might be the difference in application time. In our study, ALAPE was applied for 30 minutes and after a longer application time

period, the PpIX fluorescence kinetics might be different. The ALA-induced PpIX fluorescence is not lower than the short-chained ester-induced PpIX fluorescence after the relatively short application time of 3.5 hours (29).

ALAHE and ALAPE are both long-chained ALA esters, the only difference is that ALAHE has one more carbon atom in the alkyl chain. However, ALAHE induced much more PpIX fluorescence in (pre)malignant lesions in the bladder compared to ALAPE in the hairless mouse model (28). The difference between ALAHE in the bladder and ALAPE in the skin is likely to be caused by the differences in the structure of the skin and the bladder mucosa. Normal epithelium in the bladder has a high permeability barrier to water, protons and small ions, located in the apical membrane of the superficial epithelial cells (36-39). However, during carcinogenesis, the apical cells of (pre)malignant lesions, like carcinoma *in situ* and papillary tumors, de-differentiate and the highly impermeable membrane is replaced by a membrane that is more permeable (36,38), probably due to the more chaotically organised (pre)malignant cells. This might explain the selectivity of photodetection of (pre)malignant lesions in the bladder with ALA and ALA ester-induced PpIX fluorescence. Probably, ALAHE is enabled by its higher lipophilicity to diffuse more into the (pre)malignant lesions in the bladder than ALA does. This latter phenomenon might also occur in the hairless mouse model, but possibly to a much less extent than in the bladder. The barrier function of the stratum corneum might be changed in the UVB-induced lesions in this model, compared to that in the normal hairless mouse skin. This change might then allow a greater diffusion of ALA and ALAPE into the lesions compared to normal skin. Its higher lipophilicity may allow ALAPE to diffuse even more into these (pre)malignant lesions than ALA does.

In the microscopic fluorescence images, the ALAPE-induced PpIX fluorescence was not greater than the ALA-induced PpIX fluorescence in the epidermis of altered skin and visible lesions (figure 5b). However, ALAPE induced more PpIX fluorescence in the stratum corneum of visible lesions than ALA at 12 hours after application. This indicates that the higher ALAPE-induced PpIX fluorescence levels in the lesions as measured *in vivo* at 12 hours after application, are located in the stratum corneum. The PpIX might be produced in the living epidermal or basal cells and thereafter diffuse into the stratum corneum. Another possibility is that the living, but dying keratinizing cells in the stratum corneum are still able to produce PpIX. These keratinizing cells are the innermost layer of the stratum corneum and the microscopic fluorescence images show that the PpIX fluorescence in the stratum corneum of altered skin and visible lesions is mainly located in that innermost part of the stratum corneum (figure 4b-f). The greater ALAPE-induced PpIX fluorescence, compared to ALA, in the whole epidermis of normal skin might also be located in these keratinizing cells in the stratum corneum. However, this greater PpIX level in the microscopic fluorescence images of the normal skin epidermis (figure 5b) is not in agreement with the *in vivo* PpIX fluorescence results in the normal hairless mouse skin (figure 3a). The microscopic fluorescence images showed no difference in ALA- and

ALAPE-induced PpIX fluorescence in the epidermis without stratum corneum (of altered skin and visible lesions), dermis and muscle layer (of normal skin, altered skin and visible lesions). This indicates that ALAPE does not penetrate deeper into the skin than ALA does during and after 30 minutes application.

Conclusions

ALAPE slightly increased the *in vivo* PpIX fluorescence kinetics compared to ALA in the UVB-induced altered skin and visible lesions, but not in the normal mouse skin. The microscopic fluorescence images showed that this ALAPE-induced higher PpIX fluorescence is located in the stratum corneum and not in the dysplastic cells of the epidermis. The PpIX levels in the epidermis, dermis and muscle layer were similar after ALA and ALAPE application. This indicates that ALAPE diffuses to higher extent into the stratum corneum, but not into the dysplastic layer of the skin.

Acknowledgements

This work was supported by the European Community, contract number BMH4-CT97-2260 (JTHMvdA). We thank Henk de Vries for his assistance in synthesizing ALA pentyl ester, Otto Speelman for his assistance in performing the fluorescence kinetics measurements and Hans Vuijk for his assistance in preparing the photographs.

References

1. Henderson BW, Dougherty TJ. How does photodynamic therapy work? *Photochem Photobiol* 1992; 55(1):145-157.
2. Kennedy JC, Pottier RH, Pross DC. Photodynamic therapy with endogenous protoporphyrin IX: basic principles and present clinical experience. *J Photochem Photobiol B* 1990; 6:143-148.
3. Peng Q, Berg K, Moan J, Kongshaug M, Nesland JM. 5-Aminolevulinic acid-based photodynamic therapy: principles and experimental research. *Photochem Photobiol* 1997; 65(2):235-251.
4. Kennedy JC, Marcus SL, Pottier RH. Photodynamic therapy and photodiagnosis using endogenous photosensitization induced by 5-aminolevulinic acid: mechanisms and clinical results. *J Clin Laser Med Surg* 1996; 14(5):289-304.
5. Rhodes LE, Tsoukas MM, Anderson RR, Kollias N. Iontophoretic delivery of ALA provides a quantitative model for ALA pharmacokinetics and PpIX phototoxicity in human skin. *J Invest Dermatol* 1997; 108(1):87-91.
6. Stenzl A, Eder I, Kostron H, Klocker H, Bartsch G. Electromotive diffusion (EMD) and photodynamic therapy with δ -aminolaevulinic acid (δ -ALA) for superficial bladder cancer. *J Photochem Photobiol B* 1996; 36:233-236.
7. Ma L-W, Moan J, Peng Q, Iani V. Production of protoporphyrin IX induced by 5-aminolevulinic acid in transplanted human colon adenocarcinoma of nude mice can be increased by ultrasound. *Int J Cancer* 1998; 78:464-469.
8. Harth Y, Hirshowitz B, Kaplan B. Modified topical photodynamic therapy of superficial skin tumors, utilizing aminolevulinic acid, penetration enhancers, red light, and hyperthermia. *Dermatol Surg* 1998; 24(7):723-726.
9. Schoenfeld N, Mamet R, Nordenberg Y, Shafran M, Babushkin T, Malik Z. Protoporphyrin biosynthesis in melanoma B16 cells stimulated by 5-aminolevulinic acid and chemical inducers: characterization of photodynamic inactivation. *Int J Cancer* 1994; 56:106-112.
10. Kriegsmair M, Baumgartner R, Knuchel R, Ehsan A, Steinbach P, Lupmer W, Hofstaedter F,

Hofstetter A. Photodynamische diagnose urothelialer neoplasien nach intravesikaler instillation von 5-aminolaevulinsäure. *Urologe* 1994; 33:270-275.

11. Curnow A, McIlroy BW, Postle-Hacon MJ, Porter JB, MacRobert AJ, Bown SG. Enhancement of 5-aminolaevulinic acid induced photodynamic therapy using hydroxypyridinone iron chelating agents. *Br J Cancer* 1998; 78(10):1278-1282.

12. Bech Ø, Phillips D, Moan J, MacRobert AJ. A hydroxypyridinone (CP94) enhances protoporphyrin IX formation in 5-aminolaevulinic acid treated cells. *J Photochem Photobiol B* 1997; 41:136-144.

13. Berg K, Anholt H, Bech Ø, Moan J. The influence of iron chelators on the accumulation of protoporphyrin IX in 5-aminolevulinic acid-treated cells. *Br J Cancer* 1996; 74(5):688-697.

14. van der Veen N, de Bruijn HS, Star WM. Photobleaching during and re-appearance after photodynamic therapy of topical ALA-induced fluorescence in UVB-treated mouse skin. *Int J Cancer* 1997; 72:110-118.

15. van der Veen N, van Leengoed HLLM, Star WM. *In vivo* fluorescence kinetics and photodynamic therapy using 5-aminolevulinic acid-induced porphyrin: increased damage after multiple irradiations. *Br J Cancer* 1994; 70:867-872.

16. de Bruijn HS, van der Veen N, Robinson DJ, Star WM. Improvement of systemic 5-aminolevulinic acid-based photodynamic therapy *in vivo* using light fractionation with a 75-minute interval. *Cancer Res* 1999; 59(4):901-904.

17. van der Veen N, Hebeda KM, de Bruijn HS, Star WM. Photodynamic effectiveness and vasoconstriction in hairless mouse skin after topical 5-aminolevulinic acid and single- or two-fold illumination. *Photochem Photobiol* 1999; 70(6):921-929.

18. Curnow A, McIlroy BW, Postle-Hacon MJ, MacRobert AJ, Bown SG. Light dose fractionation to enhance photodynamic therapy using 5-aminolevulinic acid in the normal rat colon. *Photochem Photobiol* 1999; 69(1):71-76.

19. Messmann H, Mlkvy P, Buonaccorsi G, Davies CL, MacRobert AJ, Bown SG. Enhancement of photodynamic therapy with 5-aminolaevulinic acid-induced porphyrin photosensitisation in normal rat colon by threshold and light fractionation studies. *Br J Cancer* 1995; 72:589-594.

20. Robinson DJ, de Bruijn HS, van der Veen N, Stringer MR, Brown SB, Star WM. Fluorescence photobleaching of ALA-induced protoporphyrin IX

during photodynamic therapy of normal hairless mouse skin: the effect of light dose and irradiance and the resulting biological effects. *Photochem Photobiol* 1998; 67(1):140-149.

21. Robinson DJ, de Bruijn HS, van der Veen N, Stringer MR, Brown SB, Star WM. Protoporphyrin IX fluorescence photobleaching during ALA-mediated photodynamic therapy of UVB-induced tumors in hairless mouse skin. *Photochem Photobiol* 1999; 69(1):61-71.

22. Kloek J, Beijersbergen van Henegouwen GMJ. Prodrugs of 5-aminolevulinic acid for photodynamic therapy. *Photochem Photobiol* 1996; 64(6):994-1000.

23. Kloek J, Akkermans W, Beijersbergen van Henegouwen GMJ. Derivatives of 5-aminolevulinic acid for photodynamic therapy: enzymatic conversion into protoporphyrin. *Photochem Photobiol* 1998; 67(1):150-154.

24. Gaullier J-M, Berg K, Peng Q, Anholt H, Selbo PK, Ma L-W, Moan J. Use of 5-aminolevulinic acid esters to improve photodynamic therapy on cells in culture. *Cancer Res* 1997; 57:1481-1486.

25. Casas A, del C. Battle AM, Butler AR, Robertson D, Brown EH, MacRobert A, Riley PA. Comparative effect of ALA derivatives on protoporphyrin IX production in human and rat skin organ cultures. *Br J Cancer* 1999; 80(10):1525-1532.

26. Fritsch C, Homey B, Stahl W, Lehmann P, Ruzicka T, Sies H. Preferential relative porphyrin enrichment in solar keratoses upon topical application of δ -aminolevulinic acid methylester. *Photochem Photobiol* 1998; 68(2):218-221.

27. Marti A, Lange N, van den Bergh H, Sedmera D, Jichlinski P, Kucera P. Optimisation of the formation and distribution of protoporphyrin IX in the urothelium: an *in vitro* approach. *J Urol* 1999; 162:546-552.

28. Lange N, Jichlinski P, Zellweger M, Forrer M, Marti A, Guillou L, Kucera P, Wagnières GA, van den Bergh H. Photodetection of early human bladder cancer based on the fluorescence of 5-aminolaevulinic acid hexyl-ester-induced protoporphyrin IX: a pilot study. *Br J Cancer* 1999; 80(1/2):185-193.

29. Peng Q, Moan J, Warloe T, Iani V, Steen HB, Bjorseth A, Nesland JM. Build-up of esterified aminolevulinic-acid-derivative-induced porphyrin fluorescence in normal mouse skin. *J Photochem Photobiol B* 1996; 34:95-96.

30. Peng Q, Moan J, Iani V, Steen HB, Nesland JM. Studies on ALA derivative-induced protoporphyrin IX build-up in normal mouse skin. *Photochem Photobiol* 1995; 61:Abstract 82S
31. de Gruijl FR, van der Meer JWM, van der Leun JC. Dose-time dependency of tumour formation by chronic UV exposure. *Photochem Photobiol* 1983; 37:53-62.
32. de Gruijl FR, Sterenborg HJCM, Forbes PD, Davies RE, Cole C, Kelfkens G, van Weelden H, Slaper H, van der Leun JC. Wavelength dependence of skin cancer induction by ultraviolet irradiation of albino hairless mice. *Cancer Res* 1993; 53:53-60.
33. Washbrook R, Riley PA. Comparison of δ -aminolaevulinic acid and its methyl ester as an inducer of porphyrin synthesis in cultured cells. *Br J Cancer* 1997; 75(10):1417-1420.
34. Suhonen TM, Bouwstra JA, Urtti A. Chemical enhancement of percutaneous absorption in relation to stratum corneum structural alterations. *J Controlled Release* 1999; 59:149-161.
35. Williams AC, Barry BW. Skin absorption enhancers. *Crit Rev Ther Drug Carrier Syst* 1992; 9(3,4):305-353.
36. Hicks RM, Ketterer B, Warren RC. The ultrastructure and chemistry of the luminal plasma membrane of the mammalian urinary bladder: a structure with low permeability to water and ions. *Phil Trans R Soc Lond B* 1974; 268:23-38.
37. Negrete HO, Lavelle JP, Berg J, Lewis SA, Zeidel ML. Permeability properties of the intact mammalian bladder epithelium. *Am J Physiol* 1996; 271:F886-F894.
38. Fickweiler E. Biopharmacy of urologics. *Krankenhauspharmazie* 1991; 10:424-427.
39. Zeidel ML. Low permeabilities of apical membranes of barrier epithelia: what makes watertight membranes watertight? *Am J Physiol* 1996; 271:F243-F245.

CHAPTER 5

Topical application of 5-aminolevulinic acid hexyl ester and 5-aminolevulinic acid to normal nude mouse skin: Differences in protoporphyrin IX fluorescence kinetics and the role of the stratum corneum

This chapter was adapted from JTHM van den Akker, V Iani, WM Star, HJCM Sterenborg and J Moan. *Photochem Photobiol* 2000;72(5):681-689

Summary

An important limitation of topical 5-aminolevulinic acid (ALA)-based photodetection and photodynamic therapy is that the amount of the fluorescing and photosensitizing product protoporphyrin IX (PpIX) formed is limited. The reason for this is probably the limited diffusion of ALA through the stratum corneum. A solution to this problem might be found in the use of ALA derivatives, as these compounds are more lipophilic and therefore might have better penetration properties than ALA itself. Previous studies have shown that ALA hexyl ester (ALAHE) is more successful than ALA for photodetection of early (pre)malignant lesions in the bladder. However, ALA pentyl ester slightly increased the *in vivo* PpIX fluorescence in early (pre)malignant lesions in hairless mouse skin compared to ALA. However, the increased PpIX fluorescence is located in the stratum corneum and not in the dysplastic epidermal layer. In the present study, ALA- and ALAHE-induced PpIX fluorescence kinetics are compared in the normal nude mouse skin, of which the permeability properties differ from the bladder. Application times and ALA(HE) concentrations were varied, the effect of a penetration enhancer and the effect of tape stripping the skin before or after application were investigated. Only during application for 24 hours, did ALAHE induce slightly more PpIX fluorescence than ALA. After application times ranging from 1 to 60 minutes, ALA-induced PpIX fluorescence was higher than ALAHE-induced PpIX fluorescence. ALA induced also higher PpIX production than ALAHE after 10 minutes application with concentrations ranging from 0.5% to 40%. The results of experiments with the penetration enhancer and tape stripping indicated that the stratum corneum acts a barrier against ALA and ALAHE. Use of penetration enhancer or tape stripping enhanced the PpIX production more in case of ALAHE application than in case of ALA application. This, together with the results from the different application times and concentrations indicates that ALAHE diffuses more slowly across the stratum corneum than ALA.

Introduction

Administration of 5-aminolevulinic acid (ALA) to cells and tissues results in the production of protoporphyrin IX (PpIX), which can be used clinically as a photosensitizer for photodetection or photodynamic therapy (PDT) of cancer (1-3). Since ALA is a small molecule, it can penetrate through the skin and into tumors after topical application. However, an important drawback of topical application of ALA is that the bioavailability of ALA is limited by diffusion of ALA through biological barriers such as the stratum corneum. Therefore, high ALA doses have to be applied in order to achieve sufficiently high PpIX levels suitable for PDT (4-6). A solution to this problem might be the use of esterified ALA, which is more lipophilic than ALA itself. This higher lipophilicity might result in better penetration into the skin, higher PpIX levels and a more uniform and

deeper PpIX distribution.

Several ALA esters have been synthesized and tested *in vitro* in different cell lines (7-10). The long chained ALA esters were more efficient than the short ones in improving PpIX production in cells (9,10). In human and rat skin explant cultures, ALAHE proved to be successful in increasing PpIX production after incubation times of 5 and 19 hours (11). In this set-up, ALA and its derivatives are absorbed from the medium through the dermis to reach the epidermis, thus resembling more the systemic delivery of the compounds to the skin. In normal nude mouse skin, long-term application of short-chained ALA esters resulted in much higher epidermal PpIX fluorescence compared to long-term ALA application (12). Application of ALA methyl ester (ALAME) to human solar keratoses did not yield higher PpIX levels in the keratoses, but the PpIX fluorescence ratio between the keratoses and adjacent normal skin was increased (13). An *in vitro* and a clinical pilot study showed that the use of ALA hexyl ester (ALAHE) resulted in increased PpIX production in bladder dysplasia, carcinoma *in situ* and tumors (14,15). A PpIX fluorescence kinetics and fluorescence microscopy study in hairless mice with and without UVB-induced (pre)cancerous skin lesions showed that ALA pentyl ester induces only slightly more PpIX in the (pre)cancerous skin lesions compared to ALA (16). In normal skin, PpIX levels are the same after ALA and ALA pentyl ester application. The higher ALA pentyl ester-induced PpIX fluorescence in the (pre)cancerous lesions is located in the stratum corneum and not in the dysplastic epidermal layer.

The design of the present study is based on the ALA pentyl ester study in the hairless mice in which the results are, quite in contrast to our expectations, different from the results obtained with ALA hexyl ester in the bladder. Therefore, we investigated in the present study whether ALAHE and ALA have different properties regarding penetration and PpIX production in normal nude mouse skin after topical application and if possible differences in ALA and ALAHE uptake into the skin are dependent on application time and applied concentration. Another important factor in topical application is that the main limitation for diffusion of ALA and its derivatives into the skin is the skin itself. The skin consists of three layers: subcutaneous tissue, dermis and epidermis, being the outermost layer. The superficial layer of the epidermis, which is the stratum corneum, acts as the main barrier against the external environment (17-19). The barrier function of the skin is to a large extent attributed to the structure of the stratum corneum, which consists of several layers of dead cells (corneocytes, mainly containing keratin) that are embedded in a lipid matrix (17-20). This structure is often presented as a "brick and mortar" model. The diffusion of drugs through the epidermis is believed to be passive (17,18), mainly across the intact epidermis and little via the skin appendages (hair follicles and sweat glands). The rate-determining step in the epidermal route is the diffusion across the stratum corneum. The diffusion pathway through the stratum corneum can be transcellular (across the corneocytes and the intercellular lipids) or

intercellular (via the lipid matrix between the corneocytes). The latter route is believed to be the principal route and thus the major barrier for drug permeation (17,18).

A solution to the problem of getting drugs to penetrate the skin might be the use of chemicals that alter the structure and permeation properties of the stratum corneum in such a way that penetration of drugs through this major barrier is facilitated. Many groups of chemicals are known to enhance the absorption of drugs through the stratum corneum (17,18). One group of successful penetration enhancers are the azacycloalkane derivatives, like HPE-101 and Azone (17,18,21-25). The mechanism of penetration enhancement of the azacycloalkane derivatives has been thoroughly investigated with Azone (18,23,25). Azone increases the disorder in the lipids within the intercellular space of the stratum corneum by upsetting packing of the tails and increasing their fluidity, permitting easier diffusion of compounds through the stratum corneum. HPE-101 has been shown to further improve penetration as compared to Azone (21,22,24). In this study we use HPE-101 as a penetration enhancer for the diffusion of ALA and ALAHE into the normal mouse skin to investigate whether and to what extent the stratum corneum acts as a barrier for the uptake of ALA and ALAHE in the epidermis. Another approach to facilitate the penetration of drugs is removing the stratum corneum by tape stripping the skin before application. PDT effects after ALA application to normal skin of hairless guinea pigs were increased dramatically when the stratum corneum was reduced by tape stripping before ALA application (26). The results from this study indicate that the stratum corneum limits the ALA penetration into the skin.

ALA- and ALAHE-induced PpIX fluorescence in the nude mouse skin was measured after application times ranging from 1 to 60 minutes and during a 24 hours application. The influence of different ALA and ALAHE concentrations, the effect of penetration enhancer and the effect of tape stripping the skin on the PpIX production was determined after 10 minutes application. The amount of PpIX produced with this short application time is mainly limited by the diffusion of ALA or ALAHE into the skin rather than the enzymatic processes involved in the PpIX production from ALA or ALAHE.

Materials and methods

Chemicals

ALA and ALAHE were kindly supplied by Photocure AS (Oslo, Norway). The molecular structures of ALA and ALAHE are shown in figure 1. HPE-101 was a gift from Hisamitsu Pharmaceuticals (Tokyo, Japan). All other reagents and solvents were of analytical grade and were used as purchased.

Animals

Inbred female albino nude mice (BALB/c, Norwegian Radium Hospital, Oslo, Norway) were used.

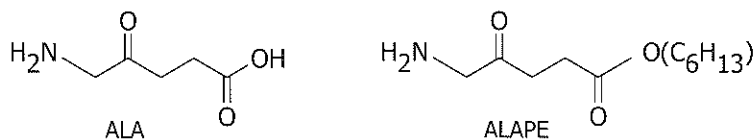


Figure 1 Structure of ALA and ALA hexyl ester (ALAHE).

Fluorescence measurements

A fiber-optic probe was coupled to a Perkin-Elmer LS50B luminescence spectrometer for *in vivo* fluorescence measurements. This probe is made of a commercially available fiber accessory (Perkin-Elmer, two 1m fussed silica fiber bundles joined in parallel at the measuring tip) fitted with a cylinder shaped aluminum spacer. This spacer is 6.5 mm in diameter and provides a constant fixed distance of 10 mm between the fibers and the tissue. This assures a relatively uniform light distribution over the measuring area and provides the maximum fluorescence signal for a given sample. Fluorescence intensity was measured at the application site as a function of time. The excitation wavelength was set at 407 nm and fluorescence was measured at 636 nm. In addition, fluorescence emission spectra were measured to verify that the fluorescence signal originated from PpIX fluorescence. The 407 nm light from the spectrophotometer was of low intensity ($1.5 \mu\text{W}/\text{cm}^2$) and did not induce photobleaching. With 400 nm light, the effective attenuation coefficient for rat skin is 34 cm^{-1} (27) and if we assume that this value is the same for mouse skin, then 50% of the initial light intensity reaches 200 μm depth. The thickness of the mouse epidermis, where PpIX localizes after topical ALA (16,28) or ALA pentyl ester (16) application, is 20-50 μm . Therefore, the 407 nm light penetrates deep enough into the skin to excite the PpIX in the epidermis and dermis.

Application of ALA and ALAHE

Prior to application of ALAHE or ALA, the animals were anaesthetized intraperitoneally with Hypnorm® (Janssen Pharmaceutica B.V., Tilburg, The Netherlands) and Dormicum® (Hoffmann-La Roche AG, Basel, Switzerland). Creams containing ALA or ALAHE were prepared in a standard oil in water emulsion (Unguentum Merck, Germany) and approximately 0.15 gram of the cream was applied to one flank of the mice. The application site (1 centimeter in diameter) was occluded with an adhesive dressing (Smith and Nephew, England) during the whole application period. Application was finished by removing the adhesive dressing, carefully wiping off the cream and washing the mouse skin with water. Application of the cream was performed under different conditions for different groups of 6 animals. The conditions are described below and a summary is given in table 1. The pH values were measured of the creams with different concentrations ALA and ALAHE.

Variation of the application time

Cream containing 10% (w/w) ALA or ALAHE, was applied for different time periods. In one group, the cream was removed immediately after application ($t=0$). This group served as a control to determine whether the washing procedure removes all the ALA or ALAHE cream from the skin surface. In the other groups, the cream was applied for 1, 5, 10, 20 or 60 minutes, respectively. Fluorescence was measured up to 8 hours after the start of the application.

Variation of the concentration

Cream containing 0.5%, 2%, 5%, 10%, 20% or 40% (w/w) ALA or ALAHE was applied for 10 minutes. Fluorescence was measured up to 8 hours after the start of the application.

Continuous application

ALA or ALAHE cream was applied with concentrations of 20%, 10%, 2% or 0.5% (w/w). Fluorescence measurements were performed until the application was stopped at 24 hours. The fluorescence could be measured through the transparent occlusion tape, because the light absorbance by the tape was negligible.

Effect of a penetration enhancer

To a control group, the standard ointment (without ALA or ALAHE) containing 3% (w/w) penetration enhancer HPE-101 was applied for 60 minutes. To four groups, cream containing 10% (w/w) ALA or ALAHE with or without 3% (w/w) HPE-101 was applied for 60 minutes. In two groups, standard ointment containing 3% (w/w) HPE-101 was applied for 1 hour before 10% (w/w) ALA or ALAHE was applied for 10 minutes. In two other groups, 10% (w/w) ALA or ALAHE cream was applied for 10 minutes. Fluorescence measurements were performed up to 14 hours after the start of the application.

Effect of tape stripping

In a pilot study, normal nude mice were tape stripped 0, 5, 10, 15 or 20 times with Scotch® tape. Hematoxylin and eosin stained microscopic histological sections showed that the mouse skin needs to be tape stripped 20 times with the Scotch® tape to obtain complete removal of the stratum corneum without disrupting the underlying living layer of the epidermis. Therefore, the skin of the animals was stripped 20 times before or immediately after the 10 minutes application of cream containing 10% (w/w) ALA or ALAHE. Two control groups received the cream with 10% (w/w) ALA or ALAHE for 10 minutes without being tape stripped. Fluorescence was measured up to 14 hours after the start of the application.

Table 1 Summary of the experimental conditions.

Compound	Concentration % (w/w)	Application time	Other
ALA	10	0, 1, 5, 10, 20 and 60 min	
ALAHE	10	0, 1, 5, 10, 20 and 60 min	
ALA	0.5, 2, 10, 20 and 40	10 min	
ALAHE	0.5, 2, 10, 20 and 40	10 min	
ALA	0.5, 2, 10 and 20	24 h	
ALAHE	0.5, 2, 10 and 20	24 h	
None	-	60 min	With PE*
ALA	10	60 min	Without PE
ALA	10	60 min	With PE
ALA	10	10 min	Without PE
ALA	10	10 min	PE before
ALAHE	10	60 min	Without PE
ALAHE	10	60 min	With PE
ALAHE	10	10 min	Without PE
ALAHE	10	10 min	PE before
ALA	10	10 min	
ALA	10	10 min	TS [†] before
ALA	10	10 min	TS after
ALAHE	10	10 min	
ALAHE	10	10 min	TS [†] before
ALAHE	10	10 min	TS after

*Penetration enhancer

†Tape stripping

Data analysis and statistics

All fluorescence measurements were corrected for the autofluorescence background. After subtraction of the autofluorescence, the corrected 636 nm fluorescence values were plotted as a function of time after start of the application. In addition, ratios (of PpIX fluorescence) between ALA and ALAHE for all time points within each group (for the groups see table 1) were calculated. When the ALA/ALAHE ratios within a group were significantly not different for all time points, as tested with analysis of variance (ANOVA), a mean ALA/ALAHE ratio was calculated for that group (table 3). In case of significantly different ALA/ALAHE ratios within a group (ANOVA), another type of ALA/ALAHE ratio was calculated; the maximal ALA-induced PpIX fluorescence was divided by the maximal ALAHE-induced PpIX fluorescence (table 3). The ALA/ALAHE ratios in table 3 were tested with the unpaired Student t-test (in case of 2 numbers per group) or with ANOVA and the Student-Newman-Keuls (SNK) test (in case of more than 2 numbers per group) to see whether they were different from each other.

Results

Varying application time

No PpIX fluorescence above the autofluorescence level was measured after 0 minutes application of ALA or ALAHE (data not shown), indicating that the removing and washing procedure was adequate. The PpIX fluorescence kinetics after the different application times of ALA and ALAHE are shown in figure 2. The PpIX fluorescence intensity maximum increases with increasing application time of ALA or ALAHE. For each application time, the maximum PpIX fluorescence is higher after ALA application than after ALAHE application. The ALA-induced PpIX fluorescence maximum shifts to later time points with increasing application time, from 1 hour (1 minute application) to 4 hours (60 minutes application) after the start of the application. The mean ALA/ALAHE ratio for the groups of 1, 5, 10 and 20 minutes application time are shown in table 3. No mean ALA/ALAHE ratio can be calculated in case of 60 minutes application time, because the maximum PpIX fluorescence is shifted from 3 hours after ALAHE application to 4 hours after ALA application. Furthermore, ALAHE-induced PpIX levels decrease from 4 hours after the start of application, while the ALA-induced PpIX remains at its maximum level till 6 hours after the start of application. Because of these differences between ALA and ALAHE application, the shapes of the ALA and the ALAHE curve are different, resulting in different ALA/ALAHE ratios per time point (ANOVA, $P<0.01$).

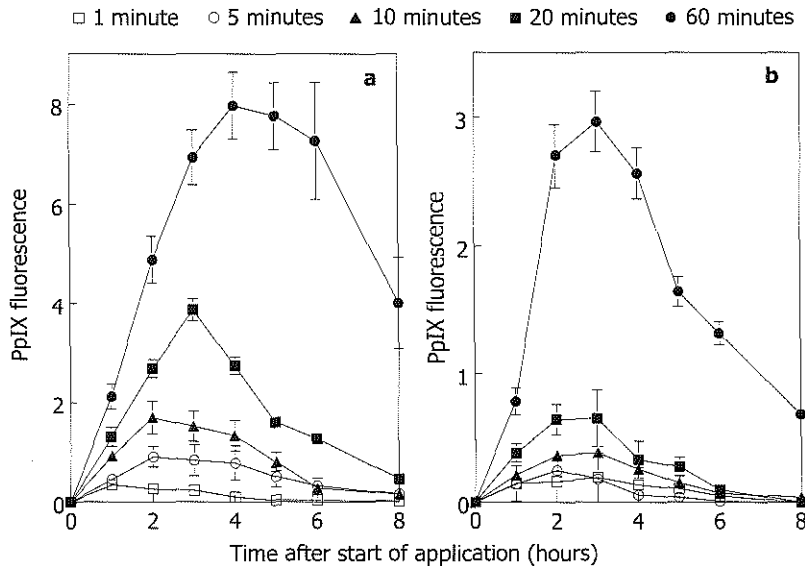


Figure 2 In vivo PpIX fluorescence kinetics in nude mouse skin after 10% (w/w) (a) ALA or (b) ALAHE application. The cream was applied for 1 (open squares), 5 (open circles), 10 (solid triangles), 20 (solid squares) or 60 (solid circles) minutes. PpIX fluorescence units are arbitrary, but comparable between all curves. Error bars indicate standard error of the mean.

Table 2 pH values of the ointments with different concentrations of ALA or ALAHE.

Concentration	pH of the ointment					
	0%	0.5%	2%	10%	20%	40%
ALA	4.8	3.9	3.0	1.9	1.4	1.1
ALAHE	4.8	4.5	4.3	4.1	3.8	3.3

Therefore, the ALA/ALAHE ratio between the maximal ALA- and the maximal ALAHE-induced PpIX fluorescence was calculated (table 3). The ALA/ALAHE ratio for the 1 minute application is significantly smaller than the 5, 10, 20 and 60 minutes application times (SNK, $P < 0.05$). The ALA/ALAHE ratios for the 5, 10, 20 and 60 minutes application time are not significantly different (SNK).

Varying concentration

The properties of the ALAHE creams were strikingly different from the ALA creams. The 0.5% and 2% ALAHE cream and the 0.5%, 2%, 10% and 20% ALA cream had a similar structure as the cream without ALA or ALAHE. The 40% ALA cream was somewhat more oily than the pure cream. The changes in the ALAHE cream are ranging from more oily than the pure cream (10% and 20%) to a fluid cream (40%). The pH value of the ALA cream decreased faster than the ALAHE cream with increasing concentration (table 2).

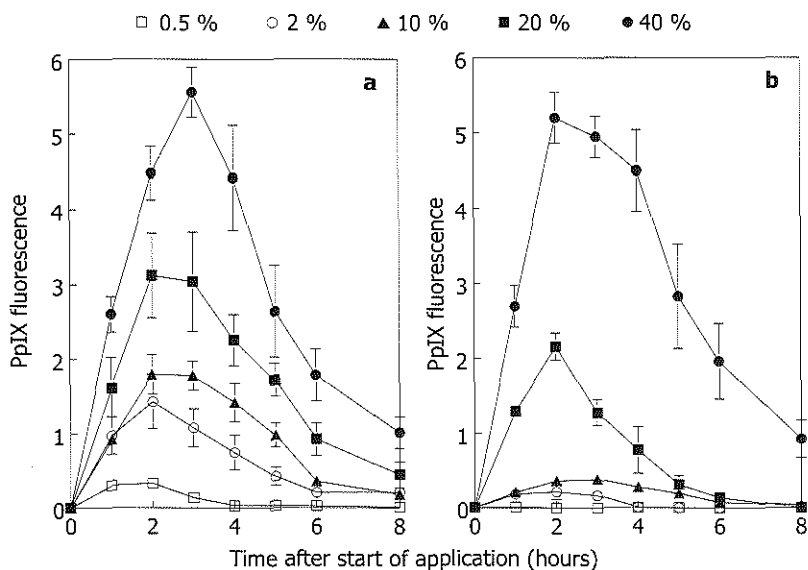


Figure 3 In vivo PpIX fluorescence kinetics in nude mouse skin after 10 minutes (a) ALA or (b) ALAHE application. The concentration of ALA or ALAHE in the cream was 0.5% (open squares), 2% (open circles), 10% (solid triangles), 20% (solid squares) or 40% (solid circles). PpIX fluorescence units are arbitrary, but comparable between all curves. Error bars indicate standard error of the mean.

Figure 3 shows that the maximum PpIX fluorescence levels increase with increasing application concentrations of ALA or ALAHE. The PpIX fluorescence maximum is the same after application of 40% ALA and 40% ALAHE. For the other concentrations, ALA-induced maximum PpIX levels are higher than the ALAHE-induced maximum PpIX levels. No PpIX fluorescence was measured after application of 0.5% ALAHE (and therefore not shown in figure 3b). The PpIX fluorescence maximum is around 2 to 3 hours after the start of the application for all application concentrations of ALA and ALAHE, possibly slightly earlier for ALAHE than for ALA.

No ALA/ALAHE ratio of the PpIX fluorescence can be calculated for the 0.5% and the 2% application concentration because the PpIX fluorescence levels are zero or too small after application of 0.5% or 2% ALAHE. Table 3 shows the ALA/ALAHE ratios of the PpIX fluorescence for 10%, 20% and 40% application. The 10% ALAHE-induced PpIX fluorescence levels are small which results in a relatively large ALA/ALAHE ratio of the PpIX fluorescence. The ALA/ALAHE ratio of the PpIX fluorescence for the 10% concentration is larger (SNK, $P < 0.01$) than the 20% and the 40%, which are not significantly different from each other (SNK).

Continuous application

The PpIX fluorescence kinetics during continuous application of ALA and ALAHE up to 14 hours after start of the application are shown in figure 4. At 24 hours after start of the

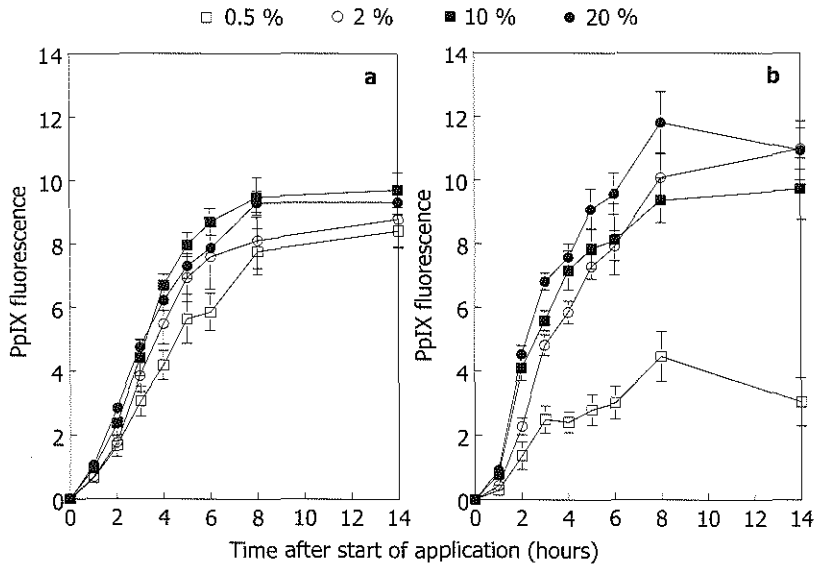


Figure 4 In vivo PpIX fluorescence kinetics in nude mouse skin during continuous application of (a) ALA or (b) ALAHE application. The concentration of ALA or ALAHE in the cream was 0.5% (open squares), 2% (open circles), 10% (solid squares) or 20% (solid circles). Error bars indicate standard error of the mean.

application, the PpIX fluorescence has decreased for all concentrations of ALA and ALAHE (data not shown). Only the 0.5% ALAHE-induced PpIX fluorescence is lower than the PpIX fluorescence after 0.5% ALA. For the other concentrations, the ALAHE-induced PpIX levels are slightly higher than the corresponding ALA-induced PpIX levels.

The ALA/ALAHE ratios are shown in table 3 and the ALA/ALAHE ratio for 0.5% application is significantly higher than the other ratios (SNK, $P < 0.01$). The 2%, 10% and 20% ALA/ALAHE ratios are the same (SNK).

Addition of penetration enhancer

Figure 5 shows that the penetration enhancer HPE-101 changes the kinetics of ALA- and ALAHE-induced PpIX. When ALA is applied 60 minutes in the presence of HPE-101, the maximum fluorescence is reached at the same time point (3 hours after start of application) and has the same level as with ALA application alone (figure 5a). However, HPE-101 induces a broader curve with a maximum shifted to a later time point, but the ALA-induced PpIX fluorescence levels with and without HPE-101 have again the same height at 14 hours from the start of application (figure 5a). When ALAHE is applied alone or together with HPE-101 for 60 minutes, maximal PpIX fluorescence is at 3 hours after start of the application (figure 5b). The PpIX fluorescence maximum after ALAHE

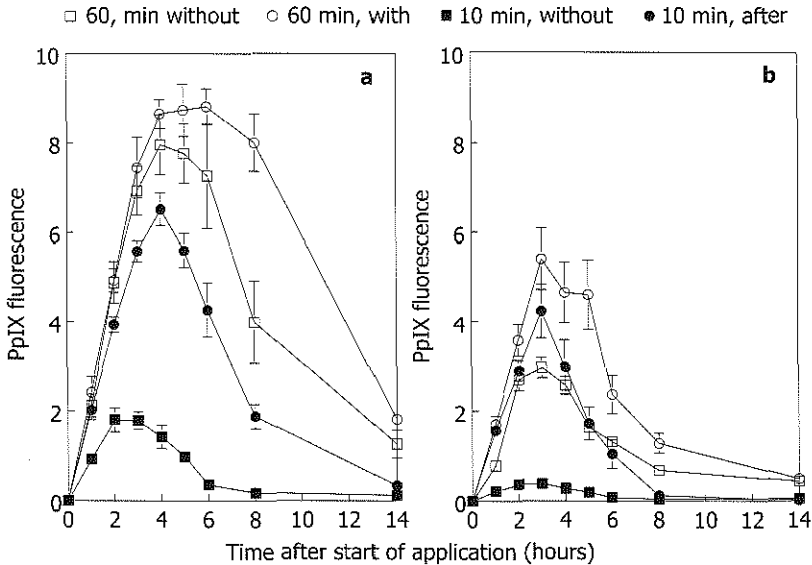


Figure 5 *In vivo* PpIX fluorescence kinetics in nude mouse skin after 10% (w/w) (a) ALA or (b) ALAHE application. The cream was applied for 60 minutes without (solid circles) or in the presence (solid squares) of 3% penetration enhancer HPE-101. The cream with ALA or ALAHE was applied for 10 minutes (open circles) or for 10 minutes after 60 minutes pretreatment (open squares) of 3% penetration enhancer HPE-101. PpIX fluorescence units are arbitrary, but comparable between all curves. Error bars indicate standard error of the mean.

together with HPE-101 is 1.8 times higher than after ALAHE alone.

Sixty minutes pretreatment with HPE-101 has a much larger effect on the ALA and ALAHE application for 10 minutes (figure 5). The PpIX fluorescence maximum induced by 10 minutes ALA after HPE-101 pretreatment is 3.6 times higher than after 10 minutes ALA alone. Furthermore the PpIX fluorescence maximum is shifted from 2 hours after start of application for ALA alone to 4 hours after start of application of ALA to skin pretreated with HPE-101 (figure 5a). When pretreated with HPE-101, the ALAHE-induced PpIX maximum fluorescence level is increased by a factor 11 and at the same time point (3 hours after start of application) as the ALAHE-induced PpIX maximum without HPE-101 pretreatment (figure 5b).

No mean ALA/ALAHE ratio for 60 minutes application without HPE-101 can be calculated, because of the different shapes of the ALA and the ALAHE curve, resulting in different ALA/ALAHE ratios per time point (ANOVA, $P < 0.01$). Therefore, the ALA/ALAHE ratio for 60 minutes application with or without HPE-101 was calculated between the maximal ALA- and the maximal ALAHE-induced PpIX fluorescence (table 3). The ALA/ALAHE ratio for the HPE-101 cotreatment is significantly lower than the ALA/ALAHE ratio without HPE-101 (t-test, $P < 0.02$).

The ALA/ALAHE ratios for 10 minutes application without and after HPE-101

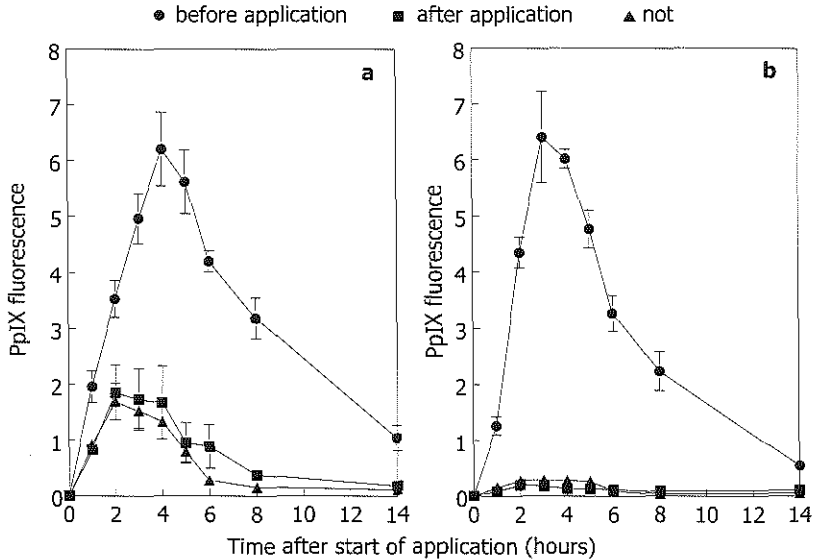


Figure 6 *In vivo* PpIX fluorescence kinetics at the application side on nude mouse skin after 10 minutes of 10% (w/w) (a) ALA or (b) ALAHE application. Skin was not tape stripped (solid triangles), tape stripped immediately after application (solid squares) or tape stripped before application (solid circles). PpIX fluorescence units are arbitrary, but comparable between all curves. Error bars indicate standard error of the mean.

pretreatment are given in table 3. The ALA/ALAHE ratio for the HPE-101 pretreatment is significantly lower than the ALA/ALAHE ratio without HPE-101 (t-test, $P < 0.01$).

Tape stripping

When the mouse skin is tape stripped before application of ALA or ALAHE, the maximum PpIX fluorescence increases dramatically and reaches the same level after ALA and ALAHE application (figure 6). The ALA- and ALAHE-induced PpIX fluorescence kinetics in the skin that is tape stripped immediately after the application are the same as those in the non tape stripped skin.

The ALA/ALAHE ratios of the three groups are given in table 3. The ratio for the tape stripped group is significantly smaller than that of the non tape stripped group and of the group stripped after application (SNK test, $P < 0.01$). The latter two groups have the same ALA/ALAHE ratio (SNK test).

Table 3 ALA/ALAHE ratios for the different experimental conditions. ALA/ALAHE ratio values within a treatment group are tested with Student t-test. All differences are considered significant at $P < 0.05$.

Treatment		ALA/ALAHE ratio Value \pm standard deviation	
Different application times	1 min	*1.2 \pm 0.74	††
	5 min	*3.5 \pm 1.6	
	10 min	*4.4 \pm 1.3	
	20 min	*4.3 \pm 1.3	
	60 min	†2.7 \pm 0.76	
Different application concentrations	10%	*4.8 \pm 1.2	††
	20%	*1.5 \pm 0.45	
	40%	*0.98 \pm 0.12	
Continuous application	0.5%	*1.7 \pm 0.31	††
	2%	*0.87 \pm 0.037	
	10%	*0.92 \pm 0.042	
	20%	*0.77 \pm 0.022	
Penetration enhancer, 60 minutes application	Without	†2.7 \pm 0.76	§
	With	†1.6 \pm 0.54	
Penetration enhancer, 10 minutes application	Without	*4.1 \pm 1.2	§
	After	*1.4 \pm 0.21	
Tape stripping	Not	*4.4 \pm 0.90	
	After	*3.2 \pm 1.3	
	Before	*1.0 \pm 0.12	††

*ALA/ALAHE ratio is the mean ALA/ALAHE ratio for all time points within the group.

†ALA/ALAHE ratio is between maximal ALA- and maximal ALAHE-induced PpIX fluorescence.

††Significantly different from the other ALA/ALAHE ratios within the treatment group, SNK test.

§Significantly different from the other ALA/ALAHE ratio within the treatment group, t-test.

Discussion

We have used PpIX fluorescence as a measure of PpIX content in the nude mouse skin. The relation between the detected fluorescence signal and the concentration is rather complicated, depending on a number of factors like the distribution of the photosensitizer in the tissue. Nevertheless, a higher PpIX content in the skin results in a higher fluorescence signal. We compare PpIX formed directly from ALA with PpIX formed from ALA after conversion of ALAHE, so we are confident that environmental factors will affect PpIX fluorescence from ALA or ALAHE in the same fashion. The fluorescence should therefore be a reliable measure of relative PpIX content for comparing ALA- and ALAHE- induced PpIX fluorescence in the nude mouse skin.

So far, ALA methyl ester, ethyl ester, propyl ester and hexyl ester are the only ALA derivatives that have been successful in improving PpIX production *in vivo* (12,13,15). Long-term application of ALA methyl, ethyl and propyl ester resulted in much higher epidermal PpIX fluorescence in normal mouse skin compared to long-term ALA application (12). ALAME is the only ALA derivative that has been used topically on the skin of patients with solar keratoses (13). ALAME did not increase the PpIX production compared to ALA in those keratoses. However, the ALAME-induced PpIX fluorescence was much lower in the adjacent normal skin compared to ALA-induced PpIX fluorescence in normal skin, resulting in an increased PpIX ratio between the keratoses and the adjacent skin. In hairless mice, ALA pentyl ester induces slightly more PpIX in the stratum corneum of (pre)cancerous skin lesions compared to ALA, but not in normal skin (16).

A clinical pilot study showed that ALAHE can improve the ALA-based photodetection of dysplasia and early bladder cancer. The instillation time could be reduced and a twofold increase in fluorescence signal was obtained with a 20 times lower concentration of ALAHE compared to ALA (15). When ALA or ALAHE is instilled in the bladder, PpIX fluorescence is found selectively in dysplasia, papillary tumors and carcinoma *in situ* (15,29,30). This selectivity and the reason why ALAHE is superior to ALA is not known, but might be explained as follows. The normal epithelium of the bladder is known to have a low permeability to water, protons and small ions (31-34). This bladder permeability barrier is localized in the apical membrane of the superficial epithelial cells (31,33). However, when lesions occur and during carcinogenesis in the bladder, structural changes occur in the apical membrane (31,33). The apical cells de-differentiate and the highly impermeable membrane is replaced by a thinner membrane, which has a higher permeability. Thus, during instillation in the bladder, little ALA or ALAHE diffuses into the normal epithelium, while much more ALA and ALAHE can diffuse into lesions like dysplasia, carcinoma *in situ* and papillary tumors. Its higher lipophilicity allows ALAHE to diffuse even more into these (pre)malignant lesions than ALA does.

In the nude mouse skin, only long-term application of 2%, 10% and 20% ALAHE induced a slight but significant larger PpIX production compared to the same concentrations of ALA (figure 4, table 3). However, this slight improvement in the skin is much less compared to what was found in *in vitro* and in clinical studies with ALAHE in the bladder (14,15). ALAHE induced a higher PpIX fluorescence than ALA in the bladder, even at lower concentrations and reduced instillation time (15). Also in the nude mouse skin, the short-chained ALA esters improved the PpIX production during continuous application much more than ALAHE in the present study (12). When 10% ALAHE and ALA were applied for 5, 10 and 20 minutes to the mouse skin, the mean ALA-induced PpIX fluorescence is higher than the corresponding ALAHE-induced PpIX fluorescence (figure 2). The ALA/ALAHE ratio is around 4 for these application times (table 3), showing that the difference between ALA and ALAHE is the same for these application times. One minute application is an exception, the PpIX fluorescence values are very low and are similar for ALA and ALAHE application (figure 2, table 3). One minute is probably too short to allow sufficient diffusion of either ALA or ALAHE into the skin.

With increasing drug concentration (and fixed application time of 10 minutes), the difference between ALA- and ALAHE-induced PpIX fluorescence decreased to zero for the 40% creams (figure 3, table 3). However, this effect might not be dependent on the concentration alone but also on the fact that the structure and properties of the ALA and ALAHE cream at higher concentrations are not the same. Creams with 10%, 20% and 40% ALAHE were more oily and in the case of 40% ALAHE, the cream was also fluid. These changes and differences in creams may affect the penetration and diffusion properties of ALA, ALAHE and the cream itself. Different studies have shown that the composition and properties of a cream can influence the skin penetration and diffusion of the compound that is dissolved in the cream (35-38). In addition, with increasing drug concentration, the pH of the ALA cream decreases much faster than the pH of the ALAHE cream (table 2). The effect of the low pH of the ALA cream is not known, but it might be a factor in influencing the permeability of the skin.

The fact that the penetration enhancer (HPE-101) increases both the ALA- and ALAHE-induced PpIX production (figure 5, table 3) indicates that the stratum corneum is an important barrier for the diffusion of both compounds into the epidermis. In case of ALA, there is a strong effect on the maximum PpIX fluorescence only in case of the short application time (figure 5a). With 60 minutes of ALA application the PpIX production was slightly increased when HPE-101 was added to the ALA cream. Probably, lengthening of the application time decreases the effect of the barrier function of the stratum corneum against ALA to a minimum. In case of ALAHE, HPE-101 has a strong positive effect on the PpIX production for short-term as well as long-term ALAHE application. Like in the case of ALA, the effect of the stratum corneum barrier function against ALAHE is decreased with increasing application time from 10 to 60 minutes (figure 5b). However, the penetration enhancer is still able to increase the PpIX

production for the 60 minutes application, showing that increasing the ALAHE application to 60 minutes is not enough to decrease the effect of the stratum corneum barrier function to a minimum as in case of ALA. This indicates that the stratum corneum barrier is more effective against ALAHE than ALA.

This is confirmed by the tape stripping experiment (figure 6, table 3). There is no difference between ALA- and ALAHE-induced PpIX production when the stratum corneum (and thus its barrier function) is removed before application. Surprisingly, the PpIX production in the living epidermal cells is the same after application of ALA and ALAHE to the tape stripped mouse skin. The higher lipophilicity of ALAHE was expected to increase the diffusion across the cell membranes when applied directly to these epidermal cells. Furthermore, the stratum corneum does not appear to act as a depot for ALA and ALAHE in case of 10 minutes application, because there is no significant difference between the PpIX production in non tape stripped mouse skin and mouse skin that had been tape stripped immediately after application. It can not be excluded that tape stripping damages the upper epidermal cells, which might result in an increased uptake of ALA and ALAHE. Furthermore, tape stripping might also have an effect on the enzymes involved in PpIX synthesis. It is known that tape stripping of hairless mouse skin induces a suppression of DNA synthesis and the mitotic rate. After 8-10 hours, this initial unspecific reaction is followed by an increase in DNA synthesis and mitotic rate (39). However, any effect of tape stripping would probably affect the ALA- and the ALAHE-induced PpIX production in the same way. Corresponding to the structural changes in the apical membrane overlying (pre)-malignant lesions in the bladder (31,33), the barrier function of the stratum corneum might be different in the skin overlying (pre)malignant skin lesions. Therefore, ALAHE- and ALA-induced PpIX fluorescence kinetics and distribution in should also be investigated in a (early) skin cancer model.

Conclusions

In normal mouse skin, ALAHE does not induce higher PpIX production compared to ALA. This is in contrast with earlier results obtained with ALAHE in the bladder (14,15). This difference might be explained by the fact that the permeability properties of the epidermis and the bladder epithelium are not the same. The results of the present study indicate that the stratum corneum is responsible for the lower ALAHE-induced PpIX production in the normal skin. Furthermore, lengthening of the application time, increasing ALA and ALAHE concentration, the use of a penetration enhancer and removing the stratum corneum accelerates the penetration of ALA and ALAHE and increases PpIX production in the skin.

Acknowledgements

This work was supported by the Norwegian Radium Hospital Research Foundation (JTHMvdA). We thank Photocure AS for supplying ALA and ALA hexyl ester.

References

- Kennedy JC, Pottier RH, Pross DC. Photodynamic therapy with endogenous protoporphyrin IX: basic principles and present clinical experience. *J Photochem Photobiol B* 1990; 6:143-148.
- Peng Q, Berg K, Moan J, Kongshaug M, Nesland JM. 5-Aminolevulinic acid-based photodynamic therapy: principles and experimental research. *Photochem Photobiol* 1997; 65(2):235-251.
- Kennedy JC, Marcus SL, Pottier RH. Photodynamic therapy and photodiagnosis using endogenous photosensitization induced by 5-aminolevulinic acid: mechanisms and clinical results. *J Clin Laser Med Surg* 1996; 14(5):289-304.
- Peng Q, Warloe T, Moan J, Heyerdahl H, Steen HB, Nesland JM, Giercksky K-E. Distribution of 5-aminolevulinic acid-induced porphyrins in nodulo-ulcerative basal cell carcinoma. *Photochem Photobiol* 1995; 62:906-913.
- Cairnduff F, Stringer MR, Hudson EJ, Ash DV, Brown SB. Superficial photodynamic therapy with topical 5-aminolevulinic acid for superficial primary and secondary skin cancer. *Br J Cancer* 1994; 69:605-608.
- Szeimies R-M, Sassy T, Landthaler M. Penetration potency of topical applied d-aminolevulinic acid for photodynamic therapy of basal cell carcinoma. *Photochem Photobiol* 1994; 59(1):73-76.
- Kloek J, Beijersbergen van Henegouwen GMJ. Prodrugs of 5-aminolevulinic acid for photodynamic therapy. *Photochem Photobiol* 1996; 64(6):994-1000.
- Kloek J, Akkermans W, Beijersbergen van Henegouwen GMJ. Derivatives of 5-aminolevulinic acid for photodynamic therapy: enzymatic conversion into protoporphyrin. *Photochem Photobiol* 1998; 67(1):150-154.
- Gaullier J-M, Berg K, Peng Q, Anholt H, Selbo PK, Ma L-W, Moan J. Use of 5-aminolevulinic acid esters to improve photodynamic therapy on cells in culture. *Cancer Res* 1997; 57:1481-1486.
- Washbrook R, Riley PA. Comparison of δ -aminolaevulinic acid and its methyl ester as an inducer of porphyrin synthesis in cultured cells. *Br J Cancer* 1997; 75(10):1417-1420.
- Casas A, del C. Battle AM, Butler AR, Robertson D, Brown EH, MacRobert A, Riley PA. Comparative effect of ALA derivatives on protoporphyrin IX production in human and rat skin organ cultures. *Br J Cancer* 1999; 80(10):1525-1532.
- Peng Q, Moan J, Warloe T, Iani V, Steen HB, Bjorseth A, Nesland JM. Build-up of esterified aminolevulinic-acid-derivative-induced porphyrin fluorescence in normal mouse skin. *J Photochem Photobiol B* 1996; 34:95-96.
- Fritsch C, Homey B, Stahl W, Lehmann P, Ruzicka T, Sies H. Preferential relative porphyrin enrichment in solar keratoses upon topical application of δ -aminolevulinic acid methylester. *Photochem Photobiol* 1998; 68(2):218-221.
- Marti A, Lange N, van den Bergh H, Sedmera D, Jichlinski P, Kucera P. Optimisation of the formation and distribution of protoporphyrin IX in the urothelium: an *in vitro* approach. *J Urol* 1999; 162:546-552.
- Lange N, Jichlinski P, Zellweger M, Forrer M, Marti A, Guillou L, Kucera P, Wagnières GA, van den Bergh H. Photodetection of early human bladder cancer based on the fluorescence of 5-aminolaevulinic acid hexylester-induced protoporphyrin IX: a pilot study. *Br J Cancer* 1999; 80(1/2):185-193.
- van den Akker JTHM, de Bruijn HS, Beijersbergen van Henegouwen GMJ, Star WM, Sterenborg HJCM. Protoporphyrin IX fluorescence kinetics and localization after topical application of ALA pentyl ester and ALA on hairless mouse skin with UVB-induced early skin cancer. *Photochem Photobiol* 2000; 72(3):399-406.
- Williams AC, Barry BW. Skin absorption enhancers. *Crit Rev Ther Drug Carrier Syst* 1992; 9(3,4):305-353.
- Suhonen TM, Bouwstra JA, Urtti A. Chemical enhancement of percutaneous absorption in relation to stratum corneum structural alterations. *J Controlled Release* 1999; 59:149-161.

19. Landmann L. The epidermal permeability barrier. *Anat Embryol* 1988; 178:1-13.
20. Menton DN, Eisen AZ. Structure and organisation of mammalian stratum corneum. *J Ultrastruct Res* 1971; 35:247-264.
21. Uekama K, Adachi H, Irie T, Yano T, Saita M, Noda K. Improved transdermal delivery of prostaglandin E1 through hairless mouse skin: combined use of carboxymethyl-ethyl- β -cyclodextrin and penetration enhancers. *J Pharm Pharmacol* 1992; 44:119-121.
22. Yano T, Higo N, Fukuda K, Tsuji M, Noda K, Otagiri M. Further evaluation of a new penetration enhancer, HPE-101. *J Pharm Pharmacol* 1993; 45:775-778.
23. Hadgraft J, Walters KA, Guy RH. Epidermal lipids and topical drug delivery. *Semin Dermatol* 1992; 11(2):139-144.
24. Yano T, Furukawa K, Tsuji M, Noda K, Otagiri M. Evaluation of a new penetration enhancer 1-[2-(decylthio)ethyl]azacyclopentan-2-one (HPE-101). *J Pharmacobiodyn* 1992; 15(9):527-533.
25. Wiechers JW, de Zeeuw RA. Transdermal drug delivery: efficacy and potential applications of the penetration enhancer azone. *Drug Des Del* 1990; 6:87-100.
26. Goff BA, Bachor R, Kollias N, Hasan T. Effects of photodynamic therapy with topical application of 5-aminolevulinic acid on normal skin of hairless guinea pigs. *J Photochem Photobiol B* 1992; 15:239-251.
27. Cheong W-F. Summary of optical properties. Appendix to Chapter 8. In *Optical-thermal response of laser-irradiated tissues*. (Edited by AJ Welch, MJC van Gemert) 1995, Plenum Press, New York and London: pp. 275-303.
28. van der Veen N, de Bruijn HS, Berg RJW, Star WM. Kinetics and localisation of PpIX fluorescence after topical and systemic ALA application, observed in skin and skin tumours of UVB-treated mice. *Br J Cancer* 1996; 73:925-930.
29. D'Hallewin M-A, Vanherzeele H, Baert L. Fluorescence detection of flat transitional cell carcinoma after intravesical instillation of aminolevulinic acid. *Am J Clin Oncol* 1998; 21(3):223-225.
30. Jichlinski P, Forrer M, Mizeret J, Glanzmann T, Braichotte D, Wagnières GA, Zimmer G, Guillo L, Schmidlin F, Graber P, van den Bergh H, Leisinger H-J. Clinical evaluation of a method for detecting superficial transitional cell carcinoma of the bladder by light-induced fluorescence of protoporphyrin IX following topical application of 5-aminolevulinic acid: preliminary results. *Lasers Surg Med* 1997; 20:402-408.
31. Hicks RM, Ketterer B, Warren RC. The ultrastructure and chemistry of the luminal plasma membrane of the mammalian urinary bladder: a structure with low permeability to water and ions. *Phil Trans R Soc Lond B* 1974; 268:23-38.
32. Negrete HO, Lavelle JP, Berg J, Lewis SA, Zeidel ML. Permeability properties of the intact mammalian bladder epithelium. *Am J Physiol* 1996; 271:F886-F894.
33. Fickweiler E. Biopharmacy of urologics. *Krankenhauspharmazie* 1991; 10:424-427.
34. Zeidel ML. Low permeabilities of apical membranes of barrier epithelia: what makes watertight membranes watertight? *Am J Physiol* 1996; 271:F243-F245.
35. Realdon N, Ragazzi E, dal Zotto M, Ragazzi E. Influence of ointment formulation on skin erythema induced by nicotinate esters. *Pharmazie* 1995; 9:603-606.
36. Tsai J-C, Chuang S-A, Hsu M-Y, Sheu H-M. Distribution of salicylic acid in human stratum corneum following topical application *in vivo*: a comparison of six different formulations. *Int J Pharm* 1999; 188:145-153.
37. Murakami T, Yoshioka M, Okamoto I, Yumoto R, Higashi Y, Okahara K, Yata N. Effect of ointment bases on topical and transdermal delivery of salicylic acid in rats: evaluation by skin microdialysis. *J Pharm Pharmacol* 1998; 50:55-61.
38. Schwarb FP, Gabard B, Ruffli T, Surber C. Percutaneous absorption of salicylic acid in man after topical administration of three different formulations. *Dermatology* 1999; 198:44-51.
39. Hennings H, Elgjo K. Epidermal regeneration after cellophane tape stripping of hairless mouse skin. *Cell Tissue Kinet* 1970; 3:243-252.

CHAPTER 6

Systemic component to protoporphyrin IX production in the nude mouse skin upon topical application of aminolevulinic acid depends on the application conditions

This chapter was adapted from JTHM van den Akker, V Iani, WM Star, HJCM Sterenborg and J Moan. *Photochem Photobiol* 2002; 75(2):172-177

Summary

Topical application of 5-aminolevulinic acid (ALA) for protoporphyrin IX (PpIX) based photodynamic therapy of skin cancer is generally considered not to induce systemic side effects, because PpIX is supposed to be formed locally. However, earlier studies with topically applied ALA have revealed that in mice PpIX is not only produced in the application area, but also in other organs including skin outside the application area, while esterified ALA does not. From these results it was concluded that it is not redistribution of circulating PpIX that causes the fluorescence distant from the ALA application site, but rather local PpIX production induced by circulating ALA. In the present study we investigate what the effect is of the ALA concentration in the cream, the application time, the presence of a penetration enhancer, the presence of the stratum corneum, or esterification of ALA, on the PpIX production in nude mouse skin outside the area where ALA is applied. For this purpose, ALA and ALA hexyl ester (ALAHE) were applied to one flank and the PpIX fluorescence was measured in the contralateral flank. During a 24 hour application of ALA, PpIX is produced in the contralateral flank. No PpIX could be detected in the contralateral flank after ALA application times ranging from 1 to 60 minutes. Tape stripping the skin prior to short-term ALA application, but not the addition of a penetration enhancer, resulted in PpIX production in the contralateral flank. When ALAHE was applied, no PpIX fluorescence was measured in the contralateral flank under any application condition. The results suggest that the systemic component to PpIX production outside the ALA application area plays no or a minor role in relevant clinical situations, when duration of ALA (ester) application is relatively short and a penetration enhancer is possibly added.

Introduction

5-Aminolevulinic acid (ALA), a precursor of protoporphyrin IX (PpIX), can be used for photodetection or photodynamic therapy of selected types of cancer (1-3). ALA penetrates through the skin (4) and into superficial skin tumors (5-11) when applied topically. Topical application of ALA is generally considered to be a route of administration that avoids systemic side effects and induces photosensitization only locally. However, the fact that ALA penetrates through the skin indicates that ALA is able to enter the circulation and induce PpIX production in other organs and skin outside the skin area where ALA is applied topically. A couple of studies on topical ALA application to mice show that PpIX production is not limited to the application area or the tumor, but that PpIX is also produced in other organs or skin outside the application area (10,12-15). After application of ALA in a saline solution to shaven mouse skin overlying a transplanted tumor, porphyrins are present in blood, liver, spleen and kidney (10). However, in case of shaven mouse skin, the stratum corneum is damaged, which results

in a facilitated penetration of compounds into and through the skin. Topical application of ALA encapsulated in liposomes induced higher porphyrin levels in blood, liver, spleen and kidney, when compared to topical application of ALA in a saline solution (14). In the same study, radioactivity was measured in the blood and liver after topical application of ^{14}C radiolabeled ALA in a saline solution with or without dimethylsulphoxide. During a 24 hour topical application of ALA to the flank of normal nude mice or to skin overlying a transplanted tumor, porphyrin fluorescence was not only measured in the application area, but also in skin outside the application area (12,13,15), liver, muscle and brain (12). The fluorescence intensity values were similar in the application area and skin outside the application area such as the ears or contralateral flank, but much lower in the liver, muscle and brain. However, during a 24 hour topical application of ALA methyl, ethyl, propyl or hexyl ester, no PpIX fluorescence above autofluorescence level was measured in skin outside the application area or in other organs (12,13,15). These ALA esters induced higher or similar porphyrin levels at the application site compared to ALA. In addition, the study with ALA and ALA hexyl ester showed that application during 24 hours of concentrations ranging from 2% to 20%, the PpIX production in the application area is not concentration dependent for ALA nor for the hexyl ester, indicating that the heme pathway is saturated (16). If this lack of ALA and ALA ester concentration dependency is due to release of surplus PpIX into the circulation, then there should be release of PpIX into the circulation and thus PpIX fluorescence outside the application area not only in case of ALA application, but also in case of ALA ester application. The fact that PpIX fluorescence is measured in organs and skin outside the application area when using ALA, but not when using ALA ester, indicates that the systemic component to distant PpIX fluorescence is not circulating surplus PpIX, but circulating ALA as a result of saturation of the heme pathway.

In the present study, we investigate whether PpIX production outside the ALA application area depends on the application conditions, such as concentration of ALA in the applied cream, duration of application, the use of a penetration enhancer and the presence of an intact stratum corneum, an important barrier for topical administration of ALA (16,17). Furthermore, ALA hexyl ester (ALAHE) was applied under the same application conditions, in order to establish if esterification of ALA results in less or no distant PpIX production under any of the application conditions tested for ALA. For these purposes, we use the nude mouse as a model in which we apply ALA and ALAHE topically to one flank and determine the PpIX fluorescence outside the application area by measuring the fluorescence in skin of the contralateral flank.

Materials and methods

Chemicals

ALA and ALAHE were supplied by Photocure AS (Oslo, Norway) and 1-[2-decylthio] -

ethyl]azacyclopentan-2-one (HPE-101) was a gift from Hisamitsu Pharmaceuticals (Tokyo, Japan). All other reagents and solvents were of analytical grade and were used as purchased.

Animals

Inbred female albino nude mice (BALB/c, Norwegian Radium Hospital, Oslo, Norway) were used. The fluorescence measurements for the present study were performed simultaneously and in the same animals described in a previous study for fluorescence measurements at the application site (16).

Fluorescence measurements

A fiber-optic probe was coupled to a Perkin-Elmer LS50B luminescence spectrometer as described previously (16) for *in vivo* fluorescence measurements. Fluorescence intensity at both flanks was measured before application of the cream (autofluorescence background) and at different time intervals during or after the application. The excitation wavelength was set at 407 nm and fluorescence was measured at 636 nm. In addition, fluorescence emission spectra were measured to verify that the fluorescence signal originated from PpIX. The low intensity (1.5 $\mu\text{W}/\text{cm}^2$) 407 nm light from the spectrophotometer did not induce photobleaching and penetrates deep enough into the skin to excite the PpIX in the epidermis and dermis (16).

Application of ALA and ALAHE

Prior to application of ALAHE or ALA, the animals were anaesthetized i.p. with Hypnorm® (Janssen Pharmaceutica B.V., Tilburg, The Netherlands) and Dormicum® (Hoffmann-La Roche AG, Basel, Switzerland). Creams containing ALA or ALAHE were prepared in an oil in water emulsion (Unguentum Merck, Germany) and approximately 0.15 gram of the cream was applied to one flank of the mice. The application site (1 cm in diameter) was occluded during the whole application period by covering the mouse all around with an adhesive dressing (Smith and Nephew, England). Application was finished by removing the adhesive dressing, carefully wiping off the cream and washing the mouse skin with water. The cream was applied to groups of 6 animals under the conditions described below and summarized in table 1.

Continuous application

The concentration of the ALA and ALAHE cream was 20%, 10%, 2% or 0.5% (w/w). Fluorescence measurements were performed until the application was stopped at 24 hours. The fluorescence was measured through the transparent occlusion tape, as the light absorption by the tape was negligible.

Variation of the application time

Cream containing 10% (w/w) ALA or ALAHE, was applied for 1, 5, 10, 20 or 60 minutes,

respectively and fluorescence was measured up to 8 hours after the start of the application.

Effect of a penetration enhancer

To a control group, the standard cream (without ALA or ALAHE) containing 3% (w/w) penetration enhancer HPE-101 was applied for 60 minutes. To four groups, cream containing 10% (w/w) ALA or ALAHE with or without 3% (w/w) HPE-101 was applied for 60 minutes. In two groups, standard cream containing 3% (w/w) HPE-101 was applied for 1 hour before 10% (w/w) ALA or ALAHE was applied for 10 minutes. In two other groups, 10% (w/w) ALA or ALAHE cream was applied for 10 minutes. Fluorescence was measured up to 14 hours after the start of the application.

Effect of tape stripping

The stratum corneum was removed by tape stripping the skin 20 times with Scotch[®] tape without disrupting the underlying living layer of the epidermis (16). Cream containing 10% (w/w) ALA or ALAHE was applied for 10 minutes to nude mouse skin that had been tape stripped. Two control groups received the cream with 10% (w/w)

Table 1 Summary of the experimental conditions.

Compound	Concentration (w/w)	% Application time	Other
ALA	0.5, 2, 10 and 20	24 h	
ALAHE	0.5, 2, 10 and 20	24 h	
ALA	10	0, 1, 5, 10, 20 and 60 min	
ALAHE	10	0, 1, 5, 10, 20 and 60 min	
None	-	60 min	With PE*
ALA	10	60 min	Without PE
ALA	10	60 min	With PE
ALA	10	10 min	Without PE
ALA	10	10 min	PE before
ALAHE	10	60 min	Without PE
ALAHE	10	60 min	With PE
ALAHE	10	10 min	Without PE
ALAHE	10	10 min	PE before
ALA	10	10 min	
ALA	10	10 min	TS† before
ALA	10	10 min	TS after
ALAHE	10	10 min	
ALAHE	10	10 min	TS† before
ALAHE	10	10 min	TS after

*Penetration enhancer

†Tape stripping

ALA or ALAHE for 10 minutes without being tape stripped before application. Fluorescence measurements were performed up to 14 hours after the start of the application.

Data analysis and statistics

All fluorescence measurements were corrected for the autofluorescence background by subtracting the autofluorescence levels (as measured before ALA or ALAHE application) from the total measured fluorescence. The corrected PpIX fluorescence levels during continuous ALA application were plotted as a function of time after the start of the application and maximum ALA- and ALAHE-induced PpIX levels from the continuous application and tape stripping experiment were plotted versus concentration and skin condition respectively. The PpIX fluorescence levels were tested against zero with the unpaired Student t-test (t-test), in order to determine whether the PpIX fluorescence level was different from the autofluorescence. PpIX fluorescence levels within the groups of different application conditions were tested against each other with the unpaired Student t-test (in case of 2 numbers) or with analysis of variance and the Student-Newman-Keuls test (SNK-test, in case of more than 2 numbers) to see whether they were significantly different from each other.

Results

The PpIX fluorescence kinetics in the application areas under different application circumstances have been presented in detail in a previous paper (16) and a selection from these results is presented in figure 2 and figure 3 for comparative purposes.

Continuous application

PpIX fluorescence appeared at the contralateral flank (figure 1) during 20%, 10% and 2% ALA application, but not during 0.5% ALA application (t-test). The maximum PpIX fluorescence (at 8 hours after start of the application) at the contralateral flank increased with increasing concentration (figure 1). Furthermore, the onset of PpIX fluorescence build-up was at later time points for lower ALA concentrations. Figure 1 shows the PpIX fluorescence kinetics up to 14 hours, as the PpIX fluorescence was decreasing after 8 hours. The measurement at 24 hours showed that the PpIX fluorescence had decreased further towards autofluorescence levels (data not shown).

Figure 2 shows the PpIX fluorescence levels in the application area and on the contralateral flank at 8 hours after the start of ALA (figure 2a) and ALAHE (figure 2b) application. The PpIX fluorescence values on the contralateral flank at 8 hours application of 20% and 10% ALA are not significantly different from each other (figure 2a; SNK-test). These contralateral PpIX fluorescence levels for the 20% and 10% ALA are both larger than for the 2% and the 0.5% ALA application (figure 2a; SNK-test, $P < 0.01$). Furthermore, there is no difference between the 2% and 0.5% concentration

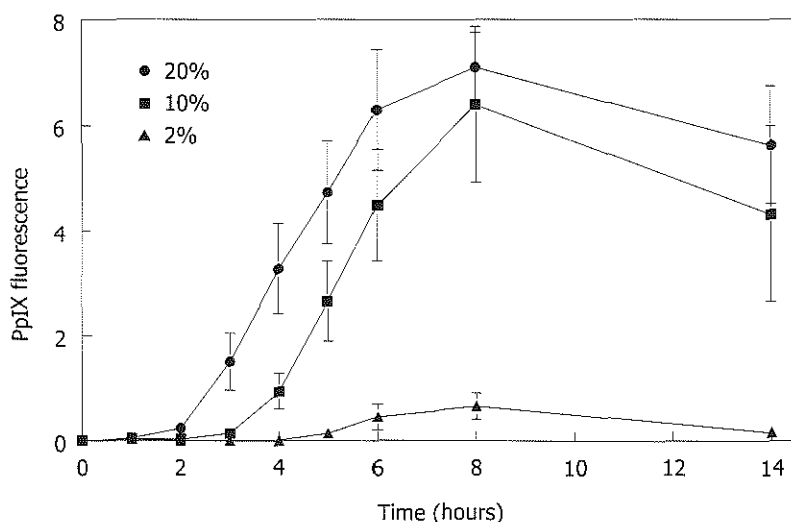


Figure 1 *In vivo* PpIX fluorescence kinetics in nude mouse skin contralateral to the flank where ALA was applied. The concentration of ALA in the cream (w/w) was 2% (triangles), 10% (squares) or 20% (circles). PpIX fluorescence units are arbitrary, but comparable between all curves and figure 2 and figure 3. Error bars indicate standard error of the mean.

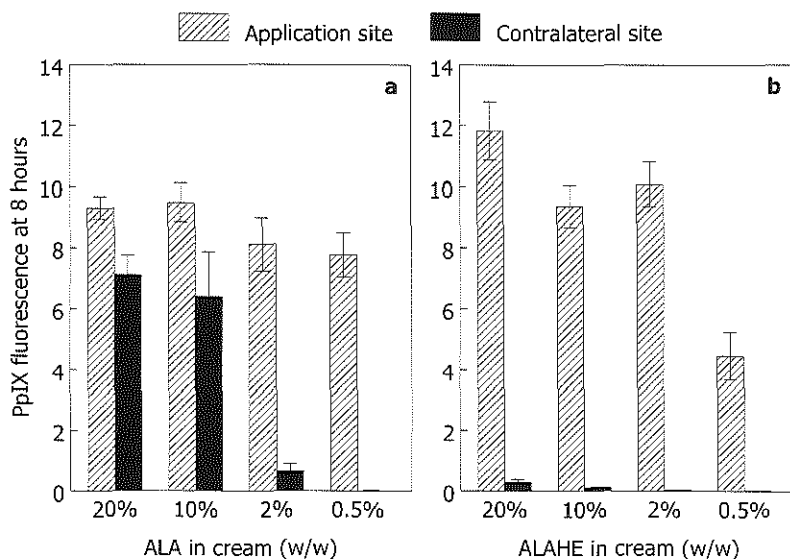


Figure 2 Maximum PpIX fluorescence in nude mouse skin at the flank where the cream was applied (shaded bars, ref (16)) and at the contralateral flank (black bars) after 8 hours application of cream with 0.5%, 2%, 10% or 20% ALA (a) or ALAHE (b). PpIX fluorescence units are arbitrary, but comparable between all bars and figure 1 and figure 3. Error bars indicate standard error of the mean.

with regard to contralateral ALA-induced PpIX levels at 8 hours after start of the application (figure 2a; SNK-test). The PpIX fluorescence levels at 8 hours are lower in the contralateral flank than in the application flank for each ALA concentration (figure 2a; t-test, $P < 0.05$)

For all concentrations of ALAHE, the PpIX fluorescence at the contralateral flanks at 8 hours after start of the application was not significantly different from autofluorescence (figure 2b; t-test).

Varying application time

The fluorescence at the contralateral flank remained at autofluorescence background levels at all time points after 1, 5, 10, 20 and 60 minutes application of 10% (w/w) ALA or 10% (w/w) ALAHE (data not shown; t-test).

Addition of penetration enhancer

No fluorescence above autofluorescence level was measured at the contralateral flank after 10 or 60 minutes application of ALA or ALAHE alone, after 60 minutes application in the presence of the penetration enhancer or after 10 minutes application to skin that was pretreated with the penetration enhancer for 60 minutes (data not shown; t-test).

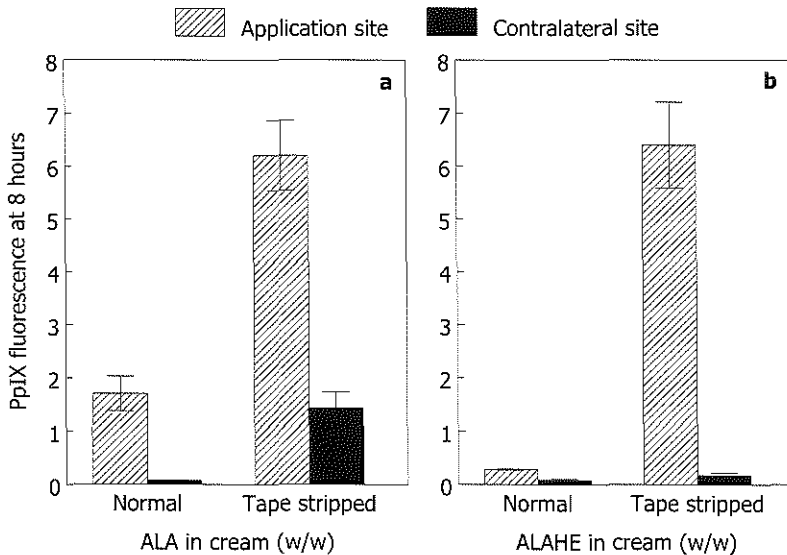


Figure 3 Maximum PpIX fluorescence in nude mouse skin at the flank where the cream was applied (shaded bars, ref (16)) and at the contralateral flank (black bars) after 10 minutes application of 10% ALA (a) or ALAHE (b). Cream was applied to untreated or tape stripped skin. PpIX fluorescence units are arbitrary, but comparable between all bars and figure 1 and figure 2. Error bars indicate standard error of the mean.

Tape stripping

The fluorescence was not significantly different from autofluorescence level at the contralateral flank when 10% ALA or ALAHE was applied for 10 minutes to non tape stripped skin (figure 3; t-test). PpIX fluorescence above autofluorescence level was measured at the contralateral flank after ALA application to skin that was tape stripped before application (figure 3a; t-test, $P < 0.01$), but not after ALAHE application to skin that was tape stripped before application (figure 3b; t-test).

Discussion

We used the nude mouse as a model to investigate the systemic component to PpIX production upon topical application of ALA. The PpIX produced in skin of the flank contralateral to the ALA application area is used as a measure for ALA that enters the circulation. In humans, topically applied ALA probably also enters the circulation, but PpIX production in skin outside the application area is not likely to happen because of the fact that the ratio between body volume and total skin area is much higher for humans compared to mice. The application area on the mice in this study (1 cm in diameter) is relatively large, resulting in a small ratio between body volume and application area. In patients, the application area has to be very large to approximate a similar small ratio between body volume and application area. This means that in humans, even in case of a large ALA application area, the concentration of ALA in the circulation is relatively much lower than in mice. The ALA concentration in human circulation after topical application is probably too low to induce significant amounts of PpIX in skin outside the application area, as there are no reports on skin photosensitivity after topical ALA application to humans.

Earlier studies have shown that there is a systemic component to PpIX production during long-term topical ALA application, but not during long-term application of ALA esters to mice (12,13,15). The present study shows that the role of the systemic component is determined by the application conditions. Substantial PpIX fluorescence is found in the flank contralateral to the application flank during continuous, but not after short-term (1 to 60 minutes) application of ALA. The amount of PpIX formed in the contralateral flank depends on the concentration of the applied ALA: no detectable PpIX is formed during 0.5% ALA application and contralateral PpIX production increases with increasing concentrations of applied ALA. The appearance of detectable PpIX fluorescence in the contralateral flank starts at later time points when ALA is applied at lower concentrations.

In a previous experiment we have shown that a 1 hour pre-treatment or co-treatment with a penetration enhancer increases the ALA-induced PpIX fluorescence in the flank where ALA is applied topically (16). This confirmed that more ALA penetrates into the skin, as expected, because penetration enhancers are chemical compounds that alter

the structure of the skin to facilitate the penetration of topically applied compounds (18,19). Although the 1 hour application of penetration enhancer is sufficient in this animal model to increase the ALA and ALAHE penetration into the skin, it does, surprisingly, not induce detectable PpIX fluorescence in the contralateral flank. Apparently, the amount of ALA in the circulation is still not high enough to induce detectable PpIX production in the contralateral flank. However, tape stripping the skin before a 10 minutes ALA application does result in detectable PpIX fluorescence in the contralateral flank. As shown before (16,17), this indicates that the stratum corneum is an important barrier for ALA penetration into the skin.

Topical application of ALAHE does not induce detectable PpIX fluorescence build-up in the contralateral flank for any of the application conditions. This is consistent with the finding that ALA methyl, ethyl, propyl or hexyl ester did not induce PpIX fluorescence in the skin outside the application area when applied to the flank of a nude mouse, much in contrast to ALA (12,13,15). At first glance this is surprising because the reason for the development of the ALA esters was that these substances were expected to penetrate better into tissue. Hence, one would expect a wider distribution of PpIX upon topical application of the ALA esters. However, the present results disprove this concept. As it is a long way from one flank of the mouse to the other, the difference between ALA- and ALAHE-induced PpIX production outside the application area can be caused by different factors. The increased lipophilicity of the esters may have boosted competing processes, like for instance plasma clearance or cellular uptake and conversion at the application side, causing a strong decrease in contralateral PpIX fluorescence. Once again, at first glance, increased cellular uptake and conversion of ALAHE at the application side does not seem to happen during long-term application, as the observed PpIX fluorescence at the application side is roughly identical for ALA and ALAHE (figure 2 and (16)). It is also clear that the PpIX fluorescence observed at the application side does not change very much with the applied concentration. This is true for ALA and also for ALAHE, although to a lesser extent. This strongly suggests that the enzymatic conversion of ALA to PpIX after topical administration in this concentration range is saturated, a conclusion also found by Aalders et al. (20) who performed extensive mathematical modeling of the PpIX kinetics after topical and systemic application of ALA. Hence, an increased cellular uptake at the application side due to the increased lipophilicity of the esters would not lead to an increase in PpIX levels.

Furthermore, the increased lipophilicity of the esters may prevent the diffusion into the circulation. The circulation is far more hydrophilic than the skin and lipophilic molecules rather remain in a lipophilic environment, i.e. the stratum corneum, epidermis or dermis. In addition, the diffusion of ALA esters may be different from ALA due to the fact that ALA esters are bigger molecules than ALA.

Conclusions

In the present study we have shown that the systemic component to PpIX production upon topical ALA application depends on the application conditions. No detectable PpIX is measured outside the application area upon topical application conditions that are relevant to clinical situations, i.e. short duration of application, addition of a penetration enhancer. This suggests that the systemic component plays no or a minor role in clinical situations.

Acknowledgements

This work was supported by the Norwegian Radium Hospital Research Foundation (JTHMvdA). We thank PhotoCure AS for supplying ALA and ALA hexyl ester.

References

- Kennedy JC, Pottier RH, Pross DC. Photodynamic therapy with endogenous protoporphyrin IX: basic principles and present clinical experience. *J Photochem Photobiol B* 1990; 6:143-148.
- Peng Q, Berg K, Moan J, Kongshaug M, Nesland JM. 5-Aminolevulinic acid-based photodynamic therapy: principles and experimental research. *Photochem Photobiol* 1997; 65(2):235-251.
- Kennedy JC, Marcus SL, Pottier RH. Photodynamic therapy and photodiagnosis using endogenous photosensitization induced by 5-aminolevulinic acid: mechanisms and clinical results. *J Clin Laser Med Surg* 1996; 14(5):289-304.
- De Rosa FS, Marchetti JM, Thomazini JA, Tedesco AC, Bentley MVLB. A vehicle for photodynamic therapy of skin cancer: influence of dimethyl-sulphoxide on 5-aminolevulinic acid *in vitro* cutaneous permeation and *in vivo* protoporphyrin IX accumulation determined by confocal microscopy. *J Control Rel* 2000; 65:359-366.
- van der Veen N, de Bruijn HS, Berg RJW, Star WM. Kinetics and localisation of PpIX fluorescence after topical and systemic ALA application, observed in skin and skin tumours of UVB-treated mice. *Br J Cancer* 1996; 73:925-930.
- Peng Q, Warloe T, Moan J, Heyerdahl H, Steen HB, Nesland JM, Giercksky K-E. Distribution of 5-aminolevulinic acid-induced porphyrins in nodulo-ulcerative basal cell carcinoma. *Photochem Photobiol* 1995; 62:906-913.
- af Klinteberg C, Enejder AMK, Wang I, Andersson-Engels S, Svanberg S, Svanberg K. Kinetic fluorescence studies of 5-aminolevulinic acid-induced protoporphyrin IX accumulation in basal cell carcinomas. *J Photochem Photobiol B* 1999; 49:120-128.
- Szeimies R-M, Sassy T, Landthaler M. Penetration potency of topical applied d-aminolevulinic acid for photodynamic therapy of basal cell carcinoma. *Photochem Photobiol* 1994; 59(1):73-76.
- Cairnduff F, Stringer MR, Hudson EJ, Ash DV, Brown SB. Superficial photodynamic therapy with topical 5-aminolevulinic acid for superficial primary and secondary skin cancer. *Br J Cancer* 1994; 69:605-608.
- Casas A, Fukuda H, del C.Battle AM. Tissue distribution and kinetics of endogenous porphyrins synthesized after topical application of ALA in different vehicles. *Br J Cancer* 1999; 81(1):13-18.
- Wennberg A-M, Larkö O, Lönnroth P, Larson G, Krogstad A-L. Delta-aminolevulinic acid in superficial basal cell carcinomas and normal skin - a microdialysis and perfusion study. *Clin Exp Dermatol* 2000; 25:317-322.
- Peng Q, Moan J, Warloe T, Iani V, Steen HB, Bjørseth A, Nesland JM. Build-up of esterified aminolevulinic-acid-derivative-induced porphyrin fluorescence in normal mouse skin. *J Photochem Photobiol B* 1996; 34:95-96.
- Sørensen R, Juzenas P, Iani V, Moan J. Formation of protoporphyrin IX in mouse skin after topical application of 5-aminolevulinic acid and its methyl ester. *Proc SPIE* 1999; 3563:77-81.
- Casas A, Fukuda H, di Venosa G, del C.Battle AM. The influence of the vehicle on the synthesis of porphyrins after topical application of

5-aminolaevulinic acid. Implications in cutaneous photodynamic sensitization. *Br J Dermatol* 2000; 143:564-572.

15. Moan J, Ma L-W, Iani V. On the pharmacokinetics of topically applied 5-aminolevulinic acid and two of its esters. *Int J Cancer* 2001; 92:139-143.

16. van den Akker JTHM, Iani V, Star WM, Sterenberg HJCM, Moan J. Topical application of 5-aminolevulinic acid hexyl ester and 5-aminolevulinic acid to normal nude mouse skin: Differences in protoporphyrin IX fluorescence kinetics and the role of the stratum corneum. *Photochem Photobiol* 2000; 72(5):681-689.

17. Goff BA, Bachor R, Kollias N, Hasan T.

Effects of photodynamic therapy with topical application of 5-aminolevulinic acid on normal skin of hairless guinea pigs. *J Photochem Photobiol B* 1992; 15:239-251.

18. Suhonen TM, Bouwstra JA, Urtti A. Chemical enhancement of percutaneous absorption in relation to stratum corneum structural alterations. *J Controlled Release* 1999; 59:149-161.

19. Williams AC, Barry BW. Skin absorption enhancers. *Crit Rev Ther Drug Carrier Syst* 1992; 9(3,4):305-353.

20. Aalders MC, van der Vange N, Star WM, Sterenberg HJCM. A mathematical evaluation of dose dependent PpIX fluorescence kinetics *in vivo*. *Photochem Photobiol* 2001; 74(2):311-317

CHAPTER 7

Comparative in vitro percutaneous penetration of 5-aminolevulinic acid and two of its esters through excised hairless mouse skin

This chapter was adapted from JTHM van den Akker, JA Holroyd, DI Vernon, HJCM Sterenborg and SB Brown. *Las Surg Med* 2003; 33(3):173-181

Summary

ALA esters have been developed to improve PpIX production in ALA-PDT, but they do not perform as well in skin as they do in cells and the bladder. The *in vitro* penetration across normal mouse skin of ALA and its methyl and hexyl ester was determined for different application concentrations. ALA and the esters were also applied to tape stripped skin to determine the effect of the stratum corneum. The penetration of ALA and the esters was higher through tape stripped skin than through normal skin ($P < 0.01$), showing that the stratum corneum is an important barrier. The experiments with different application concentrations indicated that the skin penetration through normal skin and tape stripped skin is highest for ALA and lowest for the hexyl ester. The differences in skin penetration properties could be (co-)responsible for the finding that ALA esters do not induce substantially higher PpIX levels in *in vivo* skin.

Introduction

Recently, 5-aminolevulinic acid esters have been developed to improve the efficacy of 5-aminolevulinic acid (ALA)-based photodynamic therapy (PDT) and photodetection of tumor tissue by increasing the synthesis of protoporphyrin IX (PpIX) in target tissues. Most ALA esters are more lipophilic than ALA itself (1) and they are taken up into cells to a greater extent than ALA. Several ALA esters increased the PpIX production in different cell lines, even when they were applied at dramatically lower concentrations than ALA (1-8). The increase of the PpIX production and the optimal ALA ester application concentration depends on the cell type used. Because of this increased ALA ester-induced PpIX production in cells, it was expected that ALA esters would induce more PpIX in tissues than ALA does. Indeed, ALA esters induce higher PpIX levels when applied to *in vitro* bladder mucosa (9). Furthermore, in a clinical study on PpIX-based photodetection in the bladder, ALA hexyl ester (ALAHE) induced a higher PpIX fluorescence intensity at lower concentrations and with shorter application period as compared to ALA (10).

Results for topical application to skin are however not according to the expectations based on studies in cells and bladder. The first report on the topical application of ALA esters to *in vivo* mouse skin showed promising results (2). ALA ethyl ester, ALA butyl ester and the (hydroxymethyl)tetrahydrofuranylester of ALA induced a 2 to 3 times higher PpIX production in *in vivo* mouse skin as compared to ALA after a 6 hours topical application. However, prior to the application of ALA and these esters, the skin was shaven in order to remove the hairs. Shaving results in a damaged stratum corneum and thus a facilitated penetration of the compounds into the skin. Furthermore, ALA and the esters were dissolved in 70% ethanol. Ethanol acts as a penetration enhancer by modifying the structure of the skin and thereby facilitating the skin penetration of

compounds (11). A study with normal nude mice showed that short-chained ALA esters induce higher *in vivo* PpIX levels in normal skin after 14 hours topical application (12). The PpIX fluorescence in the skin was about 2 times higher after ALA methyl, ethyl or propyl ester application as compared to ALA. Contradictory to these results, it was found in another study with nude mice that ALA methyl ester (ALAME) application for 24 hours resulted in a slower PpIX build-up and a lower PpIX maximum at a later time point as compared to the same ALA application (13).

ALAHE induced similar PpIX levels compared to ALA when applied for 24 hours to normal nude mouse skin or when applied for 10 minutes to tape stripped nude mouse skin (i.e. without stratum corneum) (14). However, ALAHE-induced PpIX levels were lower than ALA-induced PpIX levels after short-term application. In hairless mouse skin with UVB-induced early skin cancer, ALA pentyl ester induced slightly more PpIX than ALA (15). Fluorescence microscopy showed that there was no difference between ALA and ALA pentyl ester-induced PpIX levels in the dysplastic layer of the epidermis, the area of interest for PDT. Furthermore, ALA pentyl ester did not induce PpIX fluorescence in deeper layers than ALA.

Based on clinical trials in which a single PDT treatment with ALAME showed similar efficacy, better cosmetic outcome, and high patient preference compared to cryotherapy for treatment of actinic keratosis, ALAME is now a licensed drug in Europe. Other studies in which ALA esters are used for topical application to human skin have been reported (16-19). In iontophoresis studies with healthy volunteers, skin erythema after PDT was greater with ALA pentyl ester and ALAHE than with ALA (17,19). The microscopic PpIX fluorescence depth (in terms of skin layers) was the same for the three compounds, but the ALAHE- and ALA pentyl ester-induced microscopic PpIX fluorescence appeared to be distributed more homogeneously. In human skin with solar keratosis, ALAME induced lower levels of PpIX not only in the normal skin, but also in the lesions after a topical application of 6 hours (16). However, the ratio of PpIX fluorescence in lesions over normal skin was higher for ALAME than for ALA, indicating that PDT of solar keratosis with ALAME is more selective than with ALA-PDT. No difference in clinical response was observed between PDT using ALA with the penetration enhancer DMSO or PDT using ALAME in the treatment of residual and recurrent basal cell carcinomas after radiotherapy (18).

At present, it is not fully understood why ALA esters do not induce substantially higher PpIX levels than ALA upon topical application to skin, as they do *in vitro* in cells and *in vitro* and *in vivo* in the bladder. One possibility is that the epidermal cells have a lower ability to hydrolyze ALA esters to ALA prior to PpIX production, compared to cells in culture used in the *in vitro* studies (none of the cell lines originated from epidermal cells). However, an experiment with freshly isolated keratinocytes (from pig skin epidermis) showed that more PpIX was produced in these keratinocytes upon ALA ester

incubation as compared to ALA incubation. However, when ALA esters were topically applied to *ex vivo* pig skin there was no difference between ALA and the ALA esters with regard to the amount of PpIX produced in the epidermis (personal communication G.M.J. Beijersbergen van Henegouwen). Another possibility is that the skin penetration properties of ALA esters are different from the skin penetration properties of ALA.

Previous *in vivo* studies with ALA and ALA esters showed that upon topical ALA application to nude mice, ALA is taken up into the circulation in sufficiently high amounts to induce PpIX fluorescence outside the application area (12,20,21). *In vivo*, compounds that penetrate into the skin are taken up by blood vessels directly beneath the epidermis. ALA esters did not induce PpIX fluorescence outside the application area, indicating that ALA esters do not enter the circulation or enter the circulation in lower amounts than ALA. From these results it may be concluded that ALA esters do not penetrate through the epidermal layer of the skin or penetrate through the epidermis in lower amounts than ALA.

In order to investigate the hypothesis that the skin penetration properties of ALA esters are different from the skin penetration properties of ALA, we measured in an *in vitro* model the percutaneous penetration of ALA, ALAME and ALAHE through excised normal hairless mouse skin, as a measure for penetration into the skin. The *in vitro* percutaneous penetration model (Figure 1) is a well established model, generally used for measuring the permeation of a compound across skin (22). Freshly excised skin (i.e. cells in the skin are still alive) is fitted between the so-called receptor compartment and donor compartment. The compound to be investigated is put in the donor compartment on top of the skin and penetrates across the skin into the buffer or medium in the receptor compartment. It has been shown before that ALA permeates through full thickness hairless mouse skin in such an *in vitro* model (23).

In the present study, we compare ALA, ALAME and ALAHE with regard to their percutaneous penetration through normal full thickness hairless mouse skin. We determine whether the penetration of ALA, ALAME and ALAHE through skin is concentration dependent. Furthermore, we investigate if the penetration of ALA, ALAME and ALAHE across the skin increases when the stratum corneum has been reduced by tape stripping the skin prior to ALA, ALAME and ALAHE application.

Materials and methods

Chemicals

ALA, ALAME and ALAHE hydrochloride (J. Griffiths, Department of Colour Chemistry, University of Leeds, Leeds, UK) were dissolved in water. The pH of the ALA and ALA ester solutions was raised to 3 with 2N NaOH. All other reagents were of analytical grade and used as purchased.

In vitro percutaneous penetration model

Male hairless mice (9-12 weeks old, Harlan UK Ltd., Oxon, UK) were, according to local regulations, killed by CO₂ asphyxiation followed by dislocation of the neck. The dorsal skin was excised and any adhering subcutaneous fat was carefully removed. The excised skin was divided in two halves and from each half, skin was fitted into a cell of the *in vitro* percutaneous penetration model (Figure 1). The cell consists of a donor compartment, barrier compartment and receptor compartment. The skin was placed in the barrier compartment, with an effective application area of 0.56 cm² between the epidermis and the donor compartment. The dermis was in contact with the receptor buffer, a 10 mM potassium phosphate buffer pH 6.8, which was maintained at 32°C by circulating through a water bath by means of a peristaltic pump (Pharmacia, Sweden). The volume of the receptor compartment plus tubing was about 20 ml, each cell was calibrated individually. Skin samples were allowed to equilibrate in the cell for 30 minutes before application of 200 µl ALA (ester) solution in the donor compartment. The cells were placed on magnetic stirrers and stirring was maintained throughout the experiment. Any air bubbles trapped under the metal support below the dermis were removed during regular checks of the receptor compartment.

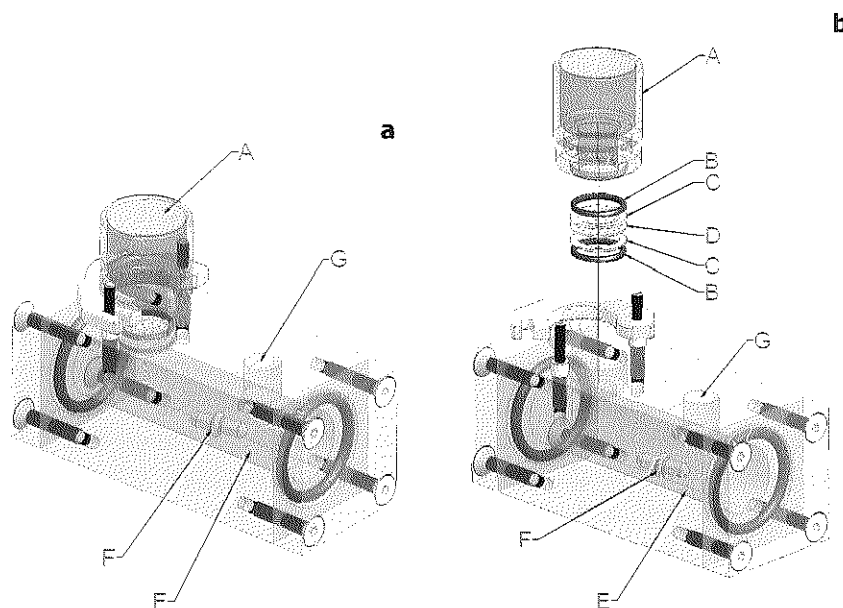


Figure 1 *In vitro* percutaneous absorption model, assembled (a) and exploded view (b). The donor compartment (A) contains the ALA (ester) solution and is placed on the barrier compartment (B-D). The barrier compartment consists of two O-rings (B) and the skin on a metal support (D) fitted between two metal rings (C). The skin in the barrier compartment is in contact with the fluid in the receptor compartment (E). The receptor fluid is stirred by a magnetic stirring bar (F) throughout the experiment and aliquot samples are withdrawn through an opening (G) in the receptor compartment.

Experimental design

Application of the ALA, ALAME and ALAHE solutions to normal skin was performed with a concentration of 500, 1500 and 3000 mM (equivalent to 7.7%, 20% and 34% (w/w), respectively). In addition, 1500 mM ALA, ALAME and ALAHE were applied to skin that was stripped 15 times with Scotch(c) tape prior to excision in order to reduce the stratum corneum thickness. For each application condition, skin from 7 different hairless mice were tested and ALA, ALAME and ALAHE accumulation in the receptor compartment was measured up to 8 hours. Aliquot samples of 1 ml were withdrawn from the receptor compartment and replaced with the equal volume of fresh receptor buffer at predetermined time intervals. The measurement of ALA, ALAME and ALAHE amounts in the receptor compartment samples was performed on the same day with a spectrophotometric method as described below.

Receptor compartment sample analysis

The spectrophotometric determination of ALA, ALAME and ALAHE amounts was based on the method described by Mauzerall and Granick (24). To a 1 ml sample, 20 μ l ethyl-acetoacetate was added and the mixture was heated in boiling water for 10 minutes. After the mixture had cooled down to room temperature, 1 ml of Ehrlich's reagent, which is 0.5 g p-dimethylaminobenzaldehyde dissolved in 21 ml glacial acetic acid plus 4 ml of 70% perchloric acid, was added. Two minutes thereafter, absorbance of the sample was measured at 553 nm in a spectrophotometer (Lambda 5 UV/VIS spectrophotometer, Perkin Elmer, \ddot{u} berlingen, Germany). A 1 ml sample of receptor buffer only served as a blank. On each experimental day, Ehrlich's reagent was freshly prepared and a calibration curve of ALA, ALAME and ALAHE in receptor buffer was measured.

Data analysis and statistics

From the spectrophotometrically determined concentrations of ALA, ALAME and ALAHE in the receptor compartment samples, the amount of ALA, ALAME and ALAHE in the receptor compartment prior to the sample withdrawal was calculated. The concentration of ALA, ALAME and ALAHE in the receptor compartment was corrected for the replenishment with fresh receptor buffer after the withdrawal of the sample. The flux of ALA, ALAME and ALAHE through the skin in each time interval was calculated from the difference in ALA, ALAME and ALAHE amounts in the receptor compartment between two sampling time points. The total ALA, ALAME and ALAHE amounts accumulated in the receptor compartment after 8 hours were tested against each other with the Mann-Whitney rank-sum test (M-W; in case of 2 groups compared with each other) or with the Kruskal-Wallis statistic (K-W; in case of more than 2 groups compared with each other). Significance was considered to be present at $p < 0.05$. When accumulated amounts within a group with more than 2 numbers proved to be not the same, pairwise comparisons were performed with the Mann-Whitney rank-sum test (M-W), including a

Bonferroni adjustment for the fact that multiple comparisons between the same observations were being made (25). We chose these nonparametric statistical methods because the distribution of the observations (i.e. the amounts of ALA, ALAME and ALAHE in the receptor compartment) is heavily skewed.

Results

The accumulation of ALA, ALAME and ALAHE in the receptor compartment during the course of the experiments with 1500 mM ALA, ALAME and ALAHE application to normal hairless mouse skin is shown in Figure 2a. The data from the 500 mM and 3000 mM ALA, ALAME and ALAHE resulted in similarly shaped curves, but at different levels of accumulated amount. During the 500 mM application (data not shown) and during the 1500 mM application (Figure 2a), ALA accumulation was higher than ALAME and ALAHE accumulation at all time points, and ALAME accumulation was higher than ALAHE accumulation at all time points, but these differences are not statistically significant. Curves for accumulated amounts during 3000 mM application of ALA, ALAME and ALAHE were the same for the three compounds (data not shown).

In Figure 2b it is shown that the accumulation of ALA in the receptor compartment du-

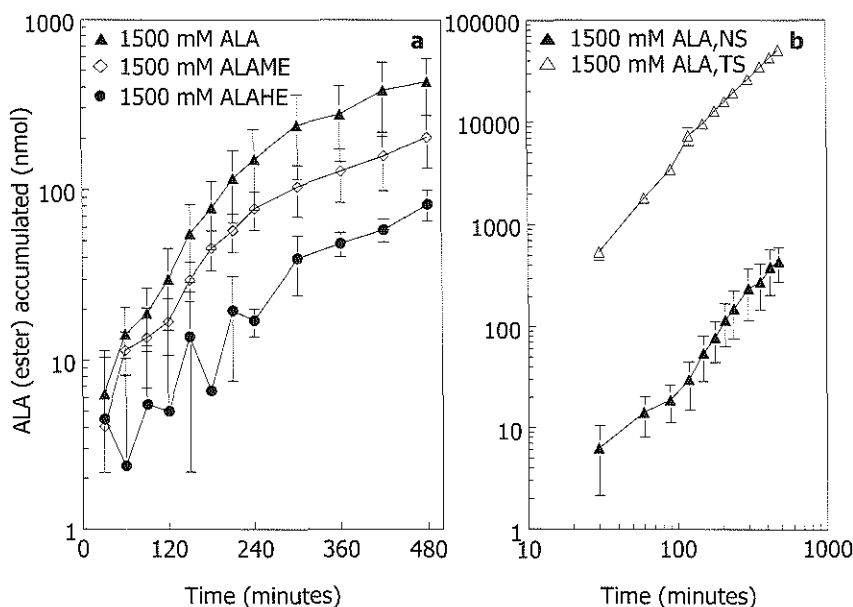


Figure 2 Accumulation of ALA (a, b), ALAME (a) and ALAHE (a) in the receptor compartment in the course of the experiment with 1500 mM ALA, ALAME and ALAHE applied to normal (a) or with 1500 mM ALA applied to normal skin (NS) and tape stripped skin (TS) (b). Error bars represent standard error of the mean. No error bar is presented when the error bar is smaller than the symbol or when the downward error bar exceeds the minimum value of the y-axis.

ring application with 1500 mM ALA to tape stripped skin is about 100 times higher than during the same application to normal skin. The data from the 1500 mM ALAME and ALAHE application to normal and tape stripped skin resulted in similarly shaped curves, but with a greater difference between them. The accumulation upon ALAME or ALAHE application to tape stripped skin is about 200 times higher than in case of normal skin.

Figure 3a shows the amounts of ALA, ALAME and ALAHE accumulated in the receptor compartment after 8 hours application with different concentrations to normal hairless mouse skin. Total accumulated amounts in the receptor compartment after 1500 mM ALA, ALAME and ALAHE application to normal and tape stripped skin are shown in Figure 3b.

The fluxes across the normal and tape stripped skin for each time interval during 1500 mM application of ALA, ALAME and ALAHE are presented in Figure 4a (ALA), Figure 4b (ALAME) and Figure 4c (ALAHE). Negative fluxes, which are a consequence of the large variation in the data (see discussion section), can not be presented in these graphs. The fluxes for ALA on normal skin and tape stripped skin (Figure 4a), for ALAME on normal skin (Figure 4b), and for ALAHE on tape stripped skin (Figure 4c) increased throughout the experiment and did not reach a steady state. Although the flux data for ALAME on tape stripped skin (Figure 4b), and for ALAHE on normal skin (Figure 4c) have a large variation, they do show the same trend that a steady state was not reached before the end of the experiment.

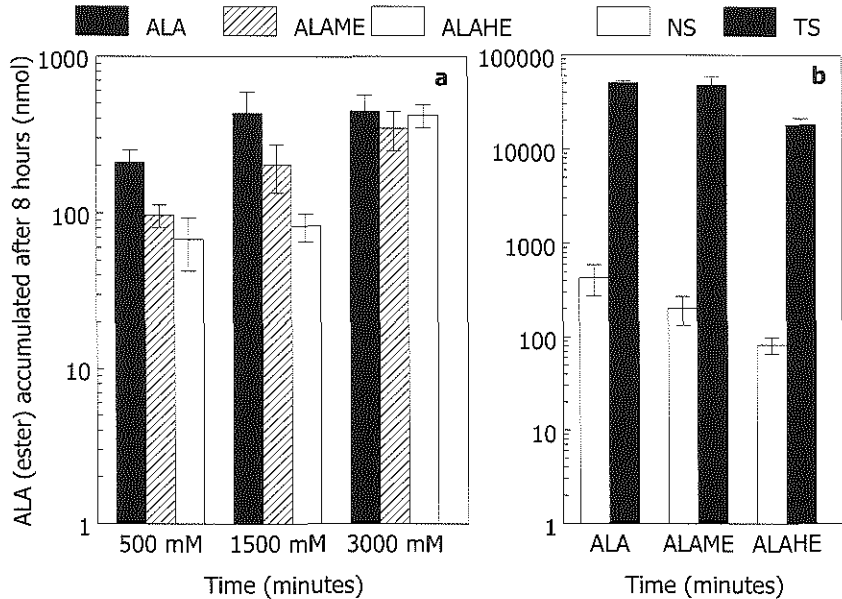


Figure 3 Total amount of ALA, ALAME and ALAHE accumulated in receptor compartment after 8 hours application to normal skin with different concentrations of ALA, ALAME and ALAHE (a) or with 1500 mM ALA, ALAME and ALAHE to normal skin (NS) and tape stripped skin (TS) (b). Error bars represent standard error of the mean.

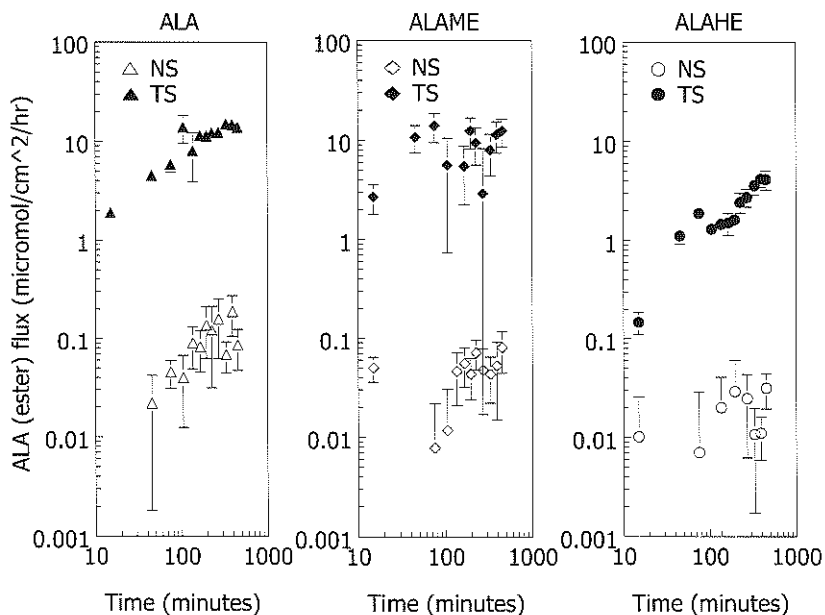


Figure 4 Flux ($\mu\text{mol}/\text{cm}^2/\text{hr}$) of ALA, ALAME and ALAHE through the skin in the course of the experiment with 1500 mM ALA (a), ALAME (b) and ALAHE (c) applied to normal skin (NS) and tape stripped skin (TS). Error bars represent standard error of the mean. No error bar is presented when the error bar is smaller than the symbol or when the downward error bar exceeds the minimum value of the y-axis.

Table 1 and table 2 give an overview of the results from the statistical tests that were performed for the comparison of the total amounts of ALA, ALAME and ALAHE that had accumulated in the receptor compartments after 8 hours. Comparing the different concentrations for each compound (table 1) showed that for ALA and for ALAME there are no significant differences in total accumulated amount between the 500 mM, 1500 mM and 3000 mM application (K-W). When the total accumulated ALAHE amounts after 500 mM, 1500 mM and 3000 mM application were compared with each other, it was found that they are significantly different from each other (K-W, $P < 0.005$). The total

Table 1 Results of Kruskal-Wallis statistic and Mann-Whitney rank-sum test when comparing the different application conditions with each other for the total amounts of ALA, ALAME and ALAHE accumulated in the receptor compartment. Differences were considered to be significant at $P < 0.05$.

	ALA	ALAME	ALAHE
500 vs. 1500 mM	n.s.*	n.s.	n.s.
500 vs. 3000 mM	n.s.	n.s.	$P < 0.05$
1500 vs. 3000 mM	n.s.	n.s.	$P < 0.05$
Normal vs. tape stripped skin	$P < 0.01$	$P < 0.01$	$P < 0.01$

*Not significant.

Table 2 Results of Kruskal-Wallis statistic and Mann-Whitney rank-sum test when comparing the total amounts of ALA, ALAME and ALAHE accumulated in the receptor compartment with each other for each application condition. Differences were considered to be significant at $P < 0.05$.

	500 mM	1500 mM	3000 mM	Tape stripped skin
ALA vs. ALAME	n.s.*	n.s.	n.s.	n.s.
ALA vs. ALAHE	$P < 0.05$	$P < 0.05$	n.s.	$P < 0.05$
ALAME vs. ALAHE	n.s.	n.s.	n.s.	n.s.

*Not significant.

accumulated amount after the 3000 mM ALAHE application was higher than after the 500 mM (M-W, $P < 0.05$) and higher than after the 1500 mM (M-W, $P < 0.05$) application. No significant difference in accumulated amount was found between the 500 mM and 1500 mM ALAHE application (M-W).

When the total accumulated amounts of ALA, ALAME and ALAHE were compared with each other for each concentration (table 2), the statistics show that in case of the 3000 mM application there are no significant differences between ALA, ALAME and ALAHE (K-W). In case of 500 and 1500 mM application, the total accumulated amounts of ALA, ALAME and ALAHE are not the same (K-W, $P < 0.05$ for both concentrations). There is a significantly lower accumulation in the receptor compartment after application of 500 mM or 1500 mM ALAHE compared to ALA (M-W, $P < 0.05$ for both concentrations). For ALAME it is not possible to show any significant difference to either ALA or ALAHE at both concentrations (M-W).

Application of ALA, ALAME and ALAHE to tape stripped skin results in a significant higher amount accumulated compared to normal skin (M-W, $P < 0.01$ for all three compounds; table 1). When comparing the accumulated amounts of ALA, ALAME and ALAHE with each other upon application to tape stripped skin, the statistics show that the accumulated amounts of ALA, ALAME and ALAHE were different from each other (K-W, $P < 0.025$). Upon ALAHE application the total amount was lower than upon ALA and ALAME application (M-W, $P < 0.05$; table 2). There was no difference between ALA and ALAME application (M-W).

Discussion

The data distribution for the amounts of ALA, ALAME and ALAHE accumulated in the receptor compartment is heavily skewed in each experimental group. This results in large standard deviations when the observations in each group are averaged. In the groups with normal skin, the standard deviations are up to nearly 100% of the mean. The distribution is less skewed in the groups with tape stripped skin and has much lower standard deviations (around 40% of the mean). A contributing factor in the relation between the large skew in the flow data and the presence of stratum corneum might be the scaly nature of the stratum corneum. Mouse stratum corneum consists of a few thin

keratinized cell layers that scale off one by one. Considering the thickness of the stratum corneum to be proportional to the number of keratinized cell layers, it is then simple to argue that the distribution of this number of layers follows a Poisson distribution. At low values of the mean, e.g. 4 layers, the distribution is strongly skewed. As a result, the flow, which can be considered inversely proportional to the thickness, can have a very large spread.

The first important step in penetration into the skin is the partitioning of ALA, ALAME and ALAHE into the stratum corneum. This is strongly influenced by several factors, including the nature of the solution on the surface of the skin, solubility of ALA, ALAME and ALAHE in the stratum corneum lipids and binding to stratum corneum proteins. One can imagine that slight differences between the skin samples regarding the stratum corneum thickness and composition have a strong effect on the penetration of ALA, ALAME and ALAHE into the skin. In addition, the epidermis and dermis thickness probably also varies between the different skin samples, resulting in differences in penetration across the skin.

The data clearly show that percutaneous penetration of ALA, ALAME and ALAHE through tape stripped skin is much larger than through normal skin (Figure 3b and table 1). Furthermore, the penetration of ALAHE through the hairless mouse skin is in most cases significantly lower than that of ALA (Figure 3 and table 2). In case of the other data, most differences between the different concentrations per compound (table 1) and most differences between ALA, ALAME and ALAHE (table 2) are not statistically significant. This is due to the large variability, but the data do show trends. The penetration of the compounds across the skin increases with increasing concentration (Figure 3a). For most application conditions the percutaneous penetration of ALA is higher than that of ALAME, which is higher than that of ALAHE (Figure 3).

The finding that ALA passes in higher amounts than ALAME and ALAHE across *in vitro* mouse skin is consistent with results from previous *in vivo* studies with ALA and ALA esters (12,20,21). In these studies it was shown that ALA is taken up into the circulation in sufficiently high amounts to induce PpIX fluorescence outside the application area. In contrast with ALA, ALA esters did not induce PpIX fluorescence outside the application area, indicating that ALA esters do not enter the circulation in sufficiently high amounts.

One can imagine that the lower percutaneous penetration of ALAME and ALAHE through full thickness skin does not necessarily mean that the penetration of ALAME and ALAHE into the skin is lower than that of ALA, as the penetration into the skin is not the only factor in percutaneous penetration. Another factor that influences the percutaneous penetration through full thickness skin may be the increased lipophilicity of ALAHE and ALAME. Diffusion from the lipophilic environment, i.e. the skin, into the far more hydrophilic circulation may be prevented by the increased lipophilicity of the ALA esters, resulting in accumulation of these two compounds in the stratum corneum, epidermis or

dermis. Furthermore, the increased lipophilicity of the ALA esters might cause a higher cellular uptake and conversion in the epidermis. As the epidermal cells are still alive during the course of the experiment, this might be a competing process for the penetration through the skin. Results from a previous study indicate that the stratum corneum does not act as a depot for ALAHE. As in this study the PpIX fluorescence kinetics (up to 14 hours) in hairless mouse skin that had been tape stripped immediately after ALAHE application was the same as the PpIX fluorescence kinetics in normal skin (14). If ALAHE accumulates in the stratum corneum, more PpIX fluorescence should be expected in the normal skin due to slow penetration of ALAHE from the stratum corneum into the epidermis where PpIX is produced.

The fluxes of ALA, ALAME and ALAHE through normal and tape stripped skin did not reach a steady-state in the course of the application period of 8 hours (Figure 4). This may be the result of the fact that the skin is being hydrated during the application of ALA, ALAME and ALAHE. The hydration level of the stratum corneum is a major factor affecting skin permeation properties, as the penetration of most compounds through the skin increases when the water content of the stratum corneum is raised (26). As ALA, ALAME and ALAHE are dissolved in water, the stratum corneum is being hydrated the application with ALA, ALAME and ALAHE solution, resulting in increasing skin permeation properties in the course of the experiment. While the skin permeation properties are changing, no steady-state flux of ALA, ALAME and ALAHE across the skin is reached.

Also in tape stripped skin, no steady-state flux of ALA, ALAME and ALAHE across the skin is reached in the course of the experiment (Figure 4). It has been shown that the progressive removal of the stratum corneum by tape stripping increases the *in vitro* skin permeability to water (27), with each layer of the stratum corneum contributing equally to the penetration barrier to water (28). Thus, the epidermis of tape stripped skin absorbs water from the ALA, ALAME and ALAHE solution and herewith probably changes its permeation properties during the application period, which results in increasing ALA, ALAME and ALAHE fluxes during the application.

It is generally recognized that skin is not only a major barrier to compounds, but that it also possesses all the major metabolizing enzyme systems (29), including the carboxylesterases that are involved in the hydrolysis of ALA esters to ALA. In a pilot study we analyzed receptor compartment samples from a few ALAME and ALAHE experiments with an HPLC-fluorescence method to investigate if ALAME and ALAHE are hydrolyzed to ALA by esterases in the skin during the penetration across the skin. With this HPLC-fluorescence method, ALA can be measured after ALA has been derivatized with a fluorescent compound. This method is currently under development in our group to measure ALA esters as well. Unfortunately, both ALAME and ALAHE standard solutions appear to be unstable to some extent during the derivatization reaction with the fluorescent compound. HPLC analysis of samples taken from the receptor

compartment show a mixture of ALA ester and ALA with the ratio between ALA and ALA ester in the mixture from the receptor compartment larger than the ALA and ALA ester ratio from a standard solution of ALA ester. This indicates that ALAME and ALAHE may be hydrolyzed by esterases in the skin. The amount of ALA ester hydrolyzed in the skin cannot be accurately quantified and the results are therefore inconclusive.

Conclusions

Data from the present study clearly show that the stratum corneum is an important barrier for the penetration of ALA, ALAME and ALAHE through skin, as the penetration through tape stripped skin is about 100 to 200 times higher than through normal skin. Furthermore, the data from the experiments with normal skin indicate that the penetration through skin is highest for ALA and lowest for ALAHE, with ALAME in between. The results suggest that the differences in penetration of ALA and ALA esters through skin may be (co-)responsible for the finding that ALA esters do not induce substantially higher PpIX levels in *in vivo* skin.

Acknowledgements

We thank J. Griffiths (Department of Colour Chemistry, University of Leeds, Leeds, UK) for supplying ALA and Jos Troquay from MATRO Engineering (Nieuw-Vennep, the Netherlands) for the drawings of the *in vitro* percutaneous penetration model.

References

1. Ühlinger P, Zellweger M, Wagnières GA, Juillerat-Jeanneret L, van den Bergh H, Lange N. 5-Aminolevulinic acid and its derivatives: physical chemical properties and protoporphyrin IX formation in cultured cells. *J Photochem Photobiol B* 2000; 54:72-80.
2. Kloek J, Beijersbergen van Henegouwen GMJ. Prodrugs of 5-aminolevulinic acid for photodynamic therapy. *Photochem Photobiol* 1996; 64(6):994-1000.
3. Gaullier J-M, Berg K, Peng Q, Anholt H, Selbo PK, Ma L-W, Moan J. Use of 5-aminolevulinic acid esters to improve photodynamic therapy on cells in culture. *Cancer Res* 1997; 57:1481-6.
4. Kloek J, Akkermans W, Beijersbergen van Henegouwen GMJ. Derivatives of 5-aminolevulinic acid for photodynamic therapy: enzymatic conversion into protoporphyrin. *Photochem Photobiol* 1998; 67(1):150-4.
5. Eléout S, Rousset N, Carre J, Bourre L, Vonarx V, Lajat Y, Beijersbergen van Henegouwen GMJ, Patrice T. *In vitro* fluorescence, toxicity and phototoxicity induced by δ -aminolevulinic acid (ALA) or ALA esters. *Photochem Photobiol* 2000; 71(4):447-54.
6. Whitaker CJ, Battah SH, Forsyth MJ, Edwards C, Boyle RW, Matthews EK. Photosensitization of pancreatic tumour cells by δ -aminolaevulinic acid esters. *Anti-Cancer Drug Design* 2000; 15:161-70.
7. Cosserat-Gerardin I, Bezdetrnaya L, Notter D, Vigneron C, Guillemin F. Biosynthesis and photodynamic efficacy of protoporphyrin IX (PpIX) generated by 5-aminolevulinic acid (ALA) or its hexylester (hALA) in rat bladder carcinoma cells. *J Photochem Photobiol B* 2000; 59:72-9.
8. Luksiene Z, Eggen I, Moan J, Nesland JM, Peng Q. Evaluation of protoporphyrin IX production, phototoxicity and cell death pathway by hexylester of 5-aminolevulinic acid in Reh and HPB-ALL cells. *Cancer Letters* 2001; 169:33-9.
9. Marti A, Lange N, van den Bergh H, Sedmera D, Jichlinski P, Kucera P. Optimisation of the formation and distribution of protoporphyrin IX in the urothelium: an *in vitro* approach. *J Urol*

1999; 162:546-52.

10. Lange N, Jichlinski P, Zellweger M, Forrer M, Marti A, Guillou L, Kucera P, Wagnières GA, van den Bergh H. Photodetection of early human bladder cancer based on the fluorescence of 5-aminolaevulinic acid hexylester-induced protoporphyrin IX: a pilot study. *Br J Cancer* 1999; 80(1/2):185-93.

11. Williams AC, Barry BW. Skin absorption enhancers. *Crit Rev Ther Drug Carrier Syst* 1992; 9(3,4):305-53.

12. Peng Q, Moan J, Warloe T, Iani V, Steen HB, Bjørseth A, Nesland JM. Build-up of esterified aminolevulinic-acid-derivative-induced porphyrin fluorescence in normal mouse skin. *J Photochem Photobiol B* 1996; 34:95-6.

13. Sørensen R, Juzenas P, Iani V, Moan J. Formation of protoporphyrin IX in mouse skin after topical application of 5-aminolevulinic acid and its methyl ester. *Proc SPIE* 1999; 3563:77-81.

14. van den Akker JTHM, Iani V, Star WM, Sterenberg HJCM, Moan J. Topical application of 5-aminolevulinic acid hexyl ester and 5-aminolevulinic acid to normal nude mouse skin: Differences in protoporphyrin IX fluorescence kinetics and the role of the stratum corneum. *Photochem Photobiol* 2000; 72(5):681-9.

15. van den Akker JTHM, de Bruijn HS, Beijersbergen van Henegouwen GMJ, Star WM, Sterenberg HJCM. Protoporphyrin IX fluorescence kinetics and localization after topical application of ALA pentyl ester and ALA on hairless mouse skin with UVB-induced early skin cancer. *Photochem Photobiol* 2000; 72(3):399-406.

16. Fritsch C, Homey B, Stahl W, Lehmann P, Ruzicka T, Sies H. Preferential relative porphyrin enrichment in solar keratoses upon topical application of 5-aminolevulinic acid methylester. *Photochem Photobiol* 1998; 68(2):218-21.

17. Gerscher S, Connolly JP, Griffiths J, Brown SB, MacRobert AJ, Wong G, Rhodes LE. Comparison of the pharmacokinetics and phototoxicity of protoporphyrin IX metabolized from 5-aminolevulinic acid and two derivatives in human skin *in vivo*. *Photochem Photobiol* 2000; 72(4):569-74.

18. Soler AM, Warloe T, Tausj J, Giercksky K-E. Photodynamic therapy of residual or recurrent basal cell carcinoma after radiotherapy using topical 5-aminolevulinic acid or methylester amino-

levulinic acid. *Acta Oncol* 2000; 39(5):605-9.

19. Gerscher S, Connolly JP, Beijersbergen van Henegouwen GMJ, MacRobert AJ, Watt P, Rhodes LE. A quantitative assessment of protoporphyrin IX metabolism and phototoxicity in human skin following dose-controlled delivery of the prodrugs 5-aminolaevulinic acid and 5-aminolaevulinic acid-n-pentylester. *Br J Dermatol* 2001; 144:983-90.

20. Moan J, Ma L-W, Iani V. On the pharmacokinetics of topically applied 5-aminolevulinic acid and two of its esters. *Int J Cancer* 2001; 92:139-43.

21. van den Akker JTHM, Iani V, Star WM, Sterenberg HJCM, Moan J. Systemic component to protoporphyrin IX production in the nude mouse skin upon topical application of aminolevulinic acid depends on the application conditions. *Photochem Photobiol* 2002; 75(2):172-7.

22. Bronaugh RL and Maibach HI, editors. *In vitro percutaneous absorption: Principles, fundamentals and applications*. 1991, CRC Press, Boca Raton, Florida.

23. De Rosa FS, Marchetti JM, Thomazini JA, Tedesco AC, Bentley MVLB. A vehicle for photodynamic therapy of skin cancer: influence of dimethylsulphoxide on 5-aminolevulinic acid *in vitro* cutaneous permeation and *in vivo* protoporphyrin IX accumulation determined by confocal microscopy. *J Control Rel* 2000; 65:359-66.

24. Mauzerall D, Granick S. The occurrence and determination of d-aminolevulinic acid and porphobilinogen in urine. *J Biol Chem* 1956; 219:435-46.

25. Glantz SA. Alternatives to analysis of variance and the t test based on ranks. In *Primer of bio-statistics*. (Edited by B Kaufman Barry and J White) 1989, McGraw-Hill, Singapore: 287-330.

26. Suhonen TM, Bouwstra JA, Urtti A. Chemical enhancement of percutaneous absorption in relation to stratum corneum structural alterations. *J Controlled Release* 1999; 59:149-61.

27. Blank IH. Further observations on factors which influence the water content of the stratum corneum. *J Invest Dermatol* 1953; 21:259

28. Blank IH. Cutaneous barriers. *J Invest Dermatol* 1965; 45:249

29. Kao J, Carver MP. Cutaneous metabolism of xenobiotics. *Drug Metab Rev* 1990; 22:363-410.

CHAPTER 8

Chronic UVB exposure enhances in vitro percutaneous penetration of 5-aminolevulinic acid in hairless mouse skin

This chapter was adapted from JTHM van den Akker, JA Holroyd, DI Vernon, HJCM Sterenborg and SB Brown. 2003; submitted to *Las Surg Med*

Summary

(Pre)Cancerous skin lesions accumulate more PpIX upon topical application of ALA than the surrounding normal skin. This might be the result of a higher percutaneous penetration of ALA into (pre)cancerous skin. ALA penetration through healthy skin with intact stratum corneum, healthy skin with reduced stratum corneum (i.e. tape stripped skin) and diseased skin with dysplastic and thickened epidermis (chronically UVB-exposed skin) was determined in an *in vitro* model with hairless mouse skin. More ALA had penetrated through chronically UVB-exposed skin than through normal non-exposed skin after 8 hours ALA application. The amount of ALA penetrated through chronically UVB-exposed skin was smaller than through tape stripped skin. The stratum corneum barrier function is less effective in chronically UVB-exposed skin than in normal non-exposed skin, but more effective than in tape stripped skin. A higher penetration rate of ALA into (pre)cancerous lesions may be (partly) responsible for the greater accumulation of PpIX in such lesions.

Introduction

Topical photodynamic therapy (PDT) and photodetection with 5-aminolevulinic acid (ALA)-induced protoporphyrin IX (PpIX) is very effective for treatment or detection of precancerous skin lesions, such as Bowen's disease (BD) and actinic keratosis (AK), and superficial cancerous lesions, such as squamous cell carcinoma (SCC) and basal cell carcinoma (BCC). Upon topical application of ALA to areas with such tumors or premalignancies, PpIX is produced to a higher extent in the lesions compared to the surrounding normal skin. The preferential accumulation of PpIX in (pre)cancerous lesions has been confirmed by fluorescence spectroscopy (1-4), fluorescence imaging (1,2,4-7), fluorescence microscopy (4,5,8-10) and biochemical analysis (8,11).

At present, it is not fully understood why the (pre)cancerous skin lesions accumulate more PpIX than the surrounding normal skin. Lower levels of iron or reduced ferrochelatase activity or a combination of both may be present in tumors compared to normal tissue which might play a role in the differential porphyrin synthesis. This would result in greater PpIX accumulation in tumors, as both ferrochelatase and iron are required for the conversion of PpIX to heme. Tumors might have a lower pH than normal tissue, which could result in higher PpIX. Furthermore, the permeability properties of the skin (i.e. stratum corneum) overlying the tumors or precancerous lesions could be different from those of normal skin, resulting in an higher penetration of ALA into the lesions than into the surrounding normal skin.

Previous data have shown that upon topical application of ALA to normal skin, the presence of the stratum corneum is an important limiting factor for PpIX production (12,13), *in vivo* ALA penetration through skin (14) and *in vitro* ALA penetration through

skin (15). The barrier function of the stratum corneum against ALA penetration into the skin is very effective and is determined by the structure and composition of the stratum corneum. The partitioning of ALA into the stratum corneum is strongly influenced by the binding of ALA to the keratin of the corneocytes and by the solubility of ALA in the lipid matrix that surrounds the corneocytes. The corneocytes originate from keratinocytes, which are formed by dividing cells in the basal layer of the epidermis. The rate of keratinocyte production and differentiation (epidermopoiesis) is regulated by a balance between stimulatory and inhibitory signals. This balance is disrupted in case of (pre)malignant conditions in the epidermis, such as AK, BCC, BD and SCC. One can imagine that disturbed epidermopoiesis can also result in a stratum corneum with a different structure and composition, and thus most probably a limited barrier function.

Indeed, several compounds permeate in higher amounts across (experimental) diseased skin as compared to normal skin (16-22). A clinical microdialysis study showed that ALA penetrates faster and in higher amounts through BCC's in patients than through normal skin from healthy volunteers (22). However, it is not clear whether the higher and faster permeation across the BCC's is due to the diseased status of the epidermis or due to the curettage of the BCC's, which was performed prior to the ALA application. The curettage itself enhances the ALA penetration, as it disrupts the stratum corneum and the underlying epidermal layer.

In the present study, we investigate the hypothesis that the preferential accumulation of PpIX BD, AK, SCC and BCC is a result of a higher penetration rate of ALA into the lesion. Such (pre)cancerous lesions may originate from chronically sun-exposed skin and we therefore use chronically UVB-exposed hairless mouse skin as a model skin condition for these (pre)cancerous lesions. In an *in vitro* model with hairless mouse skin, the percutaneous penetration of ALA was measured in healthy skin with an intact stratum corneum barrier function, in healthy skin with a reduced stratum corneum (i.e. tape stripped skin), and in chronically UVB-exposed skin.

Materials and methods

Chemicals

ALA hydrochloride (J. Griffiths, Department of Colour Chemistry, University of Leeds, Leeds, UK) was dissolved in water. All other reagents were of analytical grade and used as purchased. The pH of the ALA solution was adjusted to 3 with 2N NaOH. Ehrlich's reagent was prepared by dissolving 0.5 g p-dimethylaminobenzaldehyde in 21 ml glacial acetic acid plus 4 ml 70% perchloric acid.

Animal model and tumor induction

Inbred female albino hairless mice (SKH HR1, Dept. of Dermatology, University Hospital Utrecht, The Netherlands) were used. The dorsal skin had been irradiated daily with

UVB for 90 days according to a method described by de Gruijl et al. (23), causing small primary lesions of actinic and seborrhoeic keratosis and squamous cell carcinoma (23,24). Non-exposed animals of the same age were used for investigation of healthy skin with intact stratum corneum and healthy skin with reduced stratum corneum.

In vitro percutaneous penetration model

Mice were anaesthetized, and killed by cervical dislocation. The dorsal skin of the normal hairless mice was divided into two halves. One half was stripped 15 times with Scotch[®] tape in order to reduce the stratum corneum, the other half was not treated. From the dorsal skin of chronically UVB-exposed hairless mice, an area without visible lesions, but with dysplastic and thickened epidermis (4,25-27), was selected. The selected skin areas were excised and any adhering subcutaneous fat was carefully removed. The excised skin was fitted into the cells of the *in vitro* percutaneous penetration model as described previously in detail by van den Akker et al. (15). The dermis was in contact with the receptor buffer (10 mM potassium phosphate buffer pH 6.8) and the epidermal side of the skin was in contact with the ALA solution in the donor compartment (effective diffusional area 56 mm²). The receptor buffer was circulated through a water bath by means of a peristaltic pump (Pharmacia, Sweden) in order to maintain the temperature of the buffer and skin at 32°C. Skin samples were allowed to equilibrate in the cell for 30 minutes and then 200 µl of a 1.5 M (which is 20% (w/w)) ALA solution was applied in the donor compartment for 8 hours. Throughout the experiment, any air bubbles trapped below the dermis were removed during regular checks of the receptor compartment.

Experimental design

ALA solution with a concentration of 1.5 M (which is equivalent to 20% (w/w) ALA) was applied to full thickness normal non-exposed hairless mouse skin (n=12), non-exposed skin that was stripped 15 times with Scotch[®] tape prior to excision (n=12) and chronically UVB-exposed skin without visible lesions (n=12). The accumulation of ALA in the receptor compartment was measured up to 8 hours. Aliquot samples of 1 ml were withdrawn from the receptor compartment and replaced with the equal volume of fresh receptor buffer at predetermined time intervals. The measurement of ALA amounts in the receptor compartment samples was performed on the same day with a spectrophotometric method as described below.

Analysis of receptor compartment samples

The spectrophotometric measurement of ALA was based on the method described by Mauzerall and Granick (28). A mixture of 1 ml sample with 20 µl ethylacetoacetate was boiled for 10 minutes and then allowed to cool down to room temperature. An equal volume of freshly prepared Ehrlich's reagent was added and mixed thoroughly. After 2

min, the absorbance of the sample was measured at 553 nm in a spectrophotometer (UV-2101 pc, Shimadzu Benelux, Den Bosch, the Netherlands). A calibration curve of ALA in receptor buffer, including receptor buffer only as a blank, was measured on each experimental day.

Data analysis and statistics

The amount of ALA in the receptor compartment at each time point (prior to the sample withdrawal) was calculated from the spectrophotometrically determined concentration of ALA in the receptor compartment sample. Then, the concentration of ALA in the receptor compartment was corrected for the replenishment with fresh receptor buffer after the withdrawal of the sample. The total ALA amounts accumulated in the receptor compartment after 8 hours were tested against each other with the Kruskal-Wallis statistic (K-W), followed by pairwise comparisons with the Mann-Whitney rank-sum test (M-W), including a Bonferroni adjustment for the fact that multiple comparisons between the same observations were being made (29). We chose these nonparametric statistical methods because the distribution of the observations (i.e. the amounts of ALA in the receptor compartment) is heavily skewed.

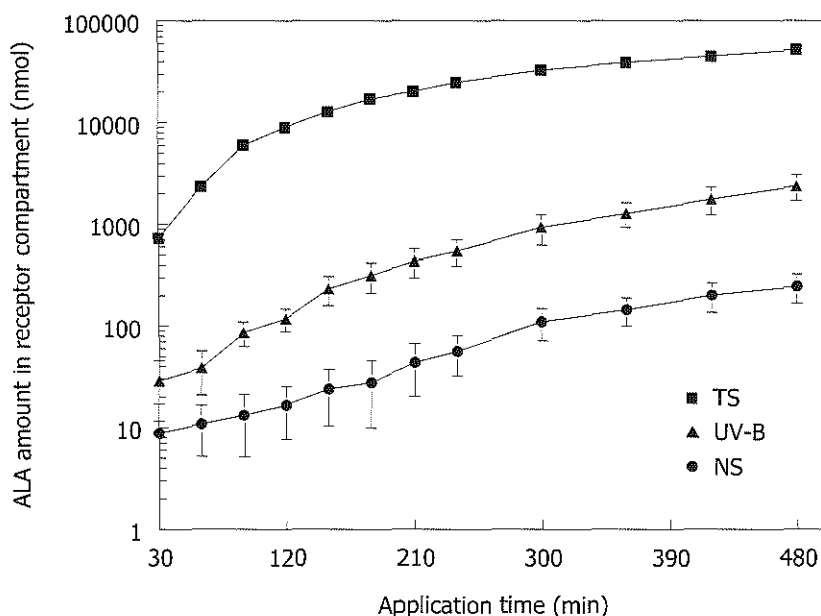


Figure 1 Time course of the accumulation of ALA in the receptor compartment in the course of the experiment depends on the condition of the skin. ALA solution was applied for 8 hours to normal non-exposed skin (NS), chronically UVB-exposed skin (UV-B) or tape stripped non-exposed skin (TS) and ALA amounts were quantified with a spectrophotometric method. Error bars represent SEM with $n=12$ for each data point. No error bar is presented when the error bar is smaller than the symbol.

Results and discussion

Figure 1 shows the time course of the accumulation of ALA in the receptor compartment in the course of the 8 hours application. At all time points, the accumulation of ALA was higher during application to chronically UVB-exposed skin than during application to normal non-exposed skin. During the application to tape stripped skin, ALA accumulation was higher than during application to chronically UVB-exposed skin or normal non-exposed skin at all time points.

The amount of ALA accumulated in the receptor compartment after 8 hours application of 1.5 M ALA to normal non-exposed skin, chronically UVB-exposed skin or tape stripped non-exposed skin is shown in figure 2. The data clearly show that according to the expectations, based on previous *in vivo* data (14) and *in vitro* data (15), the total accumulated amount of ALA was the highest upon application to tape stripped skin. The amount of ALA accumulated after application to chronically UVB-exposed skin was about 10 times higher than after application to normal non-exposed skin, showing that the stratum corneum barrier function is less effective in chronically UVB-exposed skin than in normal non-exposed skin. The ALA accumulation upon application to chronically UVB-exposed skin is about 20 times smaller than upon application to tape stripped non-exposed skin, indicating that chronically UVB-exposed skin has not lost the whole stratum corneum barrier function.

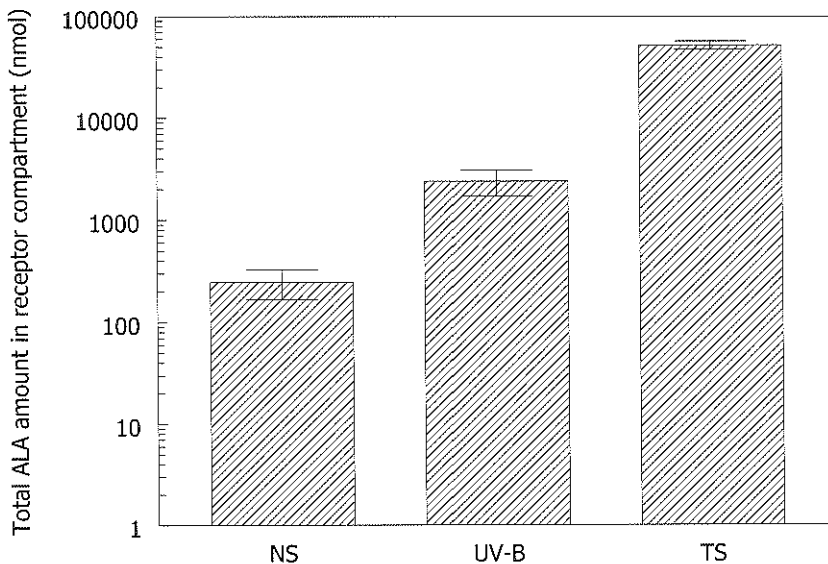


Figure 2 Total amount of ALA accumulated in the receptor compartment depends on the condition of the skin. The total amount of ALA in the receptor compartment after 8 hours of ALA application to normal non-exposed skin (NS), chronically UVB-exposed skin (UV-B) or tape stripped non-exposed skin (TS) was determined spectrophotometrically. Error bars represent SEM with $n=12$ for each data point.

The differences between the three groups regarding the total ALA accumulation were confirmed by the statistical tests which showed that the total amounts of ALA accumulated after application to normal non-exposed skin, chronically UVB-exposed skin and tape stripped non-exposed skin were not the same (K-W, $P < 0.001$) and that the total ALA accumulation for each group was different from that for the other two groups (M-W, $P < 0.001$; for each pairwise comparison).

The difference between chronically UVB-exposed skin and normal non-exposed skin with regard to ALA penetration into the skin is probably larger than the difference in penetration of ALA through the skin. The dysplastic epidermis of chronically UVB-exposed skin is several layers of keratinocytes thicker than the normal epidermis of normal non-exposed skin (4,25-27). As full thickness skin is used in the *in vitro* percutaneous penetration model, the passage of ALA through chronically UVB-exposed skin is across a longer distance than through normal non-exposed skin, resulting in a delayed accumulation of ALA in the receptor compartment underneath the chronically UVB-exposed skin. Furthermore, as there are more keratinocytes in the epidermal layer of chronically UVB-exposed skin, more ALA is absorbed by the cells in the chronically UVB-exposed skin during the passage across the skin as compared to normal non-exposed skin.

Conclusion

Many authors have suggested or assumed that the greater accumulation of PpIX in lesions, such as BD, AK, SCC and BCC, upon topical application of ALA is a result of a higher penetration rate of ALA into these lesions, as the skin overlying such lesions most likely has different permeation properties compared to the surrounding normal skin. Our study presents for the first time results that confirm the hypothesis that the preferential accumulation of PpIX in (pre)cancerous lesions is the result, or at least partly the result, of a higher penetration rate of ALA into such lesions than into normal skin. The data imply that chronic UVB exposure induces changes in the skin which results in increased percutaneous penetration of ALA and thus increased PpIX accumulation in chronically UVB-exposed skin as compared to normal skin.

Acknowledgements

This work was supported by a grant from Yorkshire Cancer Research. We thank J. Griffiths (Department of Colour Chemistry, University of Leeds, Leeds, UK) for supplying ALA.

References

1. van der Veen N, de Bruijn HS, Star WM. Photobleaching during and re-appearance after photodynamic therapy of topical ALA-induced fluorescence in UVB-treated mouse skin. *Int J Cancer* 1997; 72:110-118.

2. Wagnières GA, Star WM, Wilson BC. *In vivo* fluorescence spectroscopy and imaging for oncological applications. *Photochem Photobiol* 1998; 68(5):603-632.
3. af Klinteberg C, Enejeder AMK, Wang I, Andersson-Engels S, Svanberg S, Svanberg K. Kinetic fluorescence studies of 5-aminolaevulinic acid-induced protoporphyrin IX accumulation in basal cell carcinomas. *J Photochem Photobiol B* 1999; 49:120-128.
4. van den Akker JTHM, de Bruijn HS, Beijersbergen van Henegouwen GMJ, Star WM, Sterenberg HJCM. Protoporphyrin IX fluorescence kinetics and localization after topical application of ALA pentyl ester and ALA on hairless mouse skin with UVB-induced early skin cancer. *Photochem Photobiol* 2000; 72(3):399-406.
5. van der Veen N, de Bruijn HS, Berg RJW, Star WM. Kinetics and localisation of PpIX fluorescence after topical and systemic ALA application, observed in skin and skin tumours of UVB-treated mice. *Br J Cancer* 1996; 73:925-930.
6. Orenstein A, Kostenich G, Malik Z. The kinetics of protoporphyrin fluorescence during ALA-PDT in human malignant skin tumors. *Cancer Letters* 1997; 120:229-234.
7. Bogaards A, Aalders MC, Zeyl CC, de Blok S, Dannecker C, Hilleman P, Stepp H, Sterenberg HJCM. Localization and staging of cervical intraepithelial neoplasia using Double Ratio fluorescence imaging. *J Biomed Optics* 2002; 7(2):215-220.
8. Szeimies R-M, Sassy T, Landthaler M. Penetration potency of topical applied d-aminolevulinic acid for photodynamic therapy of basal cell carcinoma. *Photochem Photobiol* 1994; 59(1):73-76.
9. Roberts DJH, Stables GI, Ash DV, Brown SB. Distribution of protoporphyrin IX in Bowen's disease and basal cell carcinomas treated with topical 5-aminolaevulinic acid. *Proc SPIE* 1995; 2371:490-494.
10. Peng Q, Warloe T, Moan J, Heyerdahl H, Steen HB, Nesland JM, Giercksky K-E. Distribution of 5-aminolevulinic acid-induced porphyrins in nodulo-ulcerative basal cell carcinoma. *Photochem Photobiol* 1995; 62:906-913.
11. Fritsch C, Lehmann P, Schulte KW, Blohm E, Lang K, Sies H, Ruzicka T. Optimum porphyrin accumulation in epithelial skin tumours and psoriatic lesions after topical application of δ -aminolaevulinic acid. *Br J Cancer* 1999; 79(9/10):1603-1608.
12. Goff BA, Bachor R, Kollias N, Hasan T. Effects of photodynamic therapy with topical application of 5-aminolevulinic acid on normal skin of hairless guinea pigs. *J Photochem Photobiol B* 1992; 15:239-251.
13. van den Akker JTHM, Iani V, Star WM, Sterenberg HJCM, Moan J. Topical application of 5-aminolevulinic acid hexyl ester and 5-aminolevulinic acid to normal nude mouse skin: Differences in protoporphyrin IX fluorescence kinetics and the role of the stratum corneum. *Photochem Photobiol* 2000; 72(5):681-689.
14. van den Akker JTHM, Iani V, Star WM, Sterenberg HJCM, Moan J. Systemic component to protoporphyrin IX production in the nude mouse skin upon topical application of aminolevulinic acid depends on the application conditions. *Photochem Photobiol* 2002; 75(2):172-177.
15. van den Akker JTHM, Holroyd JA, Vernon DJ, Sterenberg HJCM, Brown SB. Comparative *in vitro* percutaneous penetration of 5-aminolevulinic acid and two of its esters through excised hairless mouse skin. *Lasers Surg Med* 2003; in press
16. Erlanger M, Martz G, Ott F, Storck H, Rieder J, Kessler S. Cutaneous absorption and urinary excretion of 6-14C-5-fluorouracil ointment applied in an ointment to healthy and diseased human skin. *Dermatologica* 1970; 140(Suppl. I):7-14.
17. Solomon AE, Lowe NJ. Percutaneous absorption in experimental epidermal proliferation. *Arch Dermatol* 1978; 114:1029-1030.
18. Solomon AE, Lowe NJ. Percutaneous absorption in experimental epidermal disease. *Br J Dermatol* 1979; 100:717-722.
19. Juhlin L, Häggglund G, Evers H. Absorption of lidocaine and prilocaine after application of a eutectic mixture of local anesthetics (EMLA®) on normal and diseased skin. *Acta Derm Venereol (Stockh)* 1989; 69:18-22.
20. Moon KC, Wester RC, Maibach HI. Diseased skin models in the hairless guinea pig: *in vivo* percutaneous absorption. *Dermatologica* 1990; 180:8-12.
21. Wilhelm K-P, Surber C, Maibach HI. Effect of sodium lauryl sulfate-induced skin irritation on *in vivo* percutaneous penetration. *J Invest Dermatol* 1991; 97(5):927-932.
22. Wennberg A-M, Larkö O, Lönnroth P, Larson G, Krogstad A-L. Delta-aminolevulinic acid in superficial basal cell carcinomas and normal

skin - a microdialysis and perfusion study. *Clin Exp Dermatol* 2000; 25:317-322.

23. de Gruijl FR, van der Meer JWM, van der Leun JC. Dose-time dependency of tumour formation by chronic UV exposure. *Photochem Photobiol* 1983; 37:53-62.

24. de Gruijl FR, Sterenborg HJCM, Forbes PD, Davies RE, Cole C, Kelfkens G, van Weelden H, Slaper H, van der Leun JC. Wavelength dependence of skin cancer induction by ultraviolet irradiation of albino hairless mice. *Cancer Res* 1993; 53:53-60.

25. Sterenborg HJCM, de Gruijl FR, van der Leun JC. UV-induced epidermal hyperplasia in hairless mice. *Photodermatol* 1986; 3:206-214.

26. Bissett DL, Hannon DP, Orr TV. An animal

model of solar-aged skin: histological, physical, and visible changes in UV-irradiated hairless mouse skin. *Photochem Photobiol* 1987; 46(3):367-378.

27. Kligman LH. The hairless mouse and photoaging. *Photochem Photobiol* 1991; 54(6):1109-1118.

28. Mauzerall D, Granick S. The occurrence and determination of d-aminolevulinic acid and porphobilinogen in urine. *J Biol Chem* 1956; 219:435-446.

29. Glantz SA. Alternatives to analysis of variance and the t test based on ranks. In *Primer of bio-statistics*. (Edited by B Kaufman Barry, J White) 1989, McGraw-Hill, Singapore: pp. 287-330.

CHAPTER 9

Effect of elevating the skin temperature during topical ALA application on in vitro ALA penetration through mouse skin and in vivo PpIX production in human skin

This chapter was adapted from JTHM van den Akker, K Boot, DI Vernon, SB Brown, L Groenendijk, GC van Rhoon and HJCM Sterenborg. 2003; submitted to *Photochem Photobiol Sci*

Summary

An approach to induce increased protoporphyrin IX (PpIX) production in aminolevulinic acid (ALA)-based photodynamic therapy (PDT) of basal cell carcinomas (BCC) in the skin is to elevate the skin temperature during topical ALA application. Increased skin temperature may increase the penetration (depth) of ALA into the skin which therewith may increase the PpIX production (in deeper layers). The effect of skin temperature on the *in vitro* ALA penetration into mouse skin was determined in an *in vitro* percutaneous penetration model at two different temperatures. The effect of skin temperature on the PpIX production in human skin during ALA application was measured with *in vivo* fluorescence spectroscopy measurements in temperature controlled areas (5 different temperatures). The data from the experiment with the *in vitro* percutaneous penetration model clearly show that the penetration of ALA into the skin is temperature dependent. The penetration of ALA through the *in vitro* mouse skin was higher when the skin was kept at 37°C than through skin that was kept at 32°C. The fluorescence data from the *in vivo* experiment show that the PpIX fluorescence increases with increasing temperature of the skin during the application period. The overall activation energy E_a for PpIX production was obtained with the Arrhenius equation for each hour of the ALA application period from the fluorescence data. The E_a in the first hour of ALA application was not a significant value, indicating that the PpIX production in that period is dominated by processes that are not temperature dependent, like the passive diffusion of ALA across the stratum corneum. In the second, third and fourth hour of ALA application, the E_a for PpIX production proved to be significant which indicates that the PpIX production in these time intervals is dominated by temperature dependent processes. In conclusion, the data from the present study indicate that improving ALA-based PDT of BCC might be achieved by elevating the skin temperature during the ALA application.

Introduction

Photodynamic therapy (PDT) with 5-aminolevulinic acid (ALA)-induced protoporphyrin IX (PpIX), for the treatment of basal cell carcinomas (BCC) has been evaluated in many clinical studies since 1990. In 1995, Peng et al. summarized the published clinical studies using topical ALA-PDT in superficial and nodular BCC (1). This summary showed that (in 14 clinical studies) an average of 87% complete response was achieved for superficial BCC. For nodular BCC however, the response rates after a single treatment were lower than 50%, but could be increased by repeated ALA-PDT treatments (1,2). Fluorescence microscopy studies have shown that these low response rates of nodular BCC are probably related to the little (inhomogeneous) PpIX fluorescence in the deeper layers of nodular BCC after topical application (3-4 hours) of ALA, suggesting insufficient

photosensitization of the deeper tissues (3-5). The amount and depth of PpIX in nodular BCC after topical application of ALA could be increased by using longer application times (4-6), or by addition of a penetration enhancer and an iron chelator (5), resulting in an improved response rate for ALA-PDT of nodular BCC (7,8). Reducing the volume of nodular BCC by debulking or curettage prior to the topical application of ALA is another approach to improve the response rate for nodular BCC (8-10). Furthermore, oral (11) or systemic (5) administration of ALA results in a more homogenous PpIX production throughout the nodular BCC lesion.

Elevating the local skin temperature during topical application in order to increase the penetration (depth) of ALA into the skin that thereby may increase the PpIX production (in deeper layers), could also be an approach to improve ALA-PDT of nodular BCC. The penetration of several compounds through *in vitro* skin (as measure for penetration into skin) is temperature dependent when applied topically (12-14) and this might also be the case for ALA. An *in vitro* study showed that ALA uptake into cells is increased with increasing temperature (15). In case of short-term *in vivo* application of ALA to nude mice (10 minutes) (16) or to the skin of three healthy volunteers (15 minutes) (17), PpIX production could be increased when skin temperature was increased after (16), but not when skin temperature was increased during (16,17) the 10 or 15 minutes ALA application. The PpIX production in the skin of three healthy volunteers was increased when the skin was kept at a higher temperature during a 6 hours ALA application (17).

In the present study, we investigated whether the increase in PpIX production induced by elevating the skin temperature during ALA application might result from increased ALA penetration into skin. For this purpose we used an *in vitro* model (18,19) in which the percutaneous penetration of ALA through hairless mouse skin at 32°C (normal skin temperature) and at 37°C was determined. The effect of skin temperature on *in vivo* PpIX production in human skin has so far only been determined in a small study in which the effect of skin temperature on PpIX production was investigated at three skin temperatures in three healthy volunteers (17). We therefore decided that the effect of skin temperature on PpIX production in human skin should be further investigated. We measured the *in vivo* PpIX fluorescence in the back skin of six healthy volunteers during a clinically relevant 3 to 4 hours ALA application, while the skin was kept at different temperatures.

Materials and methods

Study design in vitro experiment

Freshly excised skin of hairless mice (9-12 weeks old, Harlan UK Ltd., Oxon, UK), killed by CO₂ asphyxiation followed by dislocation of the neck, was fitted into a cell of the *in vitro* percutaneous penetration model as described previously in detail by van den Akker et al. (18). The epidermis side of the skin was in contact with the ALA solution in the

donor compartment (effective diffusional area 56 mm²) and the dermis was in contact with 10 mM potassium phosphate buffer pH 6.8 in the receptor compartment. The receptor buffer was circulated through a water bath by means of a peristaltic pump (Pharmacia, Sweden) in order to maintain the temperature of the buffer and skin at 32°C or 37°C. After the skin samples had equilibrated in the cell for 30 minutes, 200 µl of a 20% (w/w) ALA solution (J. Griffiths, Department of Colour Chemistry, University of Leeds, Leeds, UK) pH 3 was applied in the donor compartment for 8 hours. At predetermined time intervals during the ALA application, aliquots from the receptor chamber were withdrawn and replaced with an equal volume of fresh receptor buffer. The concentration of ALA in the receptor chamber was determined spectrophotometrically, based on the method described by Mauzerall and Granick (20) with some modifications (18).

Study design in vivo experiment

Six healthy volunteers (3 male, 3 female) participated in this study. Approximately 2 gram of a gel (Instillagel, Medeco BV, Oud Beijerland, The Netherlands) containing 20% ALA (w/w) was applied to 8 application areas (3 cm in diameter) on the back skin. Four application areas were each kept at a different temperature by placing bags flushed with water at a controlled temperature of 15°C, 25°C, 35°C or 41°C on these application areas. On each volunteer's back, the water bags were distributed randomly among these four application areas. The other four application areas served as controls and were covered with water bags containing water at room temperature. The temperature in each application area was continuously measured with a fibreoptic multichannel temperature measurement device (FT1210, Takaoka, Japan).

Light delivery and in vivo fluorescence measurements

For the excitation of the skin at 405 nm, light from a mercury lamp was passed through a 405 nm bandpass filter. Low-intensity light (40 µW/cm²) was used to avoid photobleaching and photodynamic damage. A Y shaped fibre (600 µm in diameter) was used to transport the excitation light from the source to the skin and the fluorescence light to an optical multi-channel analyser (InstaSpecTM-IV 77131 CCD camera coupled to a MultiSpecTM 77400 spectrometer, Oriel Instruments, Stratford, USA) with additional 500 nm longpass filter (Schott KV 500). The Y fibre was repositioned 5 times per time point yielding fluorescence from 5 different locations within every application area.

Data analysis and statistics

The amount of ALA in the receptor compartment was calculated from the spectrophotometrically determined concentrations of ALA in the receptor compartment including a correction for the replenishment with fresh receptor buffer after the withdrawal of the sample.

The total amounts of ALA accumulated in the receptor compartment after 8 hours were tested against each other with the Mann-Whitney rank-sum test (M-W). We chose this nonparametric statistical method because the distribution of the observations (i.e. the amounts of ALA in the receptor compartment) is heavily skewed.

From the *in vivo* fluorescence emission spectra, the area under the curve was determined from the 629-643 nm interval (PpIX fluorescence, F_{PpIX}) and from the 591-601 nm interval (autofluorescence, F_{auto}). A fluorescence ratio (FR) between the mean (of the 5 measurements within the application area) F_{PpIX} and F_{auto} was then calculated for each time point:

$$FR = \frac{F_{\text{PpIX}}}{F_{\text{auto}}} \quad \text{equation 1}$$

The FR is a measure for PpIX content in the skin, corrected for differences in lamp output, fibre coupling and differences in skin colour. The use of this ratio is necessary for objective data acquisition, as the redness of the skin changes in time in some application areas during the ALA application period.

The FR was plotted as a function of time and from these curves, the gradient of the FR for the 0-1 hour, 1-2 hours, 2-3 hours and 3-4 hours time interval was determined as a measure for the reaction rate k . After plotting $\ln k$ versus $1/T$, the activation energy (E_a) could be determined from the slope of the regression line (which was obtained with the method of least squares) according to the Arrhenius equation:

$$\ln k = \ln A - \frac{E_a}{RT} \quad \text{equation 2}$$

With $\ln k$ being the reaction rate ($\text{M}^{-1} \text{s}^{-1}$), A the pre-exponential factor ($\text{M}^{-1} \text{s}^{-1}$), E_a the activation energy (kJ mol^{-1}), R the gas constant ($\text{kJ mol}^{-1} \text{K}^{-1}$) and T the temperature (K). The correlation between $\ln k$ and $1/T$ for each time interval was determined by calculating the Pearson product-moment correlation coefficient (CC) for the $\ln k$ versus $1/T$ plots. Subsequently, each CC was tested with the unpaired Student t-test (t-test) to see whether the data show a significant correlation between $\ln k$ and $1/T$. The E_a for the 1-2 hours, 2-3 hours and 3-4 hours time interval were tested with the Kruskal-Wallis statistic (K-W) to see whether they are different from each other. We chose this nonparametric statistical method (K-W) because the distribution of the variable E_a is not normally distributed, but heavily skewed.

Results

The *in vitro* ALA penetration through mouse skin during 8 hours of application at 32°C and 37°C is shown in figure 1, expressed as accumulated amount of ALA in the receptor

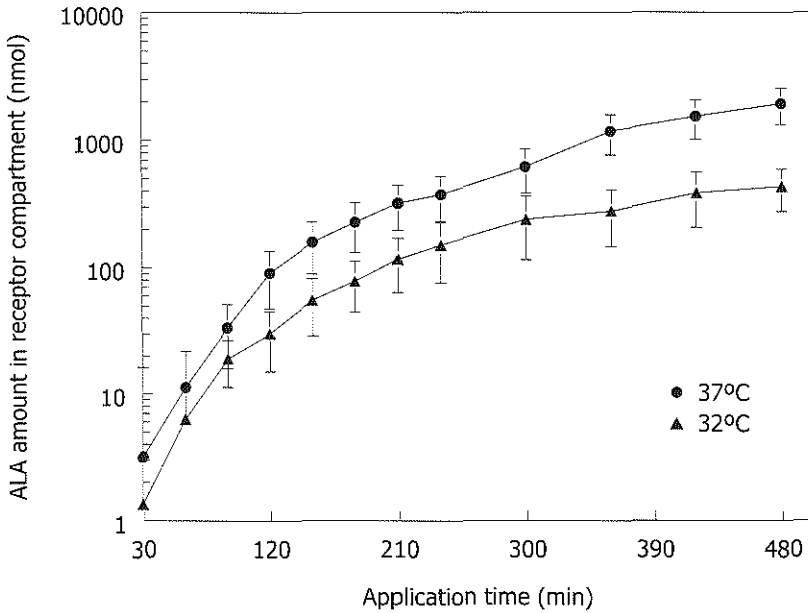


Figure 1 Accumulation of ALA in the receptor compartment in the course of the *in vitro* experiment with 20% (w/w) ALA applied to hairless mouse skin which was kept at 32°C or 37°C. Error bars represent standard error of the mean. No error bar is presented when the downward error bar exceeds the minimum value of the y-axis.

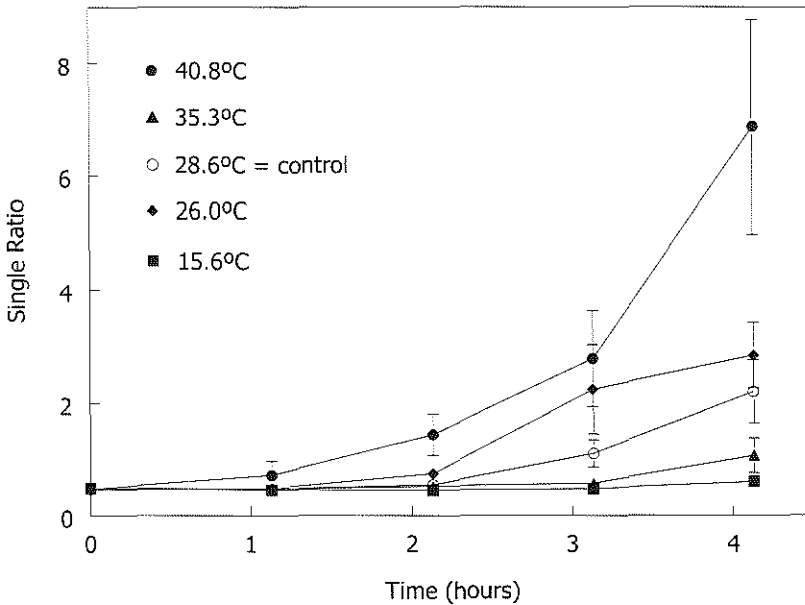
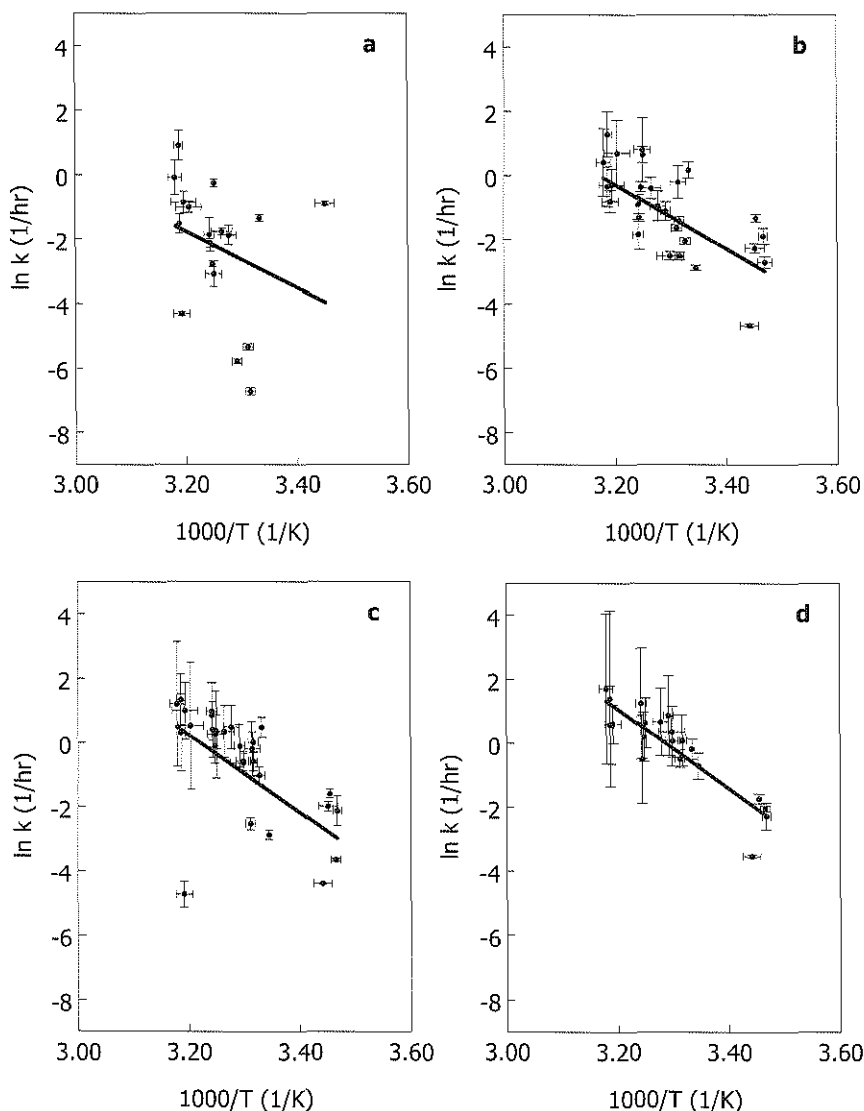


Figure 2 Temperature dependence of PpIX fluorescence kinetics in the back skin from one of the volunteers. The PpIX fluorescence kinetics in the control application areas (average temperature 28.6°C, open circles) was averaged. The 15.6°C (solid squares), 26.0°C (solid diamonds), 35.3°C (solid triangles) and 40.8°C (solid circles) curves represent PpIX fluorescence kinetics in the application areas with the 15°C, 25°C, 35°C and 42°C water bag, respectively.

Table 1 The Pearson product-moment correlation coefficients (CC) between $\ln k$ and $1/T$ from the Arrhenius plots in figure 3.

Time interval	CC	
0-1 hour	-0.28	Not significant
1-2 hours	-0.67	$P < 0.001$
2-3 hours	-0.61	$P < 0.001$
3-4 hours	-0.89	$P < 0.001$

**Figure 3** Arrhenius plots of the PpIX fluorescence data. The values for $\ln k$ for the 0-1 hour (a), 1-2 hours (b), 2-3 hours (c) and 3-4 hours (d) time interval are calculated from the slopes in the corresponding time intervals in the PpIX fluorescence kinetics during the ALA application. Linear regression lines were obtained with the method of least squares.

compartment of the *in vitro* percutaneous penetration model. The ALA accumulation is at all time points highest in case of skin that is kept at 37°C skin, although the differences between the 32°C and 37°C skin are not statistically significant.

In the *in vivo* experiment, the skin temperature in each application area remained at a constant level throughout the whole experiment (maximum standard deviation of 2.2°C). However, the influence of the temperature of the water bags on the skin temperature was different for each volunteer. Therefore, the PpIX fluorescence data from the different volunteers could not be averaged for each temperature setting of the water bags. The PpIX kinetics, expressed as FR versus time, from the application areas of one volunteer are shown in figure 2. The fluorescence data from the other volunteers resulted in similar curves, but at slightly different skin temperatures. Figure 2 clearly shows that PpIX synthesis increases with increasing temperature. No or very little PpIX production takes place when skin is cooled with the 15°C water bag and PpIX production is maximum in the application area with the highest skin temperature.

The Arrhenius plots (with regression lines) for the 0-1, 1-2, 2-3 and 3-4 hours time intervals during ALA application are shown in figure 3. The data in the Arrhenius plot for the 0-1 hour time interval do not show a significant correlation (table 1; $CC=-0.28$; t-test). For the other time intervals, the correlation between $\ln k$ and $1/T$ is significant ($P<0.001$ for all three time intervals), with $CC=-0.67$, -0.61 and -0.89 for the 1-2, 2-3

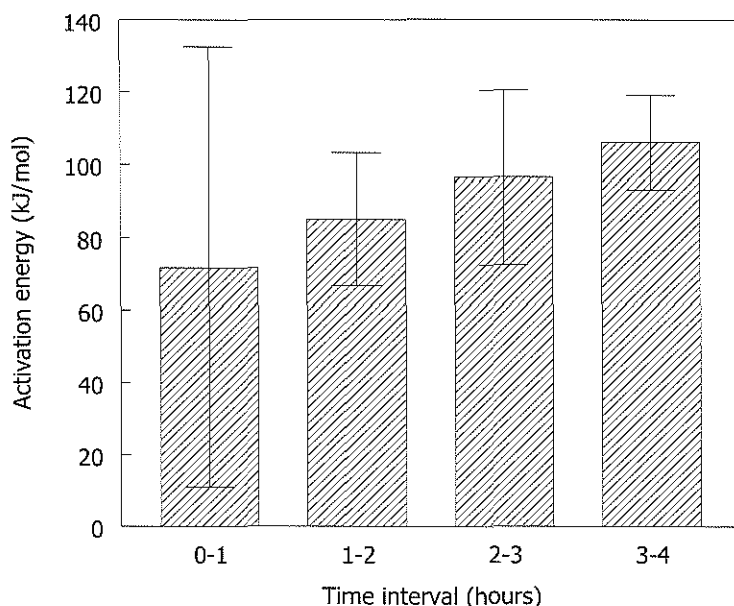


Figure 4 Activation energies for the different time intervals, as calculated from the slopes of the Arrhenius plots in figure 3. Error bars represent the standard error.

and 3-4 hours time interval (table 1), respectively.

Figure 4 shows the E_a (determined from the slopes of the regression lines in figure 3) for the four time intervals. The E_a from the 0-1 hour time interval is not significantly different from zero as a result from the fact that there is no significant correlation between $\ln k$ and $1/T$ in the corresponding Arrhenius plot. The statistics show that the E_a 's from the 1-2, 2-3 and 3-4 hours time interval are not significantly different from each other (K-W).

Discussion

Increasing ALA-induced PpIX production in cells or skin by elevating the local temperature during ALA application has been investigated previously in *in vitro* and *in vivo* experiments (15-17). It was shown in an *in vitro* study that ALA uptake into cells is increased with increasing temperature (15). A higher cellular uptake of ALA might result in increased PpIX production in the cells. From other *in vitro* experiments (17), in which the temperature was varied either during the 20 minutes ALA application to cells or during the incubation after 20 minutes ALA application at normal temperature, it was concluded that the temperature effect was more pronounced for PpIX formation than for cellular ALA uptake.

In case of a 10 minutes topical ALA application to normal nude mice, PpIX production was increased when skin temperature was increased after this short-term application (16). However, when the skin temperature was increased during a 10 minutes ALA application, no increase in PpIX production could be determined (16). In another *in vivo* study, it was found that the PpIX production in skin of three healthy volunteers could be increased during application of ALA for 6 hours (17). In the same study, the skin temperature in three healthy volunteers was elevated during a 15 minutes ALA application and then kept at normal skin temperature after the application. The data indicated, however with a large variation, that PpIX production in human skin was not increased under these circumstances.

Moan et al. concluded from the results of their study (17) and the study by Juzenas et al. (16) that the conversion of ALA to PpIX is temperature dependent, but not the penetration of ALA into the skin or cells. This conclusion is in contrast with the *in vitro* study of Rud et al. (15), who showed that ALA penetration into cells is temperature dependent. Furthermore, one should keep in mind that the authors (16,17) assume that a separate ALA-uptake and a PpIX-formation phase can be distinguished in the skin when a short-term (i.e. 10 or 15 minutes) ALA application period is used. The main process taking place during such a short application period, is the penetration of ALA into the skin. Therefore, comparing the PpIX production following different application conditions (for example the temperature) during a 10 or 15 minutes application period means comparing the influence of the application conditions on the penetration of ALA

into the skin, but not on the conversion of ALA to PpIX. However, one can not be sure that this short application period is long enough for determining a temperature effect on ALA uptake into skin. This is because of the fact that the first step of ALA penetration into the skin is the diffusion across the stratum corneum. This diffusion step can not be influenced by elevating the skin temperature as diffusion is a temperature independent process. It is not known how long the diffusion step of ALA across the stratum corneum takes, prior to ALA uptake into the epidermis where PpIX is formed. Therefore it may be the case that the application period used in those *in vivo* studies (16,17) is too short for ALA uptake into the epidermis already taking place.

The *in vitro* results from the present study contradict the earlier conclusion that the ALA penetration into the skin is not temperature dependent (16,17). The penetration of ALA into *in vitro* mouse skin, determined by measuring ALA penetration through the skin, is higher for mouse skin that was kept at 37°C than for 32°C skin (figure 1). This is in agreement with previous findings that penetration of other compounds through *in vitro* skin is also temperature dependent (12-14).

The data from the *in vivo* experiment show that the PpIX fluorescence in skin increases with increasing temperature during the application period (figure 2). The increase in PpIX fluorescence is most probably the result of three main processes involved in PpIX production which are temperature dependent: I) Increased ALA penetration into the skin (figure 1), II) increased ALA uptake by cells in the epidermis (15) and III) increased activity of the enzymes that are involved in the PpIX formation. Enzyme activity is temperature dependent and it might be that the relative optimum of the enzymes involved in PpIX formation is at higher temperature than at normal skin temperature. If this is the case, then one could expect increased PpIX formation when the skin temperature is elevated. Indeed, in previous studies it was shown that PpIX production in the skin was increased when the temperature in the application area was increased after ALA application at normal skin temperature (16,17). The enzyme ferrochelatase, involved in the conversion of PpIX to haem, might also have a higher activity at higher temperature than normal skin temperature. This would mean that not only the formation, but also the clearance of PpIX is increased at higher skin temperature. This may partly or completely compensate the gain obtained by the temperature increased ALA to PpIX conversion. The accompanying increased PpIX to haem conversion only means a faster turnover, but does not necessarily result in increased PpIX levels. Temperature induced increase in ALA penetration and cellular uptake of ALA does not have such a counteracting mechanism and will generally lead to an increase in PpIX production.

With the Arrhenius equation, the activation energy E_a for PpIX production for the four time intervals was obtained from the fluorescence data. The Arrhenius equation is a model, which generates an overall E_a for the PpIX production in the skin without knowing how many different steps are involved and which enzymes and transport

mechanisms are involved in the PpIX production. The E_a for the 0-1 hour time interval was determined from the Arrhenius plot, but is not significantly different from zero as there was no significant correlation between $\ln k$ and $1/T$ for that time interval (table 1; t-test). This result indicates that during the first hour of ALA application the PpIX production in the skin is dominated by processes that are not temperature dependent. In the first hour of ALA application the penetration into the skin is most likely mainly determined by the passive diffusion of ALA across the stratum corneum, which is the dominant process that determines the amount of ALA that penetrates into the skin (18,21).

The correlation coefficients between $\ln k$ and $1/T$ for the 1-2, 2-3 and 3-4 hours time interval proved to be significant (table 1; $P < 0.001$ for all three CC's). Thus, the data for these time intervals fit the Arrhenius equation, indicating that the PpIX production in these time intervals is dominated by a temperature dependent process. In the course of the ALA application, E_a slightly increases while the standard error decreases (figure 4). This finding indicates that during this period the balance is still slightly shifting in favour of the temperature dependent processes.

The data from the present study show that elevating the skin temperature during ALA application could be a factor in improving ALA-based PDT of BCC. The fact that the PpIX production is temperature independent in the first hour of ALA application is not a problem, as the clinically relevant application time is at least a couple of hours. Furthermore, the temperature effect on the overall PpIX production might be greater for BCC than for normal skin, as it is known that the ALA penetration into (pre)-cancerous lesions is increased compared to normal skin (19). This is the result from facilitated ALA diffusion across the stratum corneum, probably due to structural changes in this skin layer. This could result in an increased temperature effect on the PpIX production, as the temperature dependent processes (ALA penetration into the epidermis and the enzyme activity in PpIX formation) will take place in an earlier stage of the application, due to the facilitated diffusion of ALA across the stratum corneum. Further research is needed to determine what effect elevating the skin temperature during ALA application has on PpIX production in BCC lesions in patients. This further research is needed in order to determine under what circumstances (i.e. temperature of the water bags, length of ALA application period, length of water bag application period) a maximum improvement of PpIX production in the BCC lesions is achieved.

Acknowledgements

The authors wish to thank the volunteers (Angelique, Arjen, Diana, Joost, Riëtte and Willem) for participating in this study. This work was partly supported by Yorkshire Cancer Research and the Willem H. Kroger Foundation. We thank J. Griffiths (Department of Colour Chemistry, University of Leeds, Leeds, UK) for supplying ALA for the *in vitro* experiments.

References

- Peng Q, Warloe T, Berg K, Moan J, Kongshaug M, Giercksky K-E, Nesland JM. 5-Aminolevulinic acid-based photodynamic therapy. *Cancer* 1997; 79(12):2282-2308.
- Haller JC, Cairnduff F, Slack G, Schofield JS, Whitehurst C, Tunstall R, Brown SB, Roberts DJH. Routine double treatments of superficial basal cell carcinomas using aminolaevulinic acid-based photodynamic therapy. *Br J Dermatol* 2000; 143(6):1270-1274.
- Martin A, Tope WD, Grevelink JM, Starr JC, Fewkes JL, Flotte TJ, Deutsch TF, Anderson RR. Lack of selectivity of protoporphyrin IX fluorescence for basal cell carcinoma after topical application of 5-aminolevulinic acid: implications for photodynamic treatment. *Arch Dermatol Res* 1995; 287:665-674.
- Szeimies R-M, Sassy T, Landthaler M. Penetration potency of topical applied d-aminolevulinic acid for photodynamic therapy of basal cell carcinoma. *Photochem Photobiol* 1994; 59(1):73-76.
- Peng Q, Warloe T, Moan J, Heyerdahl H, Steen HB, Nesland JM, Giercksky K-E. Distribution of 5-aminolevulinic acid-induced porphyrins in nodulo-ulcerative basal cell carcinoma. *Photochem Photobiol* 1995; 62:906-913.
- Morton CA, MacKie RM, Whitehurst C, Moore JV, McColl JH. Photodynamic therapy for basal cell carcinoma: Effect of tumor thickness and duration of photosensitizer application on response. *Arch Dermatol* 1998; 134:248-249.
- Fijan S, Honigsman H, Ortel B. Photodynamic therapy of epithelial skin tumours using delta-aminolaevulinic acid and desferrioxamine. *Br J Dermatol* 1995; 133:282-288.
- Soler AM, Warloe T, Tausj t J, Berner A. Photodynamic therapy by topical aminolevulinic acid, dimethylsulphoxide and curettage in nodular basal cell carcinoma: A one-year follow-up study. *Acta Derm Venereol* 1999; 79:204-206.
- Itoh Y, Henta T, Ninomiya Y, Tajima S, Ishibashi A. Repeated 5-aminolevulinic acid-based photodynamic therapy following electrocautery for pigmented basal cell carcinoma. *J Dermatol* 2000; 27:10-15.
- Thissen MRTM, Schroeter CA, Neumann HAM. Photodynamic therapy with delta-aminolaevulinic acid for nodular basal cell carcinoma using a prior debulking technique. *Br J Dermatol* 2000; 142:338-339.
- Tope WD, Ross EV, Kollias N, Martin A, Gillies R, Anderson RR. Protoporphyrin IX fluorescence induced in basal cell carcinoma by oral δ -aminolevulinic acid. *Photochem Photobiol* 1998; 67(2):249-255.
- Chang SK, Riviere JE. Percutaneous absorption of parathion *in vitro* in porcine skin: effects of dose, temperature, humidity, and perfusate composition on absorptive flux. *Fundam Appl Toxicol* 1991; 17:494-504.
- Clarys P, Alewaeters K, Jadoul A, Barel A, Oliviera Manadas R, Preat V. In vitro percutaneous penetration through hairless rat skin: influence of temperature, vehicle and penetration enhancers. *Eur J Pharm Biopharm* 1998; 46:279-283.
- Durrheim H, Flynn GL, Higuchi WI, Behl CR. Permeation of hairless mouse skin I: Experimental methods and comparison with human epidermal permeation by alkanols. *J Pharm Sci* 1980; 69(7):781-786.
- Rud E, Gederaas O, Hogset A, Berg K. 5-Aminolevulinic acid, but not 5-aminolevulinic acid esters, is transported into adenocarcinoma cells by system BETA transporters. *Photochem Photobiol* 2000; 71(5):640-647.
- Juzenas P, S rensen R, Iani V, Moan J. Uptake of topically applied 5-aminolevulinic acid and production of protoporphyrin IX in normal mouse skin: Dependence on skin temperature. *Photochem Photobiol* 1999; 69(4):478-481.
- Moan J, Berg K, Gadmar  B, Iani V, Ma L-W, Juzenas P. The temperature dependence of protoporphyrin IX production in cells and tissues. *Photochem Photobiol* 1999; 70(4):669-673.
- van den Akker JTHM, Holroyd JA, Vernon DI, Sterenborg HJCM, Brown SB. Comparative *in vitro* percutaneous penetration of 5-aminolevulinic acid and two of its esters through excised hairless mouse skin. *Lasers Surg Med* 2003; in press.
- van den Akker JTHM, Holroyd JA, Vernon DI, Sterenborg HJCM, Brown SB. Chronic UVB exposure enhances *in vitro* percutaneous penetration of 5-aminolevulinic acid in hairless mouse skin. 2003; submitted.
- Mauzerall D, Granick S. The occurrence and determination of d-aminolevulinic acid and porphobilinogen in urine. *J Biol Chem* 1956; 219:435-446.
- van den Akker JTHM, Iani V, Star WM, Sterenborg HJCM, Moan J. Topical application of 5-aminolevulinic acid hexyl ester and 5-aminolevulinic acid to normal nude mouse skin: Differences in protoporphyrin IX fluorescence kinetics and the role of the stratum corneum. *Photochem Photobiol* 2000; 72(5):681-689.

CHAPTER 10

General discussion and summary

Tumour localisation and accumulation of carotenoporphyrins

The carotenoporphyrins (CP) were developed as a new group of photodiagnostic agents for detection of (pre)malignant lesions. The CPs have fluorescent properties similar to porphyrins, but they do not induce phototoxic reactions, as the covalently attached carotenoid moiety effectively quenches the porphyrin triplet state (1,2). *In vivo* studies in animals with transplanted tumours have shown that the CPs have promising tumour-localising properties (3-6). Chapter 3 in this thesis describes the *in vivo* fluorescence kinetics and tumour localising properties of a hexamethoxylated CP (CP6) in mice with UVB-induced early skin cancer and in rats with chemically induced mucosal dysplasia in the palate. We chose for these primary tumour models, as they present a more realistic challenge for optical detection of early cancer than models with transplanted tumours which are usually clearly visible. In accordance with the previous studies (3-6), the *in vivo* spectroscopic fluorescence measurements showed localisation of CP6 in the skin tumours and the dysplasia in the palatal mucosa. However, the fluorescence microscopy images showed that CP6 did not localise in the dysplastic epidermis nor in the dysplastic palatal mucosa, but in other tissues and structures that are not related to the malignant stage of the lesions. In conclusion, in the two primary tumour models, CP6 does not localise preferentially in pre-cancerous or cancerous tissues. Therefore, this compound was not further investigated for its use in photodetection of (pre)cancerous lesions.

Use of ALA esters for ALA-based photodetection and photodynamic therapy in skin

Ester derivatives of 5-aminolevulinic acid (ALA) have been developed in order to overcome an important limitation of topically applied ALA-based photodetection and photodynamic therapy (PDT), namely the limited amount and tumour depth of protoporphyrin IX (PpIX) produced from ALA. One of the factors that limits the production of PpIX is the low bioavailability of ALA in the skin upon topical application, which is probably due to the limited ALA penetration into the skin. ALA esters are more lipophilic than ALA (7) and may therefore penetrate in higher amounts into the skin and therewith increase the PpIX production. Several studies have demonstrated that ALA esters, and long chained ALA esters in particular, are successful in increasing PpIX production in cells (7-16) and the PpIX production and distribution in bladder mucosa (17,18).

In vivo ALA ester-induced PpIX fluorescence kinetics in normal skin

The first publications on topical application of ALA esters showed promising results

(8,19): Increased PpIX production (as compared to ALA-induced PpIX production) was measured upon topical application of the ethyl, butyl and 2-(hydroxymethyl) tetrahydrofuranyl ester to shaven mouse skin for 6 hours (8) and upon the topical application of the methyl, ethyl and propyl ester to nude mice for 14 hours (19). After application of 3.5 hours, ALA methyl, ethyl and propyl ester induced the same amounts of PpIX as ALA did (19). Contradictory to these results it was found in another study that ALAHE-induced PpIX amounts were lower than or the same as the ALA-induced PpIX amounts at all time points during a 24 hour topical application of ALA and ALA methyl ester to nude mouse skin (20). Similar results were obtained in the studies described in chapter 4 and 5.

Chapter 4 describes the PpIX fluorescence kinetics in hairless mouse skin after topical ALA pentyl ester (ALAPE) or ALA application for 30 minutes. ALAPE did not induce an increased PpIX production as compared to ALA. In fact, ALAPE-induced PpIX fluorescence was about the same as ALA-induced PpIX fluorescence at all time points after the application. The results presented in chapter 5 show that ALA hexyl ester (ALAHE) could not increase the PpIX production in normal nude mouse skin. Different application conditions of ALA and ALAHE were investigated, namely different application times, different application concentrations, the addition of a penetration enhancer and the effect of tape stripping the skin prior to the application of ALA and ALAHE. Only during 24 hour application with application concentrations of 2%, 10% or 20% (w/w), ALAHE did induce slightly more PpIX fluorescence than ALA did. ALAHE induced lower PpIX fluorescence levels than ALA in the experiments with application times up to 60 minutes and in the experiments with different concentrations (at 10 minutes application time). Using a penetration enhancer, which alters the structure of the stratum corneum, or removing the stratum corneum by tape stripping the skin, are methods used in this study to evaluate whether the stratum corneum (which is the outermost layer of the skin) is an important limiting factor for penetration of ALA and its esters into the skin (and thus PpIX production in the skin). Indeed, the stratum corneum is an important barrier against ALA and ALAHE as the PpIX production was increased when a penetration enhancer was used or when the skin was tape stripped prior to the application of ALA and ALAHE. The ALA-induced PpIX production with help of the penetration enhancer was higher than for ALAHE with help of the penetration enhancer. In tape stripped skin, the PpIX fluorescence was the same for ALA and ALAHE application. For both application circumstances (i.e. addition of penetration enhancer and tape stripped skin), the PpIX production was more increased for ALAHE than for ALA, indicating that ALAHE diffuses more slowly across the stratum corneum into the next layer of the skin, the epidermis, than ALA.

The latter result was confirmed in chapter 6, in which results are described about PpIX production outside the application area of ALA upon or during different application conditions (the same conditions as described in chapter 5). Studies with mice had

shown before that PpIX production is not restricted to the application area and that PpIX is also produced in other organs and skin outside the application area. These observations indicated that surplus PpIX or surplus ALA in the skin enters the circulation and induces PpIX fluorescence outside the ALA application area. The fact that this was observed in case of ALA application (19-23), but not in case of ALA ester application (19-21), indicates that it is not redistribution of circulating PpIX that causes the PpIX fluorescence distant from the ALA application site, but rather local PpIX production induced by circulating ALA. Chapter 6 further investigates this phenomenon and determines if the PpIX production in skin distant from ALA application area depends on the ALA concentration, the application time, the presence of a penetration enhancer, the presence of the stratum corneum, or esterification of ALA. PpIX production outside the ALA application area was only found during 24 hour ALA application or after ALA application to tape stripped skin. The amount of PpIX produced was ALA concentration dependent. No PpIX fluorescence could be detected outside the ALA application area in case of application times from 1 to 60 minutes, or when a penetration enhancer was added to the ALA cream. Furthermore, no PpIX was produced outside the application area during or after ALA hexyl ester at any application condition. These results confirm the previous findings that PpIX production outside the ALA application area can take place, but only after or during specific application conditions. The results indicate that the systemic component of PpIX production with topical ALA application plays a minor or no role in relevant clinical situations, when ALA application is relatively short, a penetration enhancer is possibly added or ALA is esterified.

ALA esters have also been investigated, and compared to ALA, in skin of healthy volunteers regarding the PpIX kinetics and phototoxicity after PDT, using iontophoresis as a quantitative delivery system (24,25). In agreement with the studies in mice (8,19,20, this thesis: chapter 4 and 5), it was found that ALA butyl ester (24), pentyl ester (25) and hexyl ester (24) could not increase the PpIX production and thus PDT phototoxicity as dramatically as they do in experiments in cells and bladder mucosa (7-18). In case of ALA butyl ester, PpIX levels and PDT effects were not increased at all as compared to ALA. PpIX fluorescence induced by ALAPE and ALAHE was not increased compared to ALA-induced PpIX fluorescence, but the peak level of ALAPE- and ALAHE-induced PpIX fluorescence was reached at an earlier time point than that of ALA-induced PpIX fluorescence. The authors observed in fluorescence microscopy images from two skin biopsies for each compound that the ester-induced PpIX fluorescence appeared to be distributed more homogeneously than ALA-induced PpIX, and that there was little difference between ALA and the esters regarding the PpIX levels in the epidermis and the depth of distribution of PpIX fluorescence in the skin.

In vivo ALA ester-induced PpIX fluorescence kinetics and tumour localisation in skin with (primary) tumours

The finding that ALA esters do not substantially increase the PpIX production in normal skin does not necessarily mean that ALA esters cannot be suitable candidates for PDT of skin cancer. A study in patients with solar keratosis showed that ALA methyl ester (ALAME) did induce lower PpIX levels in normal skin and in the lesions (26). However, the ratio of PpIX fluorescence between lesion and normal skin was higher for ALAME than for ALA.

A similar result was obtained with ALA pentyl ester (ALAPE) in the study described in chapter 4. In normal skin, ALAPE-induced PpIX levels were about the same as the ALA-induced PpIX levels. In small primary lesions of actinic and seborrhoeic keratosis and squamous cell carcinoma (induced by chronic UVB exposure of the skin (27,28)), ALAPE induced higher PpIX levels than ALA, but only at later time points. The apparently normal looking skin adjacent to the lesions is thickened and dysplastic (27,29,30 and histological examination of the skin samples) and accumulates more PpIX upon ALAPE application than upon ALA application. These *in vivo* differences between ALA and ALAPE result in ratios of PpIX fluorescence between (pre)cancerous skin and normal skin that are higher for ALAPE than for ALA. This indicates that PDT with ALA esters may be more selective than with PDT with ALA. However, the fluorescence microscopy images revealed that at these later time points the higher *in vivo* PpIX ratio between (pre)cancerous skin and normal skin for ALAPE is not related to an increased PpIX fluorescence in the dysplastic part of the epidermis, which is the area of interest for PDT. The ALAPE-induced PpIX levels in the dysplastic part of the epidermis are the same as for ALA, but the stratum corneum showed higher PpIX levels for ALAPE than for ALA.

The results from chapter 4 also reveal that the higher *in vivo* ratio of PpIX fluorescence between (pre)cancerous skin and normal skin is not the sole result of preferential accumulation of ALA- or ALA ester-induced PpIX in (pre)cancerous skin. The PpIX fluorescence measured by quantitative fluorescence microscopy in the dysplastic part of the epidermis is higher in the lesions than in the apparently normal looking adjacent skin. This strongly indicates that accumulation of ALA- or ALA ester-induced PpIX in (pre)cancerous skin takes place. However, the quantitative differences in PpIX fluorescence at microscopic level between normal and (pre)cancerous skin are not as large as could be expected on basis of the *in vivo* measurements. The fluorescence images show that the PpIX fluorescence is mainly located in the epidermis and hair follicles. The dysplastic cells are located in the epidermis, which results in differences in epidermal thickness between normal skin, the lesions and the apparently normal looking skin adjacent to the lesions. The epidermis is thickest in the lesions and thinnest in normal skin. From these observations, one can easily deduce

that the *in vivo* PpIX fluorescence signal increases with increasing epidermal thickness, which is related to the (pre)cancerous stage of the skin.

In addition to these studies on the accumulation of ALA esters in (pre)cancerous lesions, the accumulation of ALAME-induced PpIX in thick basal cell carcinomas (BCC) has been investigated (31). A highly selective and homogeneous distributed PpIX fluorescence induced by ALAME was found in all lesions studied. Unfortunately, no comparison was made with ALA-induced PpIX accumulation and distribution in similar thick BCCs. Therefore, the results are not conclusive whether ALAME increases PpIX production and/or the PpIX fluorescence ratio between lesions and normal skin as compared to ALA.

Photodynamic therapy using ALA esters

The efficacy of photodynamic therapy of basal cell carcinomas with ALA methyl ester (ALAME) has been assessed in two clinical studies (32,33). The clinical response of residual and recurrent basal cell carcinomas (BCC) to PDT was not different between PDT with ALA and dimethylsulphoxide (an established penetration enhancer) and PDT with ALAME (32). In the second study, superficial and nodular BCCs were treated with ALAME-based PDT with or without curettage (for the nodular and superficial BCCs, respectively) prior to the treatment (33). The initial complete response (after 3-6 months) was 89% (310/350 lesions) and the overall long-term complete response (after 24-48 months) was 79% (277/350 lesions). These response rates for ALAME-based PDT correspond to the response rates reported on ALA-based PDT (34).

The clinical response after ALA methyl ester-based photodynamic therapy in basal cell carcinomas appears not to be dramatically improved compared to ALA-based photodynamic therapy. In order to get a more conclusive comparison between ALA- and ALA (methyl) ester-based photodynamic therapy in (pre)cancerous skin lesions, further investigation is necessary, preferably double-blind randomised clinical studies with ALA and ALA (methyl) ester(s) being used within the same study.

In vitro percutaneous penetration of ALA and ALA esters

Normal skin penetration properties of ALA and ALA esters

Upon topical application, ALA esters do not increase the PpIX production as well in the skin as could be expected from the results obtained in cells and bladder mucosa. In chapter 7, it was investigated in an *in vitro* percutaneous penetration model whether this is caused by unexpected differences in skin penetration properties between ALA and ALA esters. The experiments with application of ALA, ALAME and ALAHE at the concentration of 500 or 1500 mM (equivalent to 7.7% and 20% (w/w), respectively) indicated that the penetration of ALA across skin is higher than that of ALAME and ALAHE. This finding is consistent with previous *in vivo* studies in which was found that

ALA, but not esterified ALA, is taken up (across the skin) into the circulation in sufficiently high amounts to induce PpIX fluorescence outside the application area (19,20,chapter 6 of this thesis). There is no difference between the ALA, ALAME and ALAHE penetration across the skin during application with the relative high concentration of 3000 mM (equivalent to 34% (w/w)).

Experiments in which ALA and the esters were applied to tape stripped skin in order to determine the effect of the stratum corneum barrier function on the skin penetration, showed that the penetration of ALA, ALAME and ALAHE through tape stripped skin is about 100 times (ALA) or about 200 times (ALAME and ALAHE) higher than through normal skin. These results confirm the finding in previous *in vivo* studies that the stratum corneum is an important barrier for the skin penetration of ALA and ALA esters (35,this thesis: chapter 5 and 6).

Penetration properties of ALA through (pre)cancerous skin versus normal skin

Upon application of ALA to skin areas with precancerous lesions, such as Bowen's disease and actinic keratosis, or superficial cancerous lesions, such as squamous cell carcinoma and basal cell carcinoma, PpIX accumulates preferentially in these (pre)malignant lesions (36-42). Many authors have suggested or assumed that the skin permeation properties of these (pre)malignant lesions are responsible for this preferential PpIX accumulation. The skin (i.e. the stratum corneum) overlying the (pre)malignant lesions most likely has different permeation properties compared to normal skin resulting in a higher penetration rate of ALA into and thus preferential PpIX accumulation in these lesions. The study described in chapter 8 of this thesis, presents for the first time results that confirm this hypothesis. Results were obtained in the *in vitro* percutaneous penetration model with dorsal skin from normal hairless mice, dorsal skin from normal hairless mice with reduced stratum corneum layer (i.e. tape stripped skin) and dorsal skin with dysplastic and thickened epidermis from chronically UVB-exposed hairless mice (29,43,44). The chronically UVB-exposed hairless mouse skin is a model skin condition for the above described (pre)cancerous skin lesions, as these lesions may originate from chronically sun-exposed skin. The penetration of ALA across chronically UVB-exposed skin was higher than across normal skin, but lower than across tape stripped skin. This indicates that the stratum corneum barrier function is less effective in chronically UVB-exposed skin than in normal skin, but more effective than in skin with (partly) removed stratum corneum.

Skin temperature during topical ALA application

Besides the use of esterified ALA, many other approaches for improving ALA-based PDT are under investigation or have been applied successfully (45-49,chapter 2). One

of the proposed approaches is to increase PpIX production in the skin by elevating the skin temperature during topical ALA application. *In vivo* studies showed increased PpIX production in mouse skin (50) and human skin (51) when skin temperature was elevated during long-term ALA application (6 hours, (51)) and after short-term ALA application (10 or 15 minutes, (50)), but not during short-term ALA application (10 or 15 minutes, (50,51)). The authors of these publications (50,51) concluded on basis of PpIX fluorescence measurements that elevating the skin temperature increases the conversion of ALA to PpIX, but does not increase the penetration of ALA into the skin or cells. This conclusion is in contrast with studies that showed temperature dependency of skin penetration of several compounds (52-54) and with a study that showed that ALA uptake by cells is temperature dependent (55).

Chapter 9 describes results from *in vitro* and *in vivo* experiments in which the effect of skin temperature during topical ALA application on the penetration of ALA through mouse skin, and the PpIX production in human skin is investigated. The data from the experiments with the *in vitro* percutaneous penetration model clearly show that the ALA penetration through skin is temperature dependent, therewith contradicting the earlier conclusion based on PpIX fluorescence measurements that ALA penetration is not temperature dependent (50,51). The *in vivo* experiments presented in chapter 9 show that the PpIX fluorescence in normal human skin increases with increasing temperature of the skin during ALA application.

General conclusions

The studies with the carotenoporphyrin and with ALA pentyl ester versus ALA have shown that (semi)quantitative fluorescence microscopy is vitally important in studies on the *in vivo* fluorescence kinetics of photodiagnostic agents that are being investigated for tumour detection.

A higher *in vivo* ratio of PpIX fluorescence between (pre)cancerous skin and normal skin is not solely due to preferential accumulation of ALA- or ALA ester-induced PpIX in (pre)cancerous skin. Differences in epidermal thickness between normal and (pre)cancerous skin also contribute to the *in vivo* PpIX fluorescence signal, as PpIX mainly localises in the epidermis and hair follicles.

Regarding the alternatives to the use of porphyrins in photodetection of (pre)cancerous lesions, it can be concluded that the carotenoporphyrin CP6 does not localise preferentially in the (pre)malignant tissues in the primary tumour models. ALA pentyl ester (ALAPE) induces preferential accumulation of PpIX in (pre)cancerous mouse skin lesions. ALAPE-induced PpIX levels in the (pre)malignant tissues of the lesions are not or not substantially higher than ALA-induced PpIX levels. The PpIX levels in normal skin are lower for ALAPE application than for ALA application. This

results in a ratio in PpIX fluorescence between (pre)cancerous and normal tissue that is higher for ALAPE than for ALA, therewith improving the photodetection of the (pre)malignant lesions and diminishing the undesirable PDT effects in normal skin.

Quite in contrast to the expectations, based on the results obtained with ALA hexyl ester (ALAHE) in the bladder mucosa, ALAHE-induced PpIX production in the skin is not substantially increased or is decreased as compared to the ALA-induced PpIX production. A (co-)responsible factor for this might be the finding that ALA and ALA esters have different *in vitro* skin penetration properties: ALA esters penetrate more slowly across the skin than ALA. This is in agreement with the *in vivo* situation in which PpIX production in skin outside the application area can take place only after or during specific application conditions for ALA but not for ALAHE.

The penetration rate of ALA into (pre)cancerous lesions is higher than into normal skin. This difference may be (partly) responsible for the preferential accumulation of PpIX in (pre)cancerous lesions.

Elevating the skin temperature increases the penetration of ALA into the skin and therewith the PpIX production in the skin and might therefore be a useful approach for improving ALA-based PDT.

References

1. Gust D, Moore TA, Moore AL, Jori G, Reddi E. The photochemistry of carotenoids. Some photosynthetic and photomedical aspects. *Ann NY Acad* 1993; 691:32-47.
2. Gust D, Moore TA, Moore AL, Devadoss C, Lidell PA, Hermant R, Nieman RA, Demanche LJ, DeGraziano JM, Gouni I. Triplet and singlet energy transfer in carotene-porphyrin dyads: role of linkage bonds. *J Am Chem Soc* 1992; 114:3590-3603.
3. Reddi E, Segalla A, Jori G, Kerrigan PK, Lidell PA, Moore AL, Moore TA, Gust D. Carotenoporphyrins as selective photodiagnostic agents for tumours. *Br J Cancer* 1994; 69:40-45.
4. Nilsson H, Johansson J, Svanberg K, Svanberg S, Jori G, Reddi E, Segalla A, Gust D, Moore AL, Moore TA. Laser-induced fluorescence in malignant and normal tissue in mice injected with two different carotenoporphyrins. *Br J Cancer* 1994; 70:873-879.
5. Nilsson H, Johansson J, Svanberg K, Svanberg S, Jori G, Reddi E, Segalla A, Gust D, Moore AL, Moore TA. Laser-induced fluorescence studies of the biodistribution of carotenoporphyrins in mice. *Br J Cancer* 1997; 76(3):355-364.
6. Saarnak AE, Rodrigues T, Schwartz J, Moore AL, Moore TA, Gust D, van Gemert MJC, Sterenborg HJCM, Thomsen SL. Influence of tumour depth, blood absorption and autofluorescence on measurements of exogenous fluorophores in tissue. *Lasers Med Sci* 1998; 13:22-31.
7. Ühlinger P, Zellweger M, Wagnières GA, Juillerat-Jeanneret L, van den Bergh H, Lange N. 5-Aminolevulinic acid and its derivatives: physical chemical properties and protoporphyrin IX formation in cultured cells. *J Photochem Photobiol B* 2000; 54:72-80.
8. Kloek J, Beijersbergen van Henegouwen GMJ. Prodrugs of 5-aminolevulinic acid for photodynamic therapy. *Photochem Photobiol* 1996; 64(6):994-1000.
9. Gaullier J-M, Berg K, Peng Q, Anholt H, Selbo PK, Ma L-W, Moan J. Use of 5-aminolevulinic acid esters to improve photodynamic therapy on cells in culture. *Cancer Res* 1997; 57:1481-1486.
10. Kloek J, Akkermans W, Beijersbergen van Henegouwen GMJ. Derivatives of 5-aminolevulinic acid for photodynamic therapy: enzymatic conversion into protoporphyrin. *Photochem*

Photobiol 1998; 67(1):150-154.

11. Whitaker CJ, Battah SH, Forsyth MJ, Edwards C, Boyle RW, Matthews EK. Photosensitization of pancreatic tumour cells by δ -aminolaevulinic acid esters. *Anti-Cancer Drug Design* 2000; 15:161-170.
12. Eléout S, Rousset N, Carre J, Bourre L, Vonarx V, Lajat Y, Beijersbergen van Henegouwen GMJ, Patrice T. *In vitro* fluorescence, toxicity and phototoxicity induced by δ -aminolaevulinic acid (ALA) or ALA esters. *Photochem Photobiol* 2000; 71(4):447-454.
13. Cosserat-Gerardin I, Bezdetnaya L, Notter D, Vigneron C, Guillemin F. Biosynthesis and photodynamic efficacy of protoporphyrin IX (PpIX) generated by 5-aminolaevulinic acid (ALA) or its hexylester (hALA) in rat bladder carcinoma cells. *J Photochem Photobiol B* 2000; 59:72-79.
14. Luksiene Z, Eggen I, Moan J, Nesland JM, Peng Q. Evaluation of protoporphyrin IX production, phototoxicity and cell death pathway by hexylester of 5-aminolaevulinic acid in Reh and HPB-ALL cells. *Cancer Letters* 2001; 169:33-39.
15. Xiang W, Weingandt H, Liessmann F, Klein S, Stepp H, Baumgartner R, Hillemans P. Photodynamic effects induced by aminolaevulinic acid esters on human cervical carcinoma cells in culture. *Photochem Photobiol* 2001; 74(4):617-623.
16. Brunner H, Hausmann F, Krieg RC, Endlicher E, Schölmerich J, Kneuchel R, Messmann H. The effects of 5-aminolaevulinic acid esters on protoporphyrin IX production in human adenocarcinoma cell lines. *Photochem Photobiol* 2001; 74(5):721-725.
17. Marti A, Lange N, van den Bergh H, Sedmera D, Jichlinski P, Kucera P. Optimisation of the formation and distribution of protoporphyrin IX in the urothelium: an *in vitro* approach. *J Urol* 1999; 162:546-552.
18. Lange N, Jichlinski P, Zellweger M, Forrer M, Marti A, Guillou L, Kucera P, Wagnières GA, van den Bergh H. Photodetection of early human bladder cancer based on the fluorescence of 5-aminolaevulinic acid hexylester-induced protoporphyrin IX: a pilot study. *Br J Cancer* 1999; 80(1/2):185-193.
19. Peng Q, Moan J, Warloe T, Iani V, Steen HB, Bjorseth A, Nesland JM. Build-up of esterified aminolaevulinic-acid-derivative-induced porphyrin fluorescence in normal mouse skin. *J Photochem Photobiol B* 1996; 34:95-96.
20. Moan J, Ma L-W, Iani V. On the pharmacokinetics of topically applied 5-aminolaevulinic acid and two of its esters. *Int J Cancer* 2001; 92:139-143.
21. Sørensen R, Juzenas P, Iani V, Moan J. Formation of protoporphyrin IX in mouse skin after topical application of 5-aminolaevulinic acid and its methyl ester. *Proc SPIE* 1999; 3563:77-81.
22. Casas A, Fukuda H, del C. Battle AM. Tissue distribution and kinetics of endogenous porphyrins synthesized after topical application of ALA in different vehicles. *Br J Cancer* 1999; 81(1):13-18.
23. Casas A, Fukuda H, di Venosa G, del C. Battle AM. The influence of the vehicle on the synthesis of porphyrins after topical application of 5-aminolaevulinic acid. Implications in cutaneous photodynamic sensitization. *Br J Dermatol* 2000; 143:564-572.
24. Gerscher S, Connelly JP, Griffiths J, Brown SB, MacRobert AJ, Wong G, Rhodes LE. Comparison of the pharmacokinetics and phototoxicity of protoporphyrin IX metabolized from 5-aminolaevulinic acid and two derivatives in human skin *in vivo*. *Photochem Photobiol* 2000; 72(4):569-574.
25. Gerscher S, Connelly JP, Beijersbergen van Henegouwen GMJ, MacRobert AJ, Watt P, Rhodes LE. A quantitative assessment of protoporphyrin IX metabolism and phototoxicity in human skin following dose-controlled delivery of the prodrugs 5-aminolaevulinic acid and 5-aminolaevulinic acid-n-pentylester. *Br J Dermatol* 2001; 144:983-990.
26. Fritsch C, Homey B, Stahl W, Lehmann P, Ruzicka T, Sies H. Preferential relative porphyrin enrichment in solar keratoses upon topical application of δ -aminolaevulinic acid methylester. *Photochem Photobiol* 1998; 68(2):218-221.
27. de Gruijl FR, van der Meer JWM, van der Leun JC. Dose-time dependency of tumour formation by chronic UV exposure. *Photochem Photobiol* 1983; 37:53-62.
28. de Gruijl FR, Sterenborg HJCM, Forbes PD, Davies RE, Cole C, Kelfkens G, van Weelden H, Slaper H, van der Leun JC. Wavelength dependence of skin cancer induction by ultraviolet irradiation of albino hairless mice. *Cancer Res* 1993; 53:53-60.
29. Sterenborg HJCM, de Gruijl FR, van der Leun JC. UV-induced epidermal hyperplasia in hairless mice. *Photodermatol* 1986; 3:206-214.
30. Sterenborg HJCM, van der Leun JC. Change in epidermal transmission due to UV-induced hyperplasia in hairless mice: a first approximation of the action spectrum. *Photodermatol* 1988;

5:71-82.

31. Peng Q, Soler AM, Warloe T, Nesland JM, Giercksky K-E. Selective distribution of porphyrins in skin thick basal cell carcinoma after topical application of methyl 5-aminolevulinate. *J Photochem Photobiol B* 2001; 62:140-145.
32. Soler AM, Warloe T, Tausj t J, Giercksky K-E. Photodynamic therapy of residual or recurrent basal cell carcinoma after radiotherapy using topical 5-aminolevulinic acid or methylester aminolevulinic acid. *Acta Oncol* 2000; 39(5):605-609.
33. Soler AM, Warloe T, Berner A, Giercksky K-E. A follow-up study of recurrence and cosmesis in completely responding superficial and nodular basal cell carcinomas treated with methyl 5-aminolevulinate-based photodynamic therapy alone and with prior curettage. *Br J Dermatol* 2001; 145:467-471.
34. Peng Q, Warloe T, Berg K, Moan J, Kongshaug M, Giercksky K-E, Nesland JM. 5-Aminolevulinic acid-based photodynamic therapy. *Cancer* 1997; 79(12):2282-2308.
35. Goff BA, Bachor R, Kollias N, Hasan T. Effects of photodynamic therapy with topical application of 5-aminolevulinic acid on normal skin of hairless guinea pigs. *J Photochem Photobiol B* 1992; 15:239-251.
36. Szeimies R-M, Sassy T, Landthaler M. Penetration potency of topical applied d-aminolevulinic acid for photodynamic therapy of basal cell carcinoma. *Photochem Photobiol* 1994; 59(1):73-76.
37. Roberts DJH, Stables GI, Ash DV, Brown SB. Distribution of protoporphyrin IX in Bowen's disease and basal cell carcinomas treated with topical 5-aminolaevulinic acid. *Proc SPIE* 1995; 2371:490-494.
38. Peng Q, Warloe T, Moan J, Heyerdahl H, Steen HB, Nesland JM, Giercksky K-E. Distribution of 5-aminolevulinic acid-induced porphyrins in nodulo-ulcerative basal cell carcinoma. *Photochem Photobiol* 1995; 62:906-913.
39. van der Veen N, de Bruijn HS, Berg RJW, Star WM. Kinetics and localisation of PpIX fluorescence after topical and systemic ALA application, observed in skin and skin tumours of UVB-treated mice. *Br J Cancer* 1996; 73:925-930.
40. Orenstein A, Kostenich G, Malik Z. The kinetics of protoporphyrin fluorescence during ALA-PDT in human malignant skin tumors. *Cancer Letters* 1997; 120:229-234.
41. Wagn  res GA, Star WM, Wilson BC. *In vivo* fluorescence spectroscopy and imaging for oncological applications. *Photochem Photobiol* 1998; 68(5):603-632.
42. af Klinteberg C, Enejeder AMK, Wang I, Andersson-Engels S, Svanberg S, Svanberg K. Kinetic fluorescence studies of 5-aminolaevulinic acid-induced protoporphyrin IX accumulation in basal cell carcinomas. *J Photochem Photobiol B* 1999; 49:120-128.
43. Bissett DL, Hannon DP, Orr TV. An animal model of solar-aged skin: histological, physical, and visible changes in UV-irradiated hairless mouse skin. *Photochem Photobiol* 1987; 46(3):367-378.
44. Kligman LH. The hairless mouse and photoaging. *Photochem Photobiol* 1991; 54(6):1109-1118.
45. Piot B, Rousset N, Lenz P, El  out S, Carr   J, Vonarx V, Bourr   L, Patrice T. Enhancement of delta aminolevulinic acid-photodynamic therapy *in vivo* by decreasing tumor pH with glucose and amiloride. *Laryngoscope* 2001; 111:2205-2213.
46. Johnson PG, Wen Hui S, Oseroff AR. Electrically enhanced percutaneous delivery of   -aminolevulinic acid using electric pulses and a DC potential. *Photochem Photobiol* 2002; 75(5):534-540.
47. de Blois AW, Thissen MRTM, de Bruijn HS, Grouls RJE, Dutrieux RP, Robinson DJ, Neumann HAM. *In vivo* pharmacokinetics of protoporphyrin IX accumulation following intracutaneous injection of 5-aminolevulinic acid. *J Photochem Photobiol B* 2001; 61:21-29.
48. Tsai J-C, Chen I-H, Wong T-W, Lo Y-L. *In vitro/in vivo* correlations between transdermal delivery of 5-aminolevulinic acid and cutaneous protoporphyrin IX accumulation and effect of formulation. *Br J Dermatol* 2002; 146:853-862.
49. Pierre MBR, Tedesco AC, Marchetti JM, Bentley MVLB. Stratum corneum lipids liposomes for the topical delivery of 5-aminolevulinic acid in photodynamic therapy of skin cancer: preparation and *in vitro* permeation study. *BMC Dermatology* 2001; 1(5)
50. Juzenas P, S  rensen R, Iani V, Moan J. Uptake of topically applied 5-aminolevulinic acid and production of protoporphyrin IX in normal mouse skin: Dependence on skin temperature. *Photochem Photobiol* 1999; 69(4):478-481.
51. Moan J, Berg K, Gadmar YB, Iani V, Ma L-W, Juzenas P. The temperature dependence of protoporphyrin IX production in cells and tissues. *Photochem Photobiol* 1999; 70(4):669-673.

52. Chang SK, Riviere JE. Percutaneous absorption of parathion *in vitro* in porcine skin: effects of dose, temperature, humidity, and perfusate composition on absorptive flux. *Fundam Appl Toxicol* 1991; 17:494-504.
53. Clarys P, Alewaeters K, Jadoul A, Barel A, Oliviera Manadas R, Preat V. *In vitro* percutaneous penetration through hairless rat skin: influence of temperature, vehicle and penetration enhancers. *Eur J Pharm Biopharm* 1998; 46:279-283.
54. Durrheim H, Flynn GL, Higuchi WI, Behl CR. Permeation of hairless mouse skin I: Experimental methods and comparison with human epidermal permeation by alkanols. *J Pharm Sci* 1980; 69(7):781-786.
55. Rud E, Gederaas O, Hogset A, Berg K. 5-Aminolevulinic acid, but not 5-aminolevulinic acid esters, is transported into adenocarcinoma cells by system BETA transporters. *Photochem Photobiol* 2000; 71(5):640-647.

Samenvatting en conclusies

Inleiding

Fotodetectie en fotodynamische therapie worden ontwikkeld om kanker en voorlopers van kanker op te kunnen sporen (detectie) of te behandelen (therapie). Bij fotodetectie en fotodynamische therapie wordt gebruik gemaakt van stoffen die door licht geactiveerd kunnen worden, de zogenaamde fotosensitizers. Zo'n fotosensitizer kan met een injectie of een zalf toegediend worden, hetgeen het geval is bij porfyrinederivaten. Ook kan de fotosensitizer in het lichaam geproduceerd worden na toediening van een geschikte bouwsteen: zo zorgt aminolevulinezuur er voor dat het lichaam de fotosensitizer protoporfyrine IX produceert.

De ideale fotosensitizer hoopt zich selectief op in (pre)maligne weefsel (tumoren en voorlopers van tumoren). Na blootstelling aan licht met de juiste golflengte, fluoresceert de fotosensitizer en gaat een reactie aan met celbestanddelen en/of produceert reactieve zuurstofvormen. Deze reactie met celbestanddelen en de reactieve zuurstofvormen zijn verantwoordelijk voor het fotodynamische effect. Hierdoor gaat de cel dood en verdwijnt het (pre)maligne weefsel. De fluorescentie-eigenschappen kunnen gebruikt worden voor diagnose van (pre)maligne weefsel dat niet voor het blote oog zichtbaar is.

Een belangrijk nadeel van fotodetectie met fotosensitizers is dat de fotodynamische eigenschappen van de porfyrinederivaten en protoporfyrine IX kunnen leiden tot ongewenste bijwerkingen zoals langdurige lichtovergevoeligheid van de huid, en erytheem. Deze bijwerkingen kunnen te sterk zijn om deze stoffen enkel voor diagnostische doeleinden te gebruiken.

Er zijn een aantal belangrijke beperkingen van fotodynamische therapie met aminolevulinezuur. De productie van protoporfyrine IX in de (pre)maligne weefsels is niet hoog genoeg en de protoporfyrine IX productie vindt niet diep genoeg in de tumoren plaats.

Het proefschrift

Na een algemene inleiding in hoofdstuk 1, beschrijft hoofdstuk 2 de principes en het werkingsmechanisme van fotodynamische therapie met aminolevulinezuur. Ook wordt in dat hoofdstuk een overzicht gegeven van behandelingen van (kwaadaardige) huid-aandoeningen met deze therapie. Daarnaast wordt beschreven hoe bepaalde nadelen van aminolevulinezuur de therapie beperken en welke methoden er onderzocht en/of toegepast worden om de therapie te verbeteren.

De hoofdstukken 3 t/m 9 behandelen een aantal mogelijke oplossingen voor de nadelen en beperkingen van porfyrine-achtige stoffen en protoporfyrine IX bij fotodetectie en fotodynamische therapie. De experimenten en resultaten uit deze hoofdstukken zijn per onderwerp samengevat op de volgende pagina's.

Tumorlokalisatie en -ophoping van carotenoporfyrines

Carotenoporfyrines zijn een nieuw soort fotosensitizers voor de fotodetectie van (pre)-maligne afwijkingen. De carotenoporfyrines hebben dezelfde fluorescentie-eigenschappen als andere porfyrines, maar ze veroorzaken geen schade omdat ze niet reageren met zuurstof en/of celbestanddelen. Uit eerdere studies bij muizen met getransplanteerde tumoren bleek dat de carotenoporfyrines goed lokaliseren in deze tumoren en zich daar ook ophopen. In hoofdstuk 3 wordt de kinetiek en tumorlokalisatie van een nieuwe carotenoporfyrine (hexamethoxy-carotenoporfyrine) onderzocht in muizen met vroege huidkanker (ontstaan door chronische blootstelling aan UVB straling), en in ratten met afwijkingen in het gehemelte (chemisch opgewekt). Deze diersmodellen met zogeheten primaire tumoren zijn in deze studie gebruikt, omdat ze realistischer zijn dan het diersmodel met een getransplanteerde tumor. Uit metingen van het fluorescentiesignaal van de carotenoporfyrine op de huid en het gehemelte blijkt dat deze nieuwe carotenoporfyrine inderdaad lokaliseert en zich ophoopt in de huidtumoren en in het afwijkende gedeelte van het gehemelte. Fluorescentiemicroscopiebeelden laten echter zien dat de carotenoporfyrine zich niet ophoopt in het echte (pre)maligne gebied van de huidtumoren en het gehemelte, maar op andere plaatsen in deze afwijkingen die niet gerelateerd zijn aan het (pre)maligne gebied.

Gebruik van aminolevulinezuur esters voor fotodetectie en fotodynamische therapie in de huid

Een mogelijke oorzaak voor het feit dat in de tumoren de productie van protoporfyrine IX uit aminolevulinezuur niet hoog genoeg is en niet in het diepere gedeelte van de tumor plaats vindt, is dat aminolevulinezuur niet diep genoeg de huid in penetreert. Aminolevulinezuur esters zijn ontwikkeld als mogelijke oplossing voor dit probleem. Zij zijn afgeleid van aminolevulinezuur en door hun structuur zouden zij beter de huid in kunnen penetreren en daarmee zorgen voor een protoporfyrine IX productie die hoger si en dieper in de tumor plaatsvindt. Vele studies hebben al laten zien dat een aantal aminolevulinezuur esters succesvol kunnen zijn in het verhogen van de protoporfyrine IX productie in gekweekte cellen.

Voor de experimenten in dit proefschrift is gebruik gemaakt van zogenaamde haarloze en naakte muizen. Deze muizen hebben nauwelijks tot geen haar groeien op hun huid, waardoor hun huid lijkt op die van een mens.

Protoporfyrine IX productie in normale huid

Uit resultaten in hoofdstuk 4 blijkt dat in het geval dat aminolevulinezuur pentyl ester gedurende 30 minuten aangebracht geweest is, de productie van protoporfyrine IX in normale huid van haarloze muizen ongeveer hetzelfde is als in het geval van

aminolevulinezuur. De resultaten in hoofdstuk 5 laten zien dat ook aminolevulinezuur hexyl ester de protoporfyrine IX productie in normale naakte muizenhuid niet of nauwelijks verhoogt ten opzichte van aminolevulinezuur. Verschillende omstandigheden waaronder aminolevulinezuur en aminolevulinezuur hexyl ester aangebracht kunnen worden zijn onderzocht, namelijk variatie in de tijd van aanbrengen, verschillende concentraties, de toevoeging van een stof die penetratie door de hoornlaag (buitenste laagje van de huid) bevordert, en de invloed van het verwijderen van de hoornlaag met plakband voorafgaand aan het aanbrengen van aminolevulinezuur hexyl ester en aminolevulinezuur. Alleen wanneer aminolevulinezuur hexyl ester en aminolevulinezuur gedurende 24 uur aangebracht zijn, zorgt de aminolevulinezuur hexyl ester voor een iets hogere protoporfyrine IX productie dan aminolevulinezuur. Wanneer ze korter aangebracht worden, dan is de protoporfyrine IX productie bij aminolevulinezuur esters lager dan bij aminolevulinezuur. Uit de experimenten met de penetratiebevorderaar en de huid met verwijderde hoornlaag blijkt dat de hoornlaag een belangrijke barrière vormt voor aminolevulinezuur en aminolevulinezuur hexyl ester. De protoporfyrine IX productie is (sterk) verhoogd in het geval dat de penetratiebevorderaar is toegevoegd of de hoornlaag verwijderd was. Ondanks de toevoeging van de penetratiebevorderaar is de protoporfyrine IX productie bij aminolevulinezuur hexyl ester lager dan bij aminolevulinezuur. In de huid zonder hoornlaag is de protoporfyrine IX productie bij aminolevulinezuur en aminolevulinezuur hexyl ester gelijk. In het geval van aminolevulinezuur hexyl ester is het verschil in protoporfyrine IX productie tussen de huid zonder hoornlaag en de gewone huid dus groter dan in het geval van aminolevulinezuur. Dit geeft aan dat aminolevulinezuur hexyl ester langzamer dan aminolevulinezuur door de hoornlaag de huid ingaat.

Het feit dat aminolevulinezuur hexyl ester langzamer de huid ingaat komt overeen met resultaten uit eerdere studies. In die studies werd gevonden dat als aminolevulinezuur lange tijd op een klein stukje huid van een muis aangebracht is, er ook protoporfyrine IX geproduceerd wordt in organen en huid buiten het gebied waar aminolevulinezuur aangebracht is. Deze bevinding geeft aan dat aminolevulinezuur door de hoornlaag en de rest van huid heen opgenomen wordt in de bloedbaan en vervolgens er voor zorgt dat er protoporfyrine IX geproduceerd wordt in andere organen en huid buiten het gebied waar aminolevulinezuur aangebracht is. In het geval van aminolevulinezuur esters vindt er geen protoporfyrine IX productie plaats buiten het stukje huid waar ze aangebracht zijn. Dit duidt aan dat aminolevulinezuur esters niet of in veel mindere mate door de huid heen gaan en dus waarschijnlijk ook in veel mindere mate door de hoornlaag heen gaan. Hoofdstuk 6 gaat dieper in op het fenomeen van protoporfyrine IX productie buiten het stukje huid waar aminolevulinezuur aangebracht wordt. In dit hoofdstuk is onderzocht of de protoporfyrine IX productie buiten het toedieningsgebied van aminolevulinezuur afhangt van de concentratie van het aminolevulinezuur, de duur van de toedieningstijd, de aanwezigheid van een penetratiebevorderaar, de

aanwezigheid van de hoornlaag, of het gebruik van een aminolevulinezuur ester. Protoporfyrine IX fluorescentie buiten het stukje huid waar aminolevulinezuur aangebracht is treedt alleen op wanneer het 24 uur lang aangebracht wordt (de hoeveelheid protoporfyrine IX is afhankelijk van de concentratie van het aminolevulinezuur) of nadat het aangebracht is op huid zonder hoornlaag. Deze resultaten bevestigen dat er protoporfyrine IX productie buiten het toedieningsgebied van aminolevulinezuur plaatsvindt, maar alleen tijdens of na specifieke omstandigheden waaronder aminolevulinezuur aangebracht wordt. Dit effect speelt derhalve niet of nauwelijks een rol in klinische situaties, waar de toediening van aminolevulinezuur relatief kort is, en mogelijk een penetratiebevorderaar toegevoegd is of een aminolevulinezuur ester gebruikt wordt.

Protoporfyrine IX productie in (pre)maligne huid

De bevinding dat aminolevulinezuur esters niet substantieel de protoporfyrine IX productie verhogen in normale huid, betekent niet per se dat de aminolevulinezuur esters geen geschikte stoffen zouden zijn voor fotodynamische therapie. Dit blijkt uit experimenten in hoofdstuk 4, waarbij gebruik gemaakt is van haarloze muizen met normale, gezonde huid en van haarloze muizen waarvan de huid chronisch blootgesteld geweest is aan UVB straling. Door de chronische blootstelling aan UVB straling (ook aanwezig in zonlicht) zijn er op de huid van deze muizen (pre)maligne afwijkingen ontstaan. De huid rondom de zichtbare afwijkingen ziet er normaal uit, maar is toch al afwijkend van, en dikker dan gezonde huid die niet chronisch blootgesteld is aan UVB straling. In normale haarloze muizenhuid waarop aminolevulinezuur pentyl ester aangebracht geweest is, zijn de protoporfyrine IX hoeveelheden ongeveer even groot als huid waarop aminolevulinezuur aangebracht geweest is. In de kleine (pre)maligne afwijkingen op de huid van de muizen die chronische blootgesteld geweest waren aan UVB straling, wordt na verloop van tijd meer protoporfyrine IX gemeten wanneer aminolevulinezuur pentyl ester aangebracht geweest is dan wanneer aminolevulinezuur aangebracht geweest is. In de huid rondom de zichtbare afwijkingen wordt meer protoporfyrine IX geproduceerd wanneer aminolevulinezuur pentyl ester aangebracht geweest is dan wanneer aminolevulinezuur aangebracht geweest is. Deze verschillen tussen aminolevulinezuur en aminolevulinezuur pentyl ester resulteren in een hogere ratio van protoporfyrine IX fluorescentie tussen (pre)maligne weefsel en normale huid voor aminolevulinezuur pentyl ester dan voor aminolevulinezuur. Dit zou betekenen dat fotodynamische therapie mogelijk selectiever zou zijn met een aminolevulinezuur ester dan met aminolevulinezuur. Echter, de fluorescentiemicroscopiebeelden tonen aan dat de hogere protoporfyrine IX hoeveelheden voor aminolevulinezuur pentyl ester zich bevinden in de hoornlaag van de afwijkingen en de daaromheen gelegen afwijkende huid en dat is niet het gedeelte van de huid wat door fotodynamische therapie behandeld wordt.

Uit de fluorescentiemicroscopiebeelden kan ook nog het volgende afgeleid worden. De hoeveelheden protoporfyrine IX in het (pre)maligne weefsel zijn hoger dan in de normale huid (bij aminolevulinezuur en aminolevulinezuur pentyl ester). Deze verschillen zijn echter niet zo groot als op basis van de metingen van het protoporfyrine IX fluorescentiesignaal aan de levende muizen verwacht werd. Dit kan verklaard worden door het feit dat (pre)maligne huid dikker is dan normale huid. Juist in het verdikte gedeelte bevindt zich het grootste deel van de hoeveelheid protoporfyrine IX. Dit betekent dat bij levende muizen de dikte van de huid ook bijdraagt aan de hoogte van het fluorescentiesignaal van protoporfyrine IX.

Penetratie van aminolevulinezuur en aminolevulinezuur esters door huid

Penetratie door normale huid

De resultaten van hoofdstuk 4 en 5 lieten zien dat de protoporfyrine IX productie in de huid met gebruik van aminolevulinezuur esters niet zo hoog was als verwacht werd op basis van eerdere studies met gekweekte cellen. In hoofdstuk 7 is onderzocht op geïsoleerde stukjes muizenhuid of de oorzaak zou kunnen liggen in onbekende verschillen in de huidpenetratie-eigenschappen van aminolevulinezuur en aminolevulinezuur esters. De resultaten geven inderdaad aan dat de penetratie (door de geïsoleerde stukjes huid heen) hoger is voor aminolevulinezuur dan voor aminolevulinezuur methyl ester en aminolevulinezuur hexyl ester. Dit resultaat komt overeen met eerdere resultaten (onder andere in hoofdstuk 6) die lieten zien dat aminolevulinezuur, maar niet een aminolevulinezuur ester, zodanig veel (door de huid heen) in de bloedbaan opgenomen wordt dat protoporfyrine IX productie geïnduceerd wordt buiten het stukje huid waar het aangebracht wordt.

Uit experimenten waarin aminolevulinezuur en aminolevulinezuur esters aangebracht werden op geïsoleerde muizenhuid waarvan de hoornlaag dunner gemaakt was (met behulp van plakband), bleek dat de penetratie door die huid heen ongeveer 100 maal (bij aminolevulinezuur) tot 200 maal (bij aminolevulinezuur esters) hoger is dan door normale huid. Deze resultaten bevestigen eerdere bevindingen (in onder andere hoofdstukken 5 en 6) dat de hoornlaag een belangrijke barrière is voor aminolevulinezuur en aminolevulinezuur esters.

Penetratie door (pre)maligne huid

Reeds lang is bekend dat na toediening van aminolevulinezuur op huid met premaligne afwijkingen zoals Bowen's disease en actinische keratose, of oppervlakkige maligne afwijkingen zoals plaveiselcel carcinomen en basaalcel carcinomen, er meer protoporfyrine IX in deze afwijkingen geproduceerd wordt dan in de omliggende normale huid. Men heeft al vaak gesuggereerd of aangenomen dat dit veroorzaakt wordt doordat de

penetratie-eigenschappen van de hoornlaag van deze (pre)maligne afwijkingen anders zijn dan van de hoornlaag van normale huid. Daardoor zou aminolevulinezuur sneller en met grotere hoeveelheden de afwijkingen binnendringen en dus zorgen voor meer protoporfyrine IX in de afwijkingen dan in de omliggende normale huid. De studie beschreven in hoofdstuk 8 presenteert voor de eerste keer resultaten die deze hypothese bevestigen. De penetratie van aminolevulinezuur door geïsoleerde stukjes haarloze muizenhuid is in dit hoofdstuk getest in normale huid, in huid met een (gedeeltelijk) verwijderde hoornlaag (met behulp van plakband), en in huid die verdikt is met premaligne cellen door chronische blootstelling aan UVB straling. Het laatste type huid is een voorloper van huid met (pre)maligne afwijkingen en staat model voor de boven beschreven premaligne en maligne huidafwijkingen, want deze afwijkingen kunnen ontstaan in een chronisch aan de zon (dus ook aan UVB straling) blootgestelde huid. De penetratie van aminolevulinezuur door de muizenhuid met premaligne afwijkingen is hoger dan door de normale huid, maar lager dan door de huid zonder hoornlaag. Dit geeft aan dat de barrière-eigenschappen van de hoornlaag minder effectief zijn in een chronisch UVB bestraalde huid dan in een normale huid, maar nog wel effectiever dan in een huid waarvan de hoornlaag (gedeeltelijk) verwijderd is.

Invloed van de huidtemperatuur tijdens toediening van aminolevulinezuur

Naast het gebruik van veresterd aminolevulinezuur zijn er vele andere mogelijkheden die onderzocht worden of al toegepast worden om fotodetectie en fotodynamische therapie met aminolevulinezuur te verbeteren. Eén van die mogelijkheden is om de huidtemperatuur tijdens de topicale toediening van aminolevulinezuur te verhogen. In hoofdstuk 9 is onderzocht wat de invloed van de huidtemperatuur tijdens de toediening van aminolevulinezuur is op de penetratie van aminolevulinezuur door de huid heen en op de protoporfyrine IX productie in de huid. De resultaten van experimenten met geïsoleerde stukjes muizenhuid laten duidelijk zien dat de penetratie van aminolevulinezuur door de huid heen hoger is bij een hogere huidtemperatuur. De experimenten met proefpersonen laten zien dat er in een gezonde mensenhuid meer protoporfyrine IX wordt geproduceerd bij hogere huidtemperaturen.

Conclusies

De studies met de carotenoporfyrine en met aminolevulinezuur en aminolevulinezuur pentyl ester hebben aangetoond dat het uitermate belangrijk is om fluorescentie-microscopie deel uit te laten maken van studies waarin nieuwe fotodiagnostische stoffen onderzocht worden voor detectie van (voorlopers van) tumoren.

Bij de metingen van het protoporfyrine IX fluorescentiesignaal bij levende muizen met of zonder (pre)maligne afwijkingen is de hoogte van het signaal niet alleen afhankelijk van de hoeveelheid protoporfyrine IX, maar ook van de dikte van de huidlaag waar de protoporfyrine IX zich bevindt.

Wat betreft nieuwe of aangepaste fotosensitizers voor fotodetectie, kan geconcludeerd worden dat de nieuwe carotenoporfyrine niet lokaliseert in (pre)maligne weefsels in de diersmodellen met primaire tumoren. Het gebruik van aminolevulinezuur pentyl ester resulteert in lagere protoporfyrine IX concentraties in normale huid en ongeveer gelijke protoporfyrine IX concentraties in (pre)maligne weefsel in vergelijking met aminolevulinezuur. Dit leidt tot een betere protoporfyrine IX ratio tussen (pre)maligne weefsel en normale huid voor aminolevulinezuur pentyl ester dan voor aminolevulinezuur. Hierdoor is een betere fotodetectie van (pre)maligne afwijkingen mogelijk met minder ongewenste fotodynamische bijwerkingen.

Tegen de verwachting in was de door aminolevulinezuur hexyl ester opgewekte protoporfyrine IX productie in de huid niet of nauwelijks hoger dan bij aminolevulinezuur. Hiervoor zou de lagere penetratie van aminolevulinezuur esters de huid in (mede)verantwoordelijk kunnen zijn. Dit komt ook overeen met de bevinding dat onder bepaalde toedieningscondities protoporfyrine IX productie plaats kan vinden buiten het opbrenggebied van aminolevulinezuur, hetgeen niet het geval is bij aminolevulinezuur hexyl ester.

De snelheid waarmee aminolevulinezuur de huid in penetreert is bij huid met (pre)maligne afwijkingen hoger dan bij normale huid. Dit verschil kan (gedeeltelijk) verantwoordelijk zijn voor de hogere protoporfyrine IX productie in deze afwijkingen.

Verhoging van de huidtemperatuur bevordert de penetratie van aminolevulinezuur de huid in en de protoporfyrine IX productie in de huid. Deze benadering zou daarom gebruikt kunnen worden ter verbetering van fotodynamische therapie met aminolevulinezuur.

Curriculum Vitae

Hanneke van den Akker werd geboren op 15 december 1971 te Helmond. In 1990 behaalde zij het diploma in het Voorbereidend Wetenschappelijk Onderwijs aan het St. Willibrord Gymnasium te Deurne. In hetzelfde jaar begon ze met de studie Biologie aan de Universiteit van Leiden. Nadat ze een jaar later de propedeuse gehaald had, zette ze haar studie voort in de bovenbouwstudie Bio-Farmaceutische Wetenschappen. In het kader van het afstuderen deed zij onderzoek bij de vakgroep Medicinale Fotochemie naar de fotoreactiviteit van een aantal 4-(nitrophenyl)-dihydropyridines. Na voltooiing van dit onderzoek, verrichtte zij onderzoek naar de fotoreactiviteit van een aantal khelline derivaten bij de afdeling Farmaceutische Wetenschappen van de Universiteit van Padua, Italië. Na haar afstuderen startte ze met haar promotieonderzoek over mogelijke oplossingen voor verbetering van fotodetectie en fotodynamische therapie met porfyrine-achtige stoffen bij de sectie Fotodynamische Therapie en Optische Spectroscopie van de afdeling Radiotherapie in de Daniel den Hoed Kliniek, Erasmus Medisch Centrum, Rotterdam. Dit onderzoek werd begeleid door dr. H.J.C.M. Sterenborg en dr. W.M. Star. Na twee jaar werd het promotieonderzoek voortgezet bij prof.dr. J. Moan van de afdeling Biofysica van het Radium Hospitaal in Oslo, Noorwegen. Het laatste gedeelte van het promotieonderzoek werd uitgevoerd bij de vakgroep Fotobiologie en Fotodynamische Therapie aan de faculteit Biochemie en Moleculaire Biologie van de Universiteit van Leeds, Verenigd Koninkrijk. Dit gedeelte van het promotieonderzoek werd begeleid door dr. D.I. Vernon, onder supervisie van prof.dr. S.B. Brown.

Na de voltooiing van haar promotieonderzoek werkte zij bij het Metabool Laboratorium van de Vrije Universiteit Medisch Centrum te Amsterdam als onderzoeker voor een Europees project over gebruik van folaten ter voorkoming van hart- en vaatziekten.

Tegenwoordig is zij clinical research associate bij NDDO Oncology te Amsterdam. Bij NDDO Oncology worden klinische en preklinische studies op het gebied van kankerbehandeling (inclusief fotodynamische therapie) ontworpen en uitgevoerd in samenwerking met farmaceutische en biotechnologische bedrijven.

List of publications

van den Akker JTHM, Speelman OC, van Staveren HJ, Moore AL, Moore TA, Gust D, Star WM, Sterenborg HJCM. Localisation and accumulation of a new carotenoporphyrin in two primary tumour models. *J Photochem Photobiol B* 2000; 54:108-115.

van den Akker JTHM, de Bruijn HS, Beijersbergen van Henegouwen GMJ, Star WM, Sterenborg HJCM. Protoporphyrin IX fluorescence kinetics and localization after topical application of ALA pentyl ester and ALA on hairless mouse skin with UVB-induced early skin cancer. *Photochem Photobiol* 2000; 72(3):399-406.

van den Akker JTHM, Iani V, Star WM, Sterenborg HJCM, Moan J. Topical application of 5-aminolevulinic acid hexyl ester and 5-aminolevulinic acid to normal nude mouse skin: Differences in protoporphyrin IX fluorescence kinetics and the role of the stratum corneum. *Photochem Photobiol* 2000; 72(5):681-689.

Moan J, van den Akker JTHM, Juzenas P, Ma L-W, Angell-Petersen E, Gadmar ØB, Iani V. On the basis for tumor selectivity in the 5-aminolevulinic acid-induced synthesis of protoporphyrin IX. *J Porphyrins Phthalocyanines* 2001; 5:170-176.

van den Akker JTHM, Brown SB. Photodynamic therapy based on 5-aminolevulinic acid: Applications in dermatology. In *Photobiology for the 21st Century*. (Edited by TP Coohill, DP Valenzano) 2001, Valdenmar Publishing Company, Kansas, USA: pp. 165-181.

van den Akker JTHM, Iani V, Star WM, Sterenborg HJCM, Moan J. Systemic component to protoporphyrin IX production in the nude mouse skin upon topical application of aminolevulinic acid depends on the application conditions. *Photochem Photobiol* 2002; 75(2):172-177.

van den Akker JTHM, Holroyd JA, Vernon DI, Sterenborg HJCM, Brown SB. Comparative *in vitro* percutaneous penetration of 5-aminolevulinic acid and two of its esters through excised hairless mouse skin. *Lasers Surg Med* 2003; 33(3):173-181.

van den Akker JTHM, Holroyd JA, Vernon DI, Sterenborg HJCM, Brown SB. Chronic UVB exposure enhances *in vitro* percutaneous penetration of 5-aminolevulinic acid in hairless mouse skin. Submitted to *Lasers Surg Med*.

van den Akker JTHM, Boot K, Vernon DI, Brown SB, Groenendijk L, van Rhoon G, Sterenborg HJCM. Effect of elevating the skin temperature during topical ALA application on *in vitro* ALA penetration through mouse skin and *in vivo* PpIX production in human skin. Submitted to *Photochem Photobiol Sci*.

Tenslotte...

Het proefschrift is af! Hoewel alleen mijn naam op de voorkant staat, is het uiteraard absoluut niet zo dat ik alles alleen heb moeten doen. Iedereen die op enige manier een bijdrage geleverd heeft wil ik bedanken, en een aantal mensen in het bijzonder.

Mijn promotoren: prof.dr. P.C. Levendag and prof.dr. S.B. Brown. Beste Peter, bedankt dat je mijn promotor wilde zijn zodat ik kan promoveren bij die afdeling waar vanaf het begin de basis van mijn promotieonderzoek geweest is. Dear Stan, thank you for giving me the opportunity to complete my PhD research in your lab in Leeds. I really appreciated and enjoyed your hospitality in the final year of my PhD research.

De basis van mijn promotieonderzoek: dr.ir. H.J.C.M. Sterenborg en dr. W.M. Star. Beste Dick, jij bent de initiator geweest achter dit proefschrift. Veel heb ik geleerd van jouw enthousiasme en kennis van het onderzoek op het gebied van de fotodetectie en de fotodynamische therapie. Altijd had je wel tijd om met me mee te denken over de experimenten, de resultaten en de publicaties. Nooit was het een probleem om me nog eens duidelijk uit te leggen hoe je de data nou ook alweer gefit had tot mooie grafieken. Veel waardering heb ik ook voor de snelheid en deskundigheid waarmee je mijn manuscripten beoordeelde en corrigeerde, ondanks je vele andere drukke werkzaamheden. Je talent, gedrevenheid en optimisme gaven mij de steun dit proefschrift te schrijven. Beste Willem, jij hebt me aangenomen voor het Rotterdamse deel van het Europees project en me binnengeleid in de wereld van de fotodynamische therapie en fotodetectie. Jouw kennis en kunde in de fotodynamische therapie kent zijn weerga niet en hebben een belangrijke bijdrage geleverd aan mijn onderzoek en de daar uit voortgekomen proefschrift en publicaties.

Rotterdamse steun en toeverlaat: de collega's. Beste Riëtte, samen met Otto heb jij mij bijgestaan bij mijn kennismaking met de praktische kant van het onderzoek op het gebied van de fotodynamische therapie en de fotodetectie. Maar het is veel meer dan dat. Vele uurtjes hebben we wat afgekletst tijdens het opmeten van tumortjes, fluorescentie opnames, congressen, mijn terugkomdagen na mijn 'Rotterdamse periode'. En niet te vergeten al die coupes die je voor me sneed, dingetjes die je voor me uitzocht en regelde, ook toen ik in Oslo en Leeds werkte. Ook de andere collega's, Otto, Hugo, Lars, Hans, Dom, Robert, Arjen, Angelique, Diana, Joost en Arjan wil ik bedanken. Voor de leuke werksfeer, de hulp in woorden en daden, de gezelligheid als ik weer eens een dagje op bezoek was om 'dingetjes' te regelen.

Degene die het mogelijk maakte dat ik met mijn promotieonderzoek door kon gaan: prof.dr. J. Moan. Dear Johan, thank you for your hospitality and the opportunity to work in your lab. This made it possible for me to continue my PhD research. I very much enjoyed my stay in the Radium Hospitalet. Thank you all colleagues in the lab and in particular Vladimir, Petras, Ma, Saulius, Even, Mario, Pål, Torunn, Kårstein, Lina and

Heidi. Thank you Julie, Gerlinde, Francesca, Aušra and Petras for your friendship, the evenings with good food and/or drinks, and the 'touristy' visits in and outside Oslo.

Degenen die me in de gelegenheid stelden om mijn promotieonderzoek af te maken: prof.dr. S.B. Brown and dr. D.I. Vernon. Dear Stan, I am honoured that you are one of my promotores. Thank you for the opportunity to work in your lab so that I could complete my PhD research. Dear Dave, I really enjoyed working with you. Thank you for your guidance and for your time you had available for discussing the problems and the results of my experiments. Thank you Julie, Ian, Emma, Cassie, Mike, Martin, Hazel, Kirste, Steve, Dave, Andy, June, Amanda and Doreen for the nice time during my stay in Leeds. I very much enjoyed working with you all, and not to forget the daily coffee breaks, the visits to the pub and all other fun outside work.

De VU collega's van het metabole lab, in het bijzonder Marcella, Desirée en Wim.

De Leidse Harmoniekapel. De muzikale ont- en inspanning op de woensdagavond is een aangename afwisseling van de werkuren. Dank aan alle medemuzikanten hiervoor. In het bijzonder wil ik Alexandra, Petra, Lex, Jeroen, Gaëlle, Elvira, Johan, Franc, Marcel, Shanna, Marco D., Marco H., Joyce, Marieke en Wilke ook bedanken voor alles wat er naast het muziekmaken bijkomt, zoals de gezelligheid aan de bar, de spelletjesavonden, de goede gesprekken en de etentjes.

Mijn 'Leidse' vriendin door de jaren heen. Lieve Jeannette, bedankt voor je vriendschap in de afgelopen jaren. We hebben wat afgebeld en kaartjes gestuurd, helaas hebben we elkaar de laatste tijd veel te weinig gezien wegens 'te druk'. Ik beloof je dat dat vanaf nu anders zal zijn!

Mijn familie. Lieve pap en mam, bedankt voor jullie liefde, jullie steun bij wat ik wilde bereiken, jullie belangstelling. Vaak zullen jullie je wel afgevraagd hebben of het proefschrift ooit nog afkwam. Zie hier dan toch het langverwachte resultaat. Ook dank aan mijn zussen en hun partners. Pap, mam, Doorke, Henrike, Paulien en Willemijntje, nu ik in de weekenden geen proefschrift meer hoeft te schrijven heb ik weer meer tijd voor familiebezoekjes.

Mijn geliefde en maatje. Lieve Paul, bedankt voor alles wat je voor me betekent.

